SMART ADSORPTION MATERIALS AND SYSTEMS FOR RECOVERY OF HIGH VALUE PROTEIN PRODUCTS

By

Ping Cao

A thesis submitted to the University of Birmingham

for the degree of

DOCTOR OF PHILOSOPHY

School of Chemical Engineering

College of Engineering and Physical Sciences

July 2015

Thesis abstract

Although liquid chromatography has been playing a key role in bioseparation since it established in 1941, scientists and engineers are still dedicated to solve its drawbacks, such as: current ‘adsorption-desorption’ processes are expensive, low productivity occurs in batch-wise operation in fixed beds, large amounts of buffer employed for equilibrating, washing, eluting and cleaning of columns, and consequently generating excessive quantities of waste.

In this context, we produced various thermoresponsive ionic exchange adsorbents via ‘grafting from’ polymerisation, and consequently applied them to a novel travelling cooling zone reactor (TCZR). Sepharose CL-6B, Superose 6 prep grade, and Superose 12 prep grade were selected as the base matrices in this study in order to find the most suitable particle size and pore diameter for the modification with thermoresponsive polymer. Both cation exchange adsorbents (thermoCEX) and anion exchange adsorbents (thermoAEX) modified with poly(*N*-isopropylacrylamide) or pNIPAAm were introduced in Chapter 2, 3, and 5. All resins’ binding affinity and maximum adsorption capacity increased with elevated temperature, however, the protein ‘adsorption-desorption’ behaviour of thermoCEX is much superior to that of thermoAEX (i.e. $q_{max,50°C}$ / $q_{max,10°C}$ ratios of thermoCEX-S6PG B2 and thermoAEX-S6PG F2 are 2.2 and 1.6 respectively). We also introduced cation exchange adsorbents with poly(ethylene glycol) or PEG in Chapter 4, although the thermoresponsiveness of thermoCEX-PEG-S6PG has been

found even better than those of thermoCEX (i.e. $q_{max,50°C}$ / $q_{max,10°C}$ ratios of thermoCEX-PEG-S6PG D2 thermoCEX-CL6B A2 and thermoCEX-S6PG B2 are 9.9, 3.3 and 2.2 respectively), the dynamic protein binding performance is limited due to its relatively lower protein binding capacity at higher temperature (i.e. $q_{max,50°C}$ of thermoCEX-PEG-S6PG D2 , thermoCEX-CL6B A2, and thermoCEX-S6PG B2 are 19.8, 55.9 and 28.6 mg/mL respectively).

Dedication

To my parents, my wife and my daughter,

for all the love and supports

Acknowledgements

I would like to thank my supervisor Professor Owen Thomas who has supported and challenged me throughout my PhD life. The knowledge of science and attitude of research from his guidance are valuable treasures not only for my PhD but also for my whole life. I am also indebted to Dr Eirini Theodossiou for the supervision, support and assistance during my PhD studies.

I am grateful to Hazel Jennings and Elaine Mitchell for their patient advice and help in the laboratory. I would like to thank all the former and current members of our research group, who provided their kind supports at different stages of my PhD project.

The novel travelling cooling zone reactor (TCZR) used in this work was designed and manufactured by Professor Matthias Franzreb and Dr Tobias Müller from KIT (Germany). The thermoresponsive chromatographic adsorbents were fabricated by me (University of Birmingham, UK). With the dedicated efforts and cooperation from both sides, Chapter 2 and Chapter 3 were published on Journal of Chromatography (A) in 2013 and 2015 respectively.

Table of Contents

List of Figures

List of Tables

Abbreviations

AAc	acrylic acid
AC	affinity chromatography
ACV	4,4'-azobis(4-cyanovaleric acid)
ATR-FTIR	attenuated total reflectance Fourier transform infrared spectroscopy
BSA	bovine serum albumin
CM	carboxymethyl
DEAE	diethylaminoethyl
DMF	*N,N*-dimethylformamide
DSP	downstream processing
ECH	epichlorohydrin
EEDQ	2-ethoxy-1-ethoxycabonyl-1,2-dihydroquinoline
FT-IR	Fourier transform infrared spectroscopy
GFC	gel filtration chromatography
GPC	gel permeation chromatography
HIC	hydrophobic interaction chromatography
HPLC	high performance liquid chromatography
IEC	ion exchange chromatography
LCST	lower critical solution temperature
LF	bovine whey lactoferrin
MBAAm	*N,N'*-methylenebisacrylamide
OVA	albumin from chicken egg white
PEG	poly(ethylene glycol)

PI	isoelectric point
pNIPAAm	poly(*N*-isopropylacrylamide)
Q	quaternary ammonium
QAE	quaternary aminoethyl
RPC	reverse phase chromatography
RT	room temperature
RTD	residence time distribution
NMR	nuclear magnetic resonance
S	methyl sulphonate
S6 PG	Superose 6 prep grade
S12 PG	Superose 12 prep grade
SEC	size exclusion chromatography
S CL-6B	Sepharose CL-6B
SP	sulphopropyl
tBAAm	*N-tert*-butylacrylamide
TCZR	travelling cooling zone reactor
THZR	travelling heating zone reactor
thermoAEX	thermoresponsive anion exchange adsorbents
thermoCEX	thermoresponsive cation exchange adsorbents
THF	tetrahydrofuran
UV	ultraviolet

1 Introduction

1.1 Project overview

This work has been supported by the European Framework Programme 7 (MagPro^{2}Life) which is aiming to develop scalable innovative nanotechnology based processes and demonstrate these at pilot-line-scale equipment for food and biopharma applications. The objective of this work is to fabricate new families of smart chromatographic adsorbents utilising the unique property of temperature-sensitive polymers (i.e. poly(*N*-isopropylacrylamide) or pNIPAAm, and poly(ethylene glycol) or PEG via graft-from polymerisation methods to modify commercial packed bed chromatographic base supports with different particle diameters and/or pores (i.e. Sepharose CL-6B, Superose 6 prep grade, and Superose 12 prep grade). Through rigorous physical-chemical characterisation, the optimal thermoresponsive chromatographic adsorbents have been found and subsequently applied into a novel travelling cooling zone reactor (TCZR) to demonstrate the dynamic 'adsorption-desorption' behaviour with high value protein products.

1.2 Downstream processing

1.2.1 Introduction

In biotechnology, any procedure of the culture broth after upstream processing (such as fermentation, animal & plant cell culture and agricultural synthesis) is classified into 'Downstream processing' (DSP). The DSP is defined as the recovery and purification operations that follow a biochemical reaction (Dunnill, 1987), and it is focusing on concentrating and purifying the target products (i.e. proteins, enzymes, plasmid DNA) to certain purity (95%, 99% or 99.9%).

Four operations are occurred sequentially in DSP stage: 1. Removal of insoluble contaminants; 2. Primary isolation; 3. Purification; and 4. Final isolation (Belter et al., 1988). The cells, cell debris and other insoluble contaminants from the fermentation broth are removed via centrifugation/ filtration/setting/sedimentation/decanting/flotation depending on the location of target product (within cells or in the liquid phase) (Thomas, 2008). High pressure homogenisation, bead milling, osmotic shock, chemical or enzymatically mediated lysis/rupture are common approaches if the target molecule is intracellular, dissolution and protein refolding are necessary in the first step if the aiming protein is produced as inclusion bodies. Although only relatively little product concentration and quality enhancement is accomplished in this step, it is essential for the following procedures in DSP. The concentration and quality of the target molecule is significant improved in

the second non-selective step ‘Primary isolation’, and liquid extraction, precipitation, flocculation and adsorption are usually applied in this step. In stark contrast, the selectivity of the following step ‘Purification’ is extremely high in order to separate the desired soluble product from impurities possessed similar physical-chemical properties. ‘Purification’ step is usually the most sophisticated in the DSP due to it’s high selective demand, and as the result, liquid chromatography is introduced for purification because of it’s advantages of high resolution and adaptability. The product’s application determines its final purity level. Size exclusion chromatography and crystallisation followed by drying treatment are heavily employed in the ‘Final isolation’ step (Thomas, 2008).

1.2.2 Protein recovery, separation and purification

In last several decades, manufacture of proteins with high purity has been attracted more and more attentions due to their high value and popularity in foods, antibodies, therapeutic or industrial and diagnostic enzyme industries (Hoare and Dunnill, 1989; Galaev and Mattiasson, 1999). Many different approaches have been developed and applied for the recovery, separation and purification of proteins due to their varieties of property arising from their own unique structures and formations. The most regularly used techniques are listed below:

Cell disruption: in more common cases, target proteins are located in the interior parts of cells, and cell disruption is consequently introduced in the

early stage of the protein DSP process. Homogenisation and bead milling by means of mechanical shear-based techniques have been utilised widely in large scale industrial applications, however, ultrasonication and osmotic shock are still popularly used at laboratory scale (Leser and Asenjo, 1994). The routinely used techniques of cell disruption are listed in Table 1.1 and Table 1.2.

Table 1.1 Release of intracellular products from cells by mechanical methods (taken from Scopes, 1982).

Technique	Principle	Stress on product	Cost
Homogenisation (blade type)	Cells chopped in Waring blender	Moderate	Moderate
Homogenisation (orifice type)	Cells forced through small orifice	Harsh	Moderate
Grinding	Cells ruptured by grinding with abrasives	Moderate	Cheap
Ultrasonication	Cells broken by ultrasound	Harsh	Expensive
Crushing in bead mill	Cells crushed between glass or steel beads	Harsh	cheap

Table 1.2 Release of intracellular products from cells by non-mechanical methods (taken from Theodossiou et al., 1997).

Technique	Principle	Stress on product	Cost
Osmotic shock	Osmotic rupture	Gentle	Cheap
Enzyme digestion	Cell wall digested	Gentle	Expensive
Solubilisation	Detergents solubilise cell membrane	Gentle	Moderate-expensive
Liquid dissolution	Organic solvent destabilises cell walls	Moderate	Cheap
Alkali treatment	Hydrolysis of cell walls and saponification of membranes	Harsh	Cheap

Aggregation: for the purpose of improving the performance of separation, the aggregation is usually utilised after cell disruption but before centrifugation and filtration processes to form solid aggregates of cells and/or debris. ‘charge neutralisation’ and ‘nucleation of adhesion by polymer bridging’ are two main techniques to increase the solid particle size (Thomas, 2008).

Precipitation: The definition of precipitation is a process in which ‘the relation between a solute and the solvent is altered, its solubility being reduced, in general by addition of a reagent or change in temperature, that changes the energy balance between the solute and the solvent’ (Kennedy and Cabral, 1993). In terms of its remarkable advantages, i.e. effective, cheap and little denaturation caused, precipitation is commonly used for recovery of bulk proteins (Scopes, 1982). Both the properties of protein (i.e. shape, size, charge and hydrophobicity) and the solvent environment (i.e. temperature, pH, salt concentration and dielectric constant) can affect the precipitation tendency of protein, consequently, salting-out through addition of neutral salts, controlling of pH (isoelectric precipitation), regulating of temperature (thermal denaturation), addition of non-ionic hydrophilic polymers, addition of miscible organic solvent, addition of polyvalent metallic ions, addition of polyelectrolytes, utilisation of carriers are commonly used precipitation methods in DSP process (Wang et al., 1979; Scopes, 1982; Kennedy and Cabral, 1993).

Centrifugation: the centrifugation is defined as ‘any separation process which uses centrifugal force to separate two liquids, or a liquid and solid(s), or a combination of all three’ (Axelsson, 1985; Belter et al., 1988). The advantages and disadvantages of some regularly used industrial centrifuges are listed in Table 1.3.

Table 1.3 Comparison of key features of industrial centrifuges (taken from Bell et al., 1983).

System	Advantages	Disadvantages
Tubular bowl	1. High centrifugal force 2. Good dewatering 3. Easy to clean 4. Simple dismantling of the bowl	1. Limited solids capacity 2. Foaming unless special skimming or centripetal pump used 3. Recovery of solids difficult
Chamber bowl	1. Clarification efficiency remains constant until sludge space full 2. Large solids holding capacity 3. Good dewatering 4. Bowl cooling possible	1. No solids discharge 2. Cleaning more difficult than tubular bowl 3. Solids recovery difficult
Disc-centrifuges	1. Solids discharge possible 2. Liquid discharge under pressure eliminates foaming 3. Bowl cooling possible	1. Poor dewatering 2. Difficult to clean
Scroll discharge	1. Continuous solids discharge 2. High feed solids concentration	1. Low centrifugal force 2. Turbulence created by scroll

Conventional filtration: Filtration is defined as a physical or mechanical process that separates and retains particulates or molecules from fluids (driven by pressure or vacuum) by means of a ‘filter media’ (Ballew, 1978). Filtration is one of the most popular approaches used at all scales and steps of operation in DSP process (Shuler and Kargi, 1992).

Chromatography: chromatography is defined as separation of various compounds by the flow of a fluid in a porous, solid sorptive medium (Shuler and Kargi, 1992). The fluid that flows through the column is mobile phase, and the medium which packed in the column is stationary phase, (the medium is also termed as adsorbent, resin, beads, supports, matrix, and gel). Today, liquid chromatography is one of the most important bioseparation approaches due to its adaptability to analytical and preparative separation tasks (Guiochon, 2002) and availability of a huge variety of differently functionalised chromatographic supports affording orthogonal separation mechanisms (Venkatramani and Zelechonok, 2003; Shi et al., 2004). Due to its significant importance in DSP process, liquid chromatography deserves detailed discussion in the following section.

1.2.3 Liquid chromatography

The liquid chromatography established by Martin and Synge in 1941 is a milestone in the history of chromatography, and this significant innovation was consequently awarded of Nobel Prize in 1952. With continuous development, liquid chromatography has played an important role in therapeutic macromolecules purification due to its highly resolution capacity and adaptability (Tiainen et al., 2007; Maharjan et al., 2008).

Nowadays, the frequently used chromatographic techniques are Size Exclusion Chromatography (SEC), Hydrophobic Interaction Chromatography (HIC), Reverse Phase Chromatography (RPC), Affinity Chromatography (AC), and Ion Exchange Chromatography (IEC). The suitability of above mentioned chromatographic techniques is listed in Table 1.4.

Table 1.4 Ranking of chromatographic techniques for suitability during capture, intermediate purification and polishing operations (taken from Thomas, 2008).

Technique	Capture	Intermediate Purification	Polishing	Some consideration
SEC		☆	☆☆☆	Can only use low samples volume and low flow rates.
HIC	☆☆	☆☆☆	☆☆	Cheap stable hydrophobic ligands, moderate binding capacity.
RPC		☆	☆☆☆	Employs 'denaturing' organic solvents and very hydrophobic solid phases. Only suitable for small proteins.
AC	☆☆☆	☆☆☆	☆☆	Protein ligands are costly, sensitive to harsh cleaning reagents, and can be leached off. Low-moderate binding capacities.
IEC	☆☆☆	☆☆☆	☆☆☆	Cheap stable charged ligands, high binding capacity.

1.2.3.1 Size Exclusion Chromatography (SEC)

Size Exclusion Chromatography is also known as Gel Filtration Chromatography (GFC), Gel Permeation Chromatography (GPC) or Molecular Sieve Chromatography, which separates molecules based upon their size differences. Rather than binding to the chromatographic resins in Ion Exchange or Affinity Chromatography, molecules in SEC do not interact with stationary phase, the mechanism of Separation in SEC is solely relied on the penetration extent of different biomolecules into the porous stationary phase, larger molecules are excluded from the gel pores and leaving from the column first, however, the smaller biomolecules are travelling a longer path in the column and passing through the column at the later stage because of their diffusion into the porous supports. Resolution is therefore not affected directly by buffer composition but the length of column (Thomas, 2008; Gel filtration - Principles and Methods, 2010). SEC can only separate the proteins with the mass difference over 500 Da, it owns the poorest resolution compared to other frequently used liquid chromatographic techniques (Gel filtration - Principles and Methods, 2010). Desalting and buffer exchange are two main applications of SEC in protein purification schemes, and Sephadex G-10, G-25 and G-50 are commonly employed supports in SEC (Thomas, 2008). The process of SEC is demonstrated in Fig. 1.1.

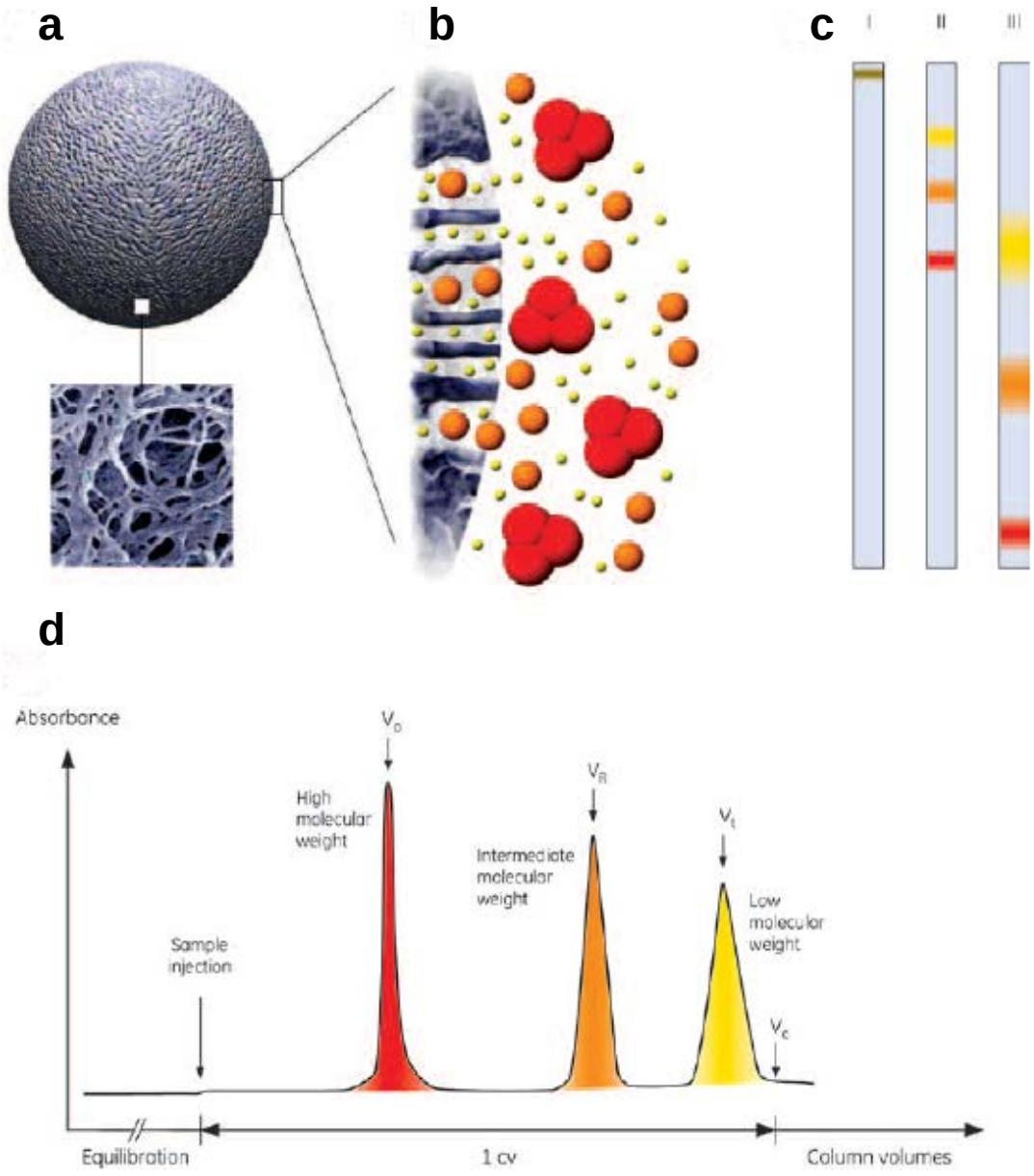

Fig. 1.1 Process of SEC (a) An electron microscopic enlargement picture of a bead packed in SEC column. (b) Schematic drawing of biomolecules with different sizes diffusing into bead pores with various extents. (c) Graphical description of separation: the largest molecule (red) passing through first from the column, the smallest molecule (yellow) passing through last from the column. (d) Schematic chromatogram (taken from Gel filtration - Principles and Methods, 2010).

1.2.3.2 Hydrophobic Interaction Chromatography (HIC)

The mechanism of HIC to separate biomolecules is via utilising reversible interaction between the hydrophobic surface of a HIC resin and the biomolecules on the basis of differences in their surface hydrophobicity, salts (i.e. ammonium sulphate) are usually selected to expose hydrophobic areas of hydrophilic proteins (Hydrophobic Interaction and Reversed Phase Chromatography Handbook, 2006; Thomas, 2008). The type of ligand, degree of ligand substitution, type of base matrix, type and concentration of salt, pH, Temperature, and Additives are important parameters to optimise HIC purification process. C4 – C8 alkyl chains or aromatic phenyl- groups are common used hydrophobic ligands in HIC, and they are primarily responsible for the protein 'adsorption-desorption' behaviours. The typical ligand substitution degree in HIC is 10 – 50 µmol/mL gel C2 – C8, protein binding capacities of HIC matrices increase with longer chain at a constant degree of substitution. The Hofmeister series (classifying ions ability to salt out/in proteins) is the principle for choosing the suitable salts for different HIC system, the order of decreasing precipitation (salting-out) effect in anions is: PO_4^{3-}, SO_4^{2-}, $CH3COO^-$, Cl^-, Br^-, NO_3^-, ClO_4^-, I^-, SCN^-; the order of increasing chaotropic (salting-in) effect in cations is: NH_4^+, Rb^+, K^+, Na^+, Cs^+, Li^+, Mg^{2+}, Ca^{2+}, Ba^{2+}. pH is a key parameter in HIC system, the hydrophobic interaction is improved at decreased pH but reduced at increased pH value. The influence of temperature on hydrophobic interaction is complex due to the varieties of conformational states and solubilities in aqueous solutions of different proteins (Hydrophobic Interaction and Reversed Phase

Chromatography Handbook, 2006; Thomas, 2008). The typical steps in a HIC process are illustrated in Fig. 1.2.

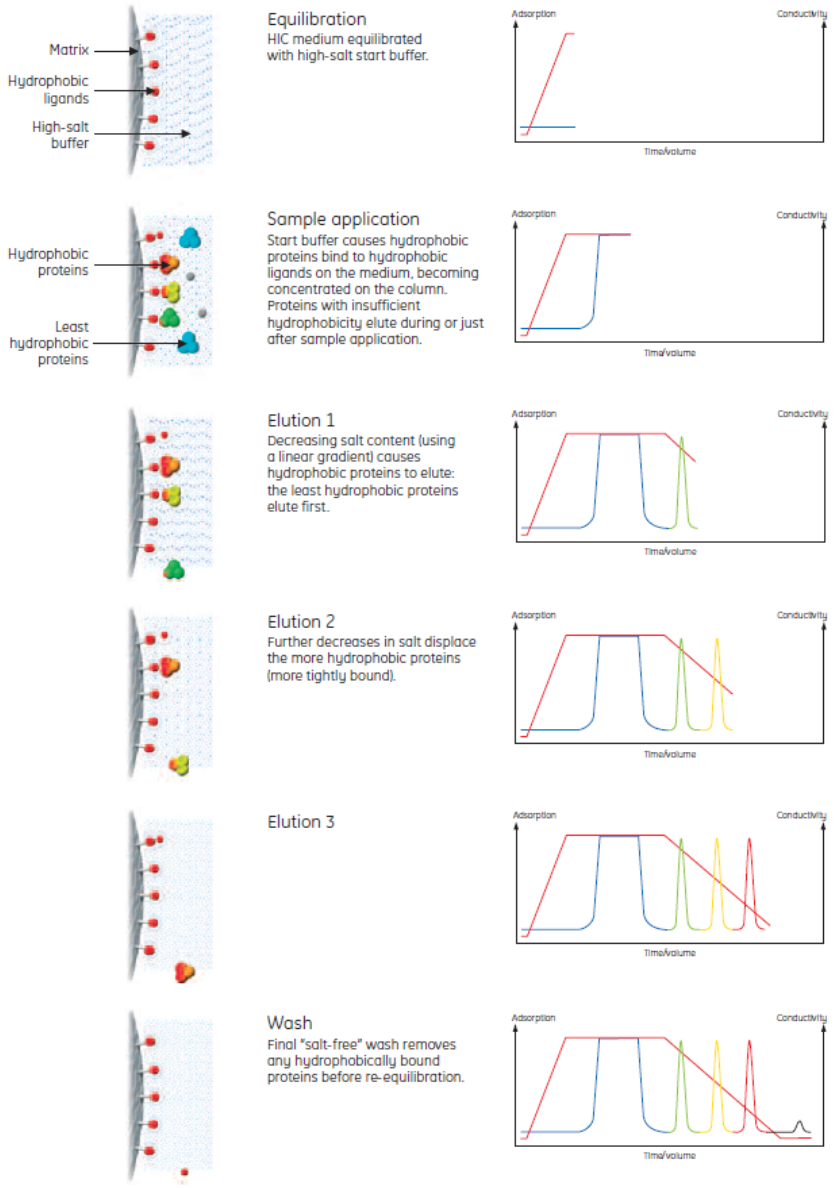

Fig. 1.2 Typical steps in HIC process (taken from Hydrophobic Interaction and Reversed Phase Chromatography Handbook, 2006).

1.2.3.3 Reverse Phase Chromatography (RPC)

Although the fundamental principle of both HIC and RPC is on the basis of interactions between the hydrophobic surfaces of chromatographic supports and hydrophobic patches on the surface of biomolecules, the hydrophobic interactions occurred in RPC is stronger than that in HIC directly resulting from the more hydrophobic ligands employed (i.e. C_8 – C_{18} alkyl chains), the extremely high resolution and great flexibility in terms of separation conditions can be achieved in RPC, which means the mixed biomolecules with very small differences in hydrophobicity can be separated via PRC technique, nonetheless, denaturation of proteins in loading/binding step caused by strong hydrophobic interactions and the utilisation of organic solvent leading to the waste treatment problems are two major concerns of RPC (Hydrophobic Interaction and Reversed Phase Chromatography Handbook, 2006). The term 'Reversed Phase Chromatography' indicates the mobile phase is more polar than stationary phase, and gradient elution is more regularly used than isocratic elution for the purpose of saving run time (Thomas, 2008). Some major differences between HIC and PRC are listed in Table 1.5.

Table 1.5 Some major differences between HIC and RPC, (taken from Thomas, 2008).

HIC	RPC
Substitution 10 – 50 µmol/mL Gel C_2 – C_8, Alkyl-, Aryl-, Phenyl- Ligands	Substitution 500 – 1000 µmol/mL gel C_4 – C_{18}, Alkyl- Ligands
Weak binding of proteins	Strong binding of proteins
Requires addition of suitable salts	Addition of ion pairing reagents (TFA) to suppress charges
Elution by decreasing salt concentration	Elution by increasing concentration of organic solvents
Mild conditions	Usually denaturating proteins
High protein yield	Low protein yield
Ideal of proteins	Ideal for peptides and small biomolecules

1.2.3.4 Affinity Chromatography (AC)

The theoretical principle of AC is based on a reversible biological interaction between the target biomolecules and the solid phase containing affinity ligands. Various interactions have been successfully employed in AC (i.e. electrostatic, hydrophobic interactions, van der Waal's forces, and hydrogen bonding) in order to purify the target biomolecules from other contaminants, and the target biomolecules can be reverse eluted via using a competitive ligand, changing the pH, ionic strength or polarity (Affinity chromatography - Principles and Methods, 2007). The most outstanding advantage of AC is its high selectivity, hence high resolution, and high capacity, highly purified and concentrated (i.e. >95%) targets can be obtained via AC technique, although the cost of AC is usually high (Thomas, 2008). The typical AC purification steps are illustrated in Fig. 1.3.

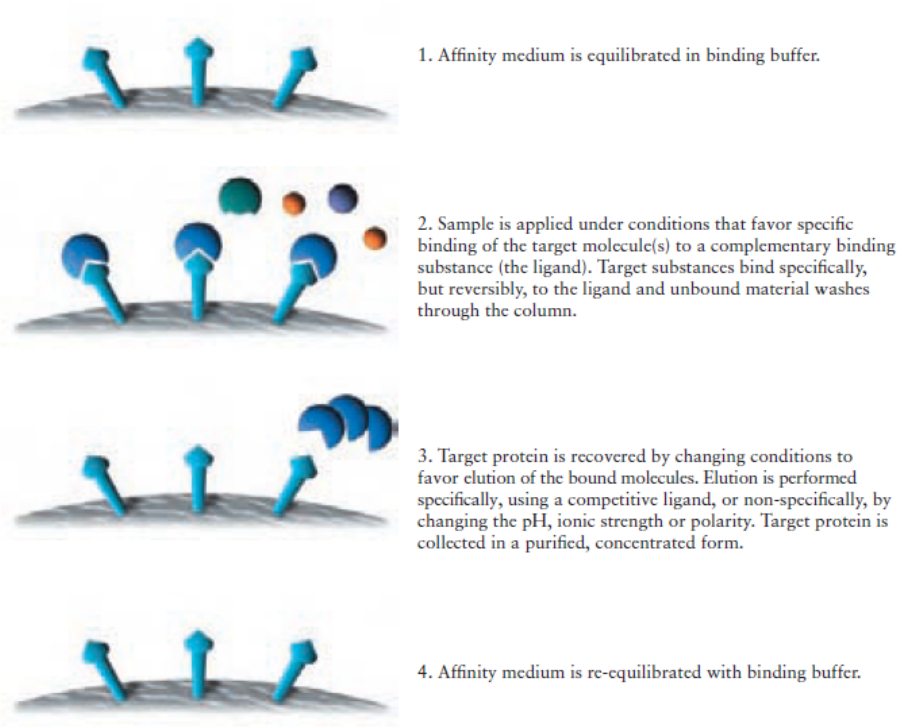

Fig. 1.3 Typical Affinity Chromatography purification steps, (taken from Affinity chromatography - Principles and Methods, 2007).

1.2.3.5 Ion Exchange Chromatography (IEC)

Since IEC was introduced in 1960s, it has been developed into one of the most common employed chromatographic techniques for the separation and purification of biomolecules due to its advantages of high resolution, high binding capacity, and straightforward principles of operation (Janson and Rydén, 1998). It is well known that all proteins are amphoteric and have their

unique pI points, proteins will exhibit a net surface positive charge when pH of the solution is below their pI points and therefore bind to negatively charged ion exchangers (cation exchangers), and vice versa, proteins will show a net surface negative charge when pH of the solution is above their pI points and bind to positively charged ion exchangers (anion exchangers), the theoretical protein titration curves are illustrated in Fig. 1.4 and the principles of an anion exchanger separation are illustrated in Fig. 1.5 (Ion Exchange Chromatography & Chromatofocusing - Principles and Methods, 2004).

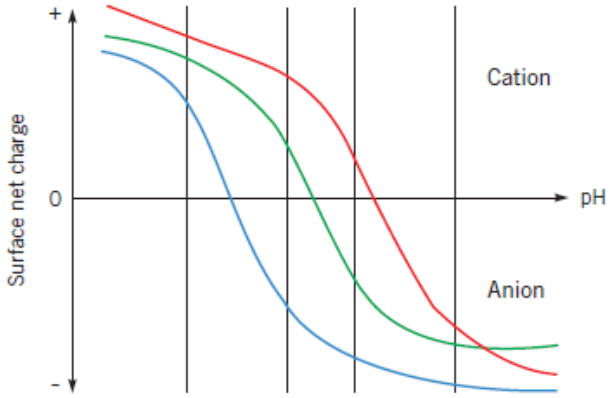

Fig. 1.4 The relationship between the net surface charge of proteins and pH, (taken from Ion Exchange Chromatography & Chromatofocusing - Principles and Methods, 2004).

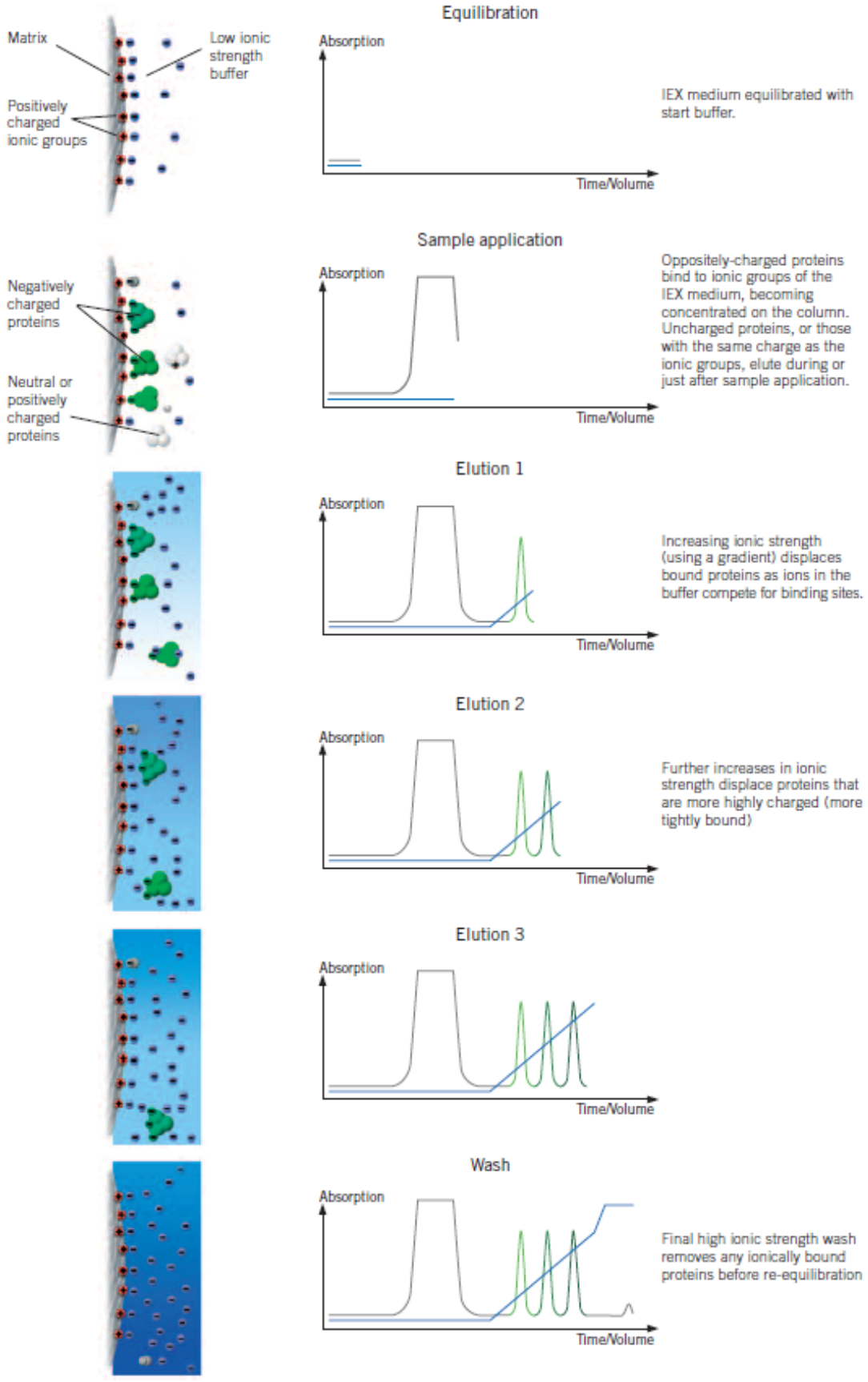

Fig. 1.5 Principles of an anion exchange separation, (taken from Ion Exchange Chromatography & Chromatofocusing - Principles and Methods, 2004).

In order to provide high internal surface area, the IEC media are always porous and their surface is covalently attached with negatively or positively charged groups. The frequently used ion exchangers are listed in Table 1.6.

Table 1.6 Common types of ion exchangers (taken from Thomas, 2008).

Type	Recommended pH range	Ligands
Weak anion exchangers	2 – 9	-Diethylaminoethyl (DEAE)
Strong anion exchangers	2 – 10	-Quaternary Aminoethyl (QAE)
Strong anion exchangers	2 – 10	-Quaternary Ammonium (Q)
Weak cation exchangers	6 – 10	-Carboxymethyl (CM)
Strong cation exchangers	2 – 10	-Sulphopropyl (SP)
Strong cation exchangers	2 – 10	-Methyl Sulphonate (S)

NB: 'strong' and 'weak' ion exchangers indicate to the extent to which they can maintain their charge, and not to their strength.

1.2.3.6 Steps in liquid chromatography

In most cases, there are four main steps in a batchwise liquid chromatography: equilibration, load, wash and elution.

Equilibration: utilising proper buffer to equilibrate the stationary phase in order to create the suitable conditions before the column is loaded by mobile phase.

Load: applying the components to be purified into the column to achieve the adsorption between media and mobile phase.

Wash: removing the contaminants in the mobile phase which adsorbed in the load stage.

Elution: desorbing the adsorbed components (usually the final products) via changing the composition of the mobile phase.

1.2.3.7 Drawbacks of chromatography

Although the so-called ‘workhorse’ – chromatography has been playing a key role in bioseparation in last several decades, it is not surprising that there are still some drawbacks existing. The majority of current frequently used chromatographic techniques are expensive, batch-wise chromatography in fixed bed suffers relatively low productivity (Przybycien et al., 2004; Jagschies, 2008; Maharjan et al., 2008), highly clarifying requirement of mobile phase before entering into the chromatography column is necessary, large amount of buffer for equilibrating, washing, eluting and cleaning of columns is needed, excessive quantities of waste are generated as the consequence (Thömmes and Etzel, 2007), the overall yield and economics are highly affected by every extra unit operation adding in DSP process, the porous stationary phase is prone to be clogging and fouling (Munro et al., 1977; Eveleigh, 1978).

1.3 Smart thermoresponsive polymers

Smart temperature-sensitive or thermoresponsive polymers are widely studied and applied in biomedicine and biotechnology due to its unique property of exhibiting inverse temperature solubility behaviour, i.e. they are water-soluble at low temperature and insoluble at high temperature, above a critical temperature known as the lower critical solution temperature (LCST) (Taylor and Cerankowski, 1975). Two thermoresponsive polymers are employed in

this thesis, i.e. poly(*N*-isopropylacrylamide) or pNIPAAm and poly(ethylene glycol) or PEG. pNIPAAm is the most studied smart thermoresponsive polymer thus far, it undergoes an abrupt reversible 'hydrophilic coil – hydrophobic globule' phase transition in water at a LCST of 32 – 34 °C (Heskins and Guillet, 1968; Kubota et al., 1990). We also introduced a more cost-effective and environmentally friendly polymer – PEG in the latter stage of this thesis. Although the different LCST of each individual macromonomer in PEG families limited its applications in bioseparation field, the lower LCST of pMEO_2MA (i.e. 28 °C) is precisely the significant advantage for us to take into the protein 'adsorption and desorption' studies with thermoresponsive adsorbents (Duncan, 2003; Han et al., 2003; Lutz and Hoth, 2006).

1.4 Outline of thesis

The main focus of this thesis is on: Preparation and characterisation of various temperature-controlled ionic exchange adsorbents modified with different smart thermoresponsive polymers (i.e. pNIPAAm and PEG), Integration of the optimised self-produced thermoresponsive ionic exchange adsorbents with the novel travelling zone reactor (TCZR) to exploit dynamic protein 'adsorption-desorption' behaviour.

The integrated approach involving NIPAAm grafted thermoresponsive cation exchange adsorbents based on Sepharose CL-6B and TCZR arrangement is discussed in Chapter 2 of this thesis. In Chapter 3, the base matrices of NIPAAm grafted thermoresponsive cation exchange resins are extended to not only Sepharose CL-6B, but also Superose 6 prep grade and Superose 12

prep grade, meanwhile, the continuous TCZR chromatography is discussed besides the batch mode TCZR chromatography in this chapter. In Chapter 4, another more cost-effective and environmentally friendly thermoresponsive polymer–PEG is introduced to substitute NIPAAm for the preparation of a new type of thermoresponsive cation exchange adsorbents. Chapter 5 covers the studies of NIPAAm grafted thermoresponsive anion exchange media based on Sepharose CL-6B and Superose 6 prep grade, and also their application on TCZR. Finally, the main conclusions drawn from this thesis and future work are briefly presented in Chapter 6.

2 Integrated system for temperature-controlled fast protein liquid chromatography. I. Improved thermoresponsive cation exchange adsorbents and a travelling cooling zone reactor arrangement

2.1 Abstract

An integrated approach to temperature-controlled chromatography, involving copolymer modified agarose adsorbents and a novel travelling cooling zone reactor (TCZR) arrangement, is described. Sepharose CL-6B was transformed into a thermoresponsive cation exchange adsorbent (thermoCEX) in four synthetic steps: (i) epichlorohydrin activation; (ii) amine capping; (iii) 4,4'-azobis(4-cyanovaleric acid) immobilisation; and (iv) 'graft from' polymerisation of poly(*N*-isopropylacrylamide-*co*-*N*-tert-butylacrylamide-*co*-acrylic acid-co-*N,N'*-methylenebisacrylamide). FT-IR, ^{1}H NMR, gravimetry and chemical assays allowed precise determination of the adsorbent's copolymer composition and loading, and identified the initial epoxy activation step as a critical determinant of 'on-support' copolymer loading, and in turn, protein binding performance. In batch binding studies with lactoferrin, thermoCEX's binding affinity and maximum adsorption capacity rose smoothly with temperature increase from 20 to 50 °C. In temperature shifting chromatography experiments employing thermoCEX in thermally jacketed columns, 44-51% of the lactoferrin adsorbed at 42 °C could be desorbed under binding conditions by cooling the column to 22 °C, but the elution peaks exhibited strong tailing. To more fully exploit the potential of thermoresponsive

chromatography adsorbents, a new column arrangement, the TCZR, was developed. In TCZR chromatography, a narrow discrete cooling zone (special assembly of copper blocks and Peltier elements) is moved along a bespoke fixed-bed separation column filled with stationary phase. In tests thermoCEX, it was possible to recover 65% of the lactoferrin bound at 35 °C using 8 successive movements of the cooling zone at a velocity of 0.1 mm/s; over half of the recovered protein was eluted in the first peak in more concentrated form than in the feed. Intra-particle diffusion of desorbed protein out of the support pores, and the ratio between the velocities of the cooling zone and mobile phase were identified as the main parameters affecting TCZR performance. In contrast to conventional systems, which rely on cooling the whole column to effect elution and permit only batch-wise operation, TCZR chromatography generates sharp concentrated elution peaks without tailing effects and appears ideally suited for continuous operation.

2.2 Introduction

Bioprocess chromatography suffers from several problems that compromise its sustainability. Current ‘adsorption-desorption’ processes are expensive, suffer from low productivity (given that most involve batch-wise operation in fixed beds), and employ large volumes of buffer for equilibrating, washing, eluting and cleaning of columns, generating as a consequence excessive quantities of waste (Przybycien et al., 2004; Jagschies, 2008; Maharjan et al., 2008). Effective solutions to these significant problems have not yet been forthcoming, but would clearly make for much cleaner, greener, and more

sustainable manufacturing of valuable bio-commodities (Maharjan et al., 2008).

In this context, we introduce an integrated bioseparation concept, which makes use of discrete 'local' changes in temperature to control 'adsorption-desorption' equilibria, and relies on the combined use of chromatographic supports modified with a methylene bisacrylamide (MBAAm) cross-linked temperature-sensitive anionic copolymer, i.e. poly(*N*-isopropylacrylamide-*co*-*N*-*tert*-butylacrylamide-*co*-acrylic acid) (abbreviated to pNIPAAm-*co*-tBAAm-*co*-AAc), and a novel device that permits continuous thermally mediated bioseparation.

Smart temperature-sensitive or thermoresponsive polymers are polymers that exhibit inverse temperature solubility behaviour, i.e. they are water-soluble at low temperature, and insoluble at high temperature above a critical temperature known as the lower critical solution temperature (LCST) (Taylor and Cerankowski, 1975). They have been shown as potentially useful in diverse biomedical and biotechnological applications (Galaev and Mattiasson, 1999; Hoffman and Stayton, 2004; Matsuda et al., 2007; Maharjan et al., 2008). By far the most studied species is pNIPAAm (Heskins and Guillet, 1968; Kubota et al., 1990; Schild, 1992). pNIPAAm undergoes an abrupt reversible 'hydrophilic coil-hydrophobic globule' phase transition in water at an LCST of 32-34 °C (Heskins and Guillet, 1968; Kubota et al., 1990), and

importantly its LCST is relatively insensitive to variation in pH, concentration or chemical environment (Kubota et al., 1990; Schild, 1992).

A significant body of work on the modification of chromatographic packing materials with thermoresponsive polymers (mostly pNIPAAm or pNIPAAm based copolymers) has appeared since the first reports in the early-mid 1990s (Gewehr et al., 1992; Hosoya et al., 1994, 1995). Most of this has concentrated on exploiting the principle of thermally induced extension and collapse of polymer chains for modulating the fractionation range in size exclusion chromatography (Gewehr et al., 1992; Hosoya et al., 1994; Adrados et al., 2001), hydrophobicity in HPLC (Hosoya et al., 1995; Kanazawa et al., 1997; Yakushiji et al., 1999; Teal et al., 2000; Ayano et al., 2006b), and balancing electrostatic and hydrophobic interactions in ion exchange chromatography, through the use of copolymers containing both thermoresponsive and ion exchange components (Kobayashi et al., 2002, 2003; Sakamoto et al., 2004; Ayano et al., 2006a; Kanazawa et al., 2008; Maharjan et al., 2009; Nagase et al., 2010), rather than mitigating ligand masking and 'forced elution' in pseudoaffinity chromatography (Yoshizako et al., 2002; Maharjan et al., 2008). To this day, the vast body of work on thermoresponsive chromatography pertains to the modification and subsequent use of small pored inorganic (glass, silica) or hydrophobic (polystyrene based) chromatography supports in analytical HPLC separations of small biomolecules (especially steroids). By contrast, applications involving soft macroporous supports, appropriate for bioprocess scale separations of large macromolecular targets (globular proteins, nucleic acids, viruses) have

received very little attention thus far. In some respects this is surprising, given that the use of temperature responsive chromatography materials offers cost-effective environmentally friendly solutions to the isolation of commercially valuable biocomponents from biopharma, bioindustry, agricultural, food and other complex process streams (Maharjan et al., 2008, 2009). Though not discussed in the literature, one of the main reasons for this is likely to be difficulties in scaling up thermo-responsive chromatography with such media and column formats, and further, that macromolecules tend to be much more thermally labile than their smaller counterparts. On the latter point, Maharjan and co-workers highlighted the attraction of this type of chromatography for the separation of thermally robust targets, such as lactoferrin (LF) from ultra-high volumes of bovine whey feedstocks. Using methods originally applied to silica matrices, these authors were the first to prepare thermoresponsive cation exchange adsorbents (modified with lightly cross-linked pNIPAAm-*co*-tBAAm-*co*-AAc) from cross-linked beaded agarose supports. In the same report the authors subsequently demonstrated both temperature dependent adsorption of LF and thermally mediated elution of the adsorbed protein in batch and dynamic column experiments; the latter being conducted tempering the whole column in a water bath.

In this study, we extend upon Maharjan and co-workers work by integrating the use of thermoresponsive cation exchangers (hereafter referred to as thermoCEX) with a new column arrangement specifically tailored for thermoresponsive chromatography. Our solution is, rather than subject the whole column to temperature changes in a water bath or via a surrounding

jacket, we subject only a small part of it via a computer controlled motor-driven travelling Peltier block arrangement. In this study involving inverse temperature responsive copolymer modified adsorbents, where elution is observed on cooling, we term the set up a travelling cooling zone reactor (TCZR). Note, in the opposite case, i.e. where the modifying polymer exhibits normal temperature solubility behaviour and/or elution occurs on heating, a travelling heating zone reactor (THZR) would be appropriate.

We first describe the preparation, characterisation and comparison of thermoCEX adsorbents prepared for this study with those reported by Maharjan et al. (2009). Subsequently, we compare their chromatographic behaviour in the TCZR (under batch-wise operation) with that in a jacketed column, and further, identify the main parameters affecting the TCZR's performance, as intra-particle diffusion of desorbed protein out of the pores of the support, and the ratio between the velocities of the cooling zone and mobile phase. Finally, we address the steps that will be required to make preparative TCZR chromatography, and temperature-controlled 'adsorption-desorption' chromatography in general, attractive propositions for the future.

2.3 Experimental

2.3.1 Materials

Bovine whey lactoferrin (MLF-1, Lot. no. 12011506, ~96%) was received as a gift from Milei GmbH (Leutkirch, Germany). Sepharose CL-6B (Cat. no. 170160-01, Lot no. 10040943) was obtained from GE Healthcare Life Sciences (Little Chalfont, Bucks, UK). The chemicals, *N*-isopropylacrylamide (Cat. no. 415324, 97%; NIPAAm), *N*-*tert*-butylacrylamide (Cat. no. 411779, 97%; tBAAm), acrylic acid (Cat. no. 147230, anhydrous, 99%, AAc), 2-ethoxy-1-ethoxycabonyl-1,2-dihydroquinoline (Cat. no. 149837, ≥99%; EEDQ), 4,4'-azobis(4-cyanovaleric acid) (Cat. no. 11590, ≥98%; ACV), *N,N*-dimethylformamide (Cat. no. 270547, >99.9%; DMF), *N,N'*-methylenebisacrylamide (Cat. no. 146072, 99%; MBAAm), epichlorohydrin (Cat. no. E1055, 99%; ECH), tetrahydrofuran (Cat. no. 34865, >99%; THF), diethyl ether (Cat. no. 309966, >99.9%), sodium borohydride (Cat. no. 71321, >99%) and sodium hydroxide (Cat. no. S5881, anhydrous, >98%) were purchased from the Sigma-Aldrich Company Ltd (Poole, Dorset, UK), whereas absolute ethanol (Cat. no. E/0650DF/17, 99.8+%) and ammonia solution (Cat. no. A/3280/PB15, AR grade, 0.88 S.G., 35%) were acquired from Fisher Scientific UK Ltd (Loughborough, Leics, UK), di-sodium hydrogen phosphate (Cat. no. 4984.1, dihydrate, ≥99.5%) was from Carl Roth GmbH+Co.KG (Karlsruhe, Germany), and bottled oxygen-free nitrogen gas was supplied by the British Oxygen Co Ltd (Windlesham, Surrey, UK).

2.3.2 Preparation of thermoresponsive cation exchange (thermoCEX) chromatography adsorbents

The methods used to convert underivatised Sepharose CL-6B supports into thermoresponsive cation exchange matrices (thermoCEX) involve four successive steps – epoxide activation, amine capping, initiator immobilisation and 'graft from' polymerisation. These are detailed below and summarised schematically in Fig. 2.1.

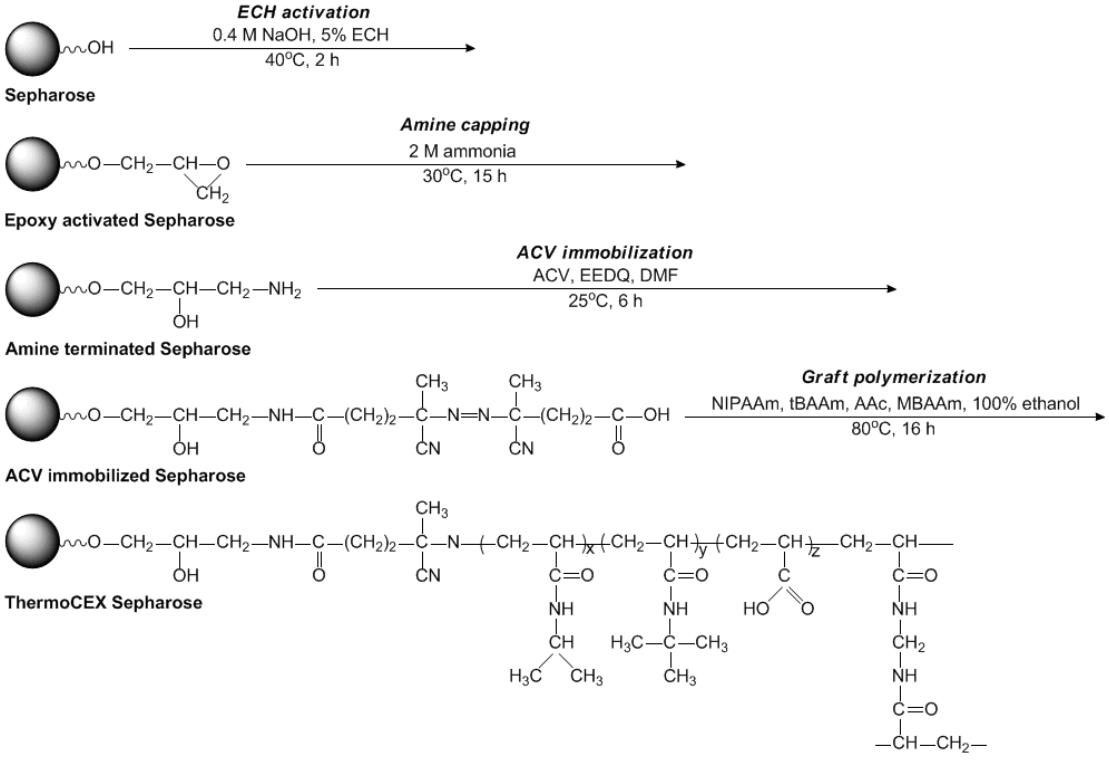

Fig. 2.1 Schematic illustration of steps involved in converting Sepharose CL-6B into thermoCEX adsorbents (see text for details)

2.3.2.1 **Epoxy activation** (Matsumoto et al., 1979)

Washed suction-drained Sepharose CL-6B (50 g, 71 mL) were mixed with 85 mL of water in 250 mL Pyrex® conical flasks and 40 mL of 2 M NaOH before placing in a 40 °C shaking water bath (Julabo SW22, Labortechnik GmbH, Seelbach, Germany) reciprocating at 150 rpm for 0.5 h. Ten millilitres of ECH

(99%) was then added to a final concentration of ~5% (v/v), and reaction was allowed to proceed at 40 °C with shaking for an additional 2 h. The resulting epoxy-activated supports were washed copiously with water under vacuum.

2.3.2.2 Amine capping

After washing, the oxirane groups of epoxy-activated Sepharose CL-6B were reacted and capped with ammonium ions using a procedure adapted from Hermansson et al. (1992). The support (47.5 g, 65 mL) were resuspended as a ~57% (v/v) slurry with 50 mL of 2 M ammonium hydroxide. After incubating overnight (~20 h) at ~30 °C with shaking at 150 rpm, the amine-terminated supports were recovered, washed exhaustively at room temperature with water in a sintered glass filter under vacuum, and then stored in 20% (v/v) ethanol at 4 °C until required.

2.3.2.3 Initiator immobilisation

The radical initiator ACV was coupled to amine-terminated Sepharose CL-6B using a modified version of Maharjan and co-workers' procedure (2009), one adapted from methods originally applied to aminated silica matrices (Kanazawa et al., 1997; Yakushiji et al., 1999; Sakamoto et al., 2004; Ayano et al., 2006a), employing EEDQ as the condensing agent. Amine-terminated supports were washed sequentially with 5 volumes each of 50%, 75% and 100% (v/v) ethanol. For each wash, the supports were mixed 'end-over-end' (0.25 h, RT, 35 rpm) on a Stuart Scientific SB1 tube rotator (Bibby Scientific Ltd, Stone, Staffs, UK), before recovering by vacuum filtration and

resuspending in the next wash solution in the series. Subsequently, the drained supports (45 g, 56 mL) were resuspended with 145 mL of DMF containing 75 mM ACV and 150 mM EEDQ. While housed in a zipper-locked inflatable glove box (AtmosBag, Sigma-Aldrich, UK), nitrogen gas was bubbled through the support slurries, before tightly sealing the reaction flasks with suba-Seal® rubber stoppers (Sigma-Aldrich, UK) and transferring to a shaking (150 rpm) water bath for 6 h of reaction at ~25 °C. The ACV coupled matrices were recovered from reaction solvent by vacuum filtration and then washed by end-over-end mixing (0.33 h, RT) and recovered by vacuum filtration, first with 5 volumes of DMF and subsequently with 5 volumes of absolute ethanol.

2.3.2.4 Graft from polymerisation of poly(NIPAAm-*co*-tBAAm-*co*-AAc-co-MBAAm) on ACV-linked Sepharose CL-6B

The surfaces of ACV-Sepharose CL-6B were grafted with an immobilised lightly cross-linked (i.e. MBAAm as 1% of the total monomers) copolymer network of poly(NIPAAm-*co*-tBAAm-*co*-AAc-*co*-MBAAm) using optimal monomer ratios identified by Maharjan et al. (2009). The method employed in this work was essentially that described by these authors, with minor modifications to pre and post washing regimes and reaction conditions. Suction-dried ACV-linked Sepharose CL-6B (25 g, 35 mL) was sequentially washed with 125 mL aliquots of 20%, 50%, 75% and 100% (v/v) ethanol in cycles of resuspension, ‘end-over-end’ mixing (0.33 h, RT, 20 rpm) and vacuum filtration. Subsequently, the supports were resuspended with 125 mL of ethanol containing the dissolved monomers NIPAAm (900 mM), tBAAm (50

mM) and AAc (50 mM), and the cross-linking monomer MBAAm (10 mM), before transferring to the environment of a glove box and bubbling nitrogen gas through the reaction slurries. After 0.5 h the reaction flasks were tightly stoppered, and placed in a shaking water bath operated at 150 rpm and 80 °C for 16 h. The reaction mixtures were cooled to room temperature and the poly(NIPAAm-*co*-tBAAm-*co*-AAc-*co*-MBAAm) grafted supports were recovered by vacuum filtration, before successively cycling through a descending ethanol concentration wash series (100%, 75%, 50%, 20%, v/v) and then with water. Each cycle involved mixing the support with 5 volumes of the appropriate solvent (0.33 h, RT, 20 rpm), followed by vacuum filtration. After the final wash, the polymer grafted supports were resuspended with 20% (v/v) ethanol and stored at 4 °C until required. The washes were retained for subsequent analysis (see Section 2.3.7).

2.3.3 Batch adsorption experiments

For batch binding tests, pure LF solutions of defined concentrations (c_0 = 1-40 mg/mL) were prepared in 10 mM sodium phosphate pH 6.5. Aliquots (0.9 mL) of these LF solutions were added to 0.1 mL volumes of settled thermoCEX supports before mixing at various temperatures between 20 and 50 °C, for 1 h with shaking (1000 rpm, Thermomixer Comfort shaker, Eppendorf, Hamburg, Germany). After an additional 0.5 h at the selected incubation temperature without shaking, the supernatants were analysed for residual protein content (see Section 2.3.7). The protein bound to the supports was determined from the difference between the protein concentration in the starting binding

solution and the supernatant after binding, and where appropriate the data were fitted to the Langmuir Equation (2.1):

$$q^* = \frac{q_{max} c^*}{K_d + c^*} \qquad \text{Eq 2.1}$$

Where q^* and c^* represent the equilibrium concentrations of adsorbed and liquid-phase protein respectively; q_{max} is the maximum protein binding capacity of the support; and K_d is the dissociation constant. Data were fitted to the model using the x^2 minimisation procedure of SigmaPlot software version 12.5 (Systat Software Inc, CA, USA).

2.3.4 Thermoresponsive CEX chromatography of LF in jacketed columns

Fixed-beds (4.3-4.7 mL) of thermoCEX matrix contained in glass C10/20 columns (internal diameter = 10 mm, length = 20 cm) equipped with JC 10/20 water jackets (GE Healthcare, Uppsala, Sweden) were initially employed for thermoresponsive CEX chromatography of LF. The column was connected to an Äkta Explorer 100 Air chromatography workstation (GE Healthcare, Uppsala, Sweden). The temperature within the column was adjusted via the column's water jacket by continuously circulating water through it from a 42 or 22 °C water bath and also by immersing the mobile phase reservoirs employed within the same water baths. Mobile phase entered the column from the buffer reservoirs via a spirally wound hollow stainless steel tube. Temperature switching was done manually, and experiments were performed in the following way. Columns were: (i) equilibrated with 10 mM sodium

phosphate buffer, pH 6.5 (7.3-10.2 CV) at either 22 or 42 °C, (ii) saturated with LF (supplied as a 14 mg/mL suspension in equilibration buffer; 5.0-8.8 CV) at the same temperature; (iii) washed with equilibration buffer (13.6-15.7 CV) maintained at loading temperature; then (iv) subjected to either single or multiple temperature transitions (without change in the mobile phase composition); before finally (v) eluting residually bound LF at 22 °C using 1 M NaCl in 10 mM sodium phosphate buffer, pH 6.5 (9-13.2 CV). A mobile phase velocity (*u*) of 300 cm/h was employed throughout.

2.3.5 Travelling cooling zone reactor (TCZR)

2.3.5.1 Design of the TCZR

The novel reactor device employed in this study (Fig. 2.2) comprises two main parts, namely (i) a bespoke fixed-bed column filled with a thermoresponsive stationary phase, and fabricated from stainless steel to ensure good heat conductance through the reactor wall; and (ii) a movable assembly of copper blocks and Peltier elements surrounding a small discrete zone of the separation column. The central part of this assembly can be cooled through adjustments to the Peltier elements, and the whole unit can be moved vertically up or down along the separation column, so that adsorbed protein in the cooling zone's region desorbs in response to a localised reduction in the column's temperature and consequent weakening of the bound species affinity for the thermoresponsive chromatography matrix. The temperatures of the column and movable assembly are measured and controlled with Pt 100

thermocouples linked to LabView Software (National Instruments, Austin, TX, USA), and motion of the copper block-Peltier assembly is accomplished via a ball bearing guided linear motorised axis capable of a minimum constant movement of 0.1 mm/s (Festo AG, Munich, Germany) controlled by Festo's dedicated PC based software package (FCT – Festo Configuration Tool). The 'sandwich-like' construction of the travelling cooling zone assembly (depicted in Fig. 2.2b) consisting of three copper blocks and two Peltier elements (Type TB-109-1,4-1,5CH, Kryotherm, St. Petersburg, Russia), generating axial heat transfer from the 18 mm thick central cooling block to 3 mm thick top and bottom copper blocks. The Peltier elements, sandwiched between the top and middle, and middle and bottom copper blocks, are operated by a MTTC-1410 controller (Laird Technologies, Chesterfield, MO, USA). To ensure maximal and homogeneous radial heat transfer, the thickness of the separation column's steel wall is just 1 mm. The inner diameter and length of the separation column are 6 mm and 10 cm, respectively, and the internal volume is 2.83 mL.

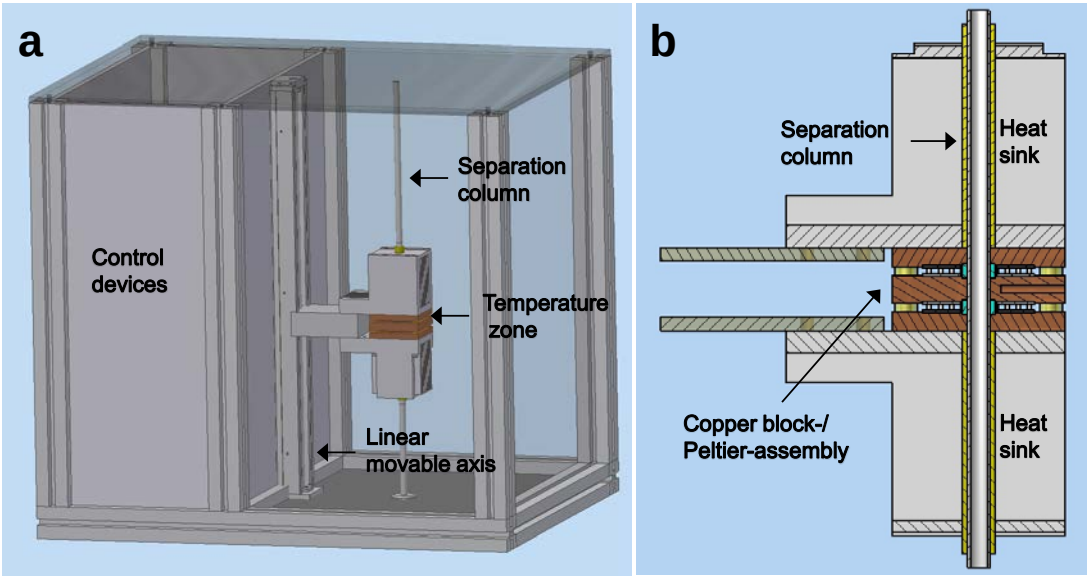

Fig. 2.2 CAD drawings of (a) the TCZR assembly and (b) temperature zone (blown up cross-section). Control devices are integrated in the closed box (a, left) and the separation column is encased within the temperature zone assembly and connected to a linear movable axis (a, right). The stainless steel column is packed with a thermoresponsive chromatography matrix. Mobile phase enters the column at the top and exiting flow is connected directly to an ÄKTA Explorer 100 Air chromatography system (not shown). The separation column is surrounded by (b) an assembly of Peltier elements, copper blocks (a central cooling block flanked on either side by a heating block) and heat sinks at the top and bottom of the whole arrangement. The Peltier elements are sandwiched between the top and middle and middle and bottom copper blocks.

2.3.5.2 Theoretical considerations

Fig. 2.3 depicts theoretical concentration and loading profiles of a single adsorbed protein species, during the course of one complete movement of the travelling cooling zone along the full length of the separation column. For simplicity, a temperature-mediated ‘all or nothing’ affinity of the protein to the thermoresponsive solid phase is assumed, i.e. full binding at the elevated temperature and no binding at the reduced temperature in the cooling zone. During batch-wise operation of the TCZR a defined volume of protein solution is initially fed to the column, whist the TCZR is switched off or parked at a position distant from the matrix filled part of the column. At the elevated

temperature, complete adsorption of the protein adsorbate on the column is assumed. Immediately on completion of protein loading, binding buffer is applied as the mobile phase (Fig. 2.3, left). The middle section of Fig. 2.3 shows the situation after the cooling zone has begun to move. Within the cooling zone, protein desorbs from the matrix into the interstitial liquid phase and is pumped through the column. Should any desorbed protein molecules move beyond the travelling cooling zone's influence, they will, given the elevated column temperature elsewhere, rebind to the matrix. As the cooling zone continues to travel along the column's length, it follows that the protein concentration in the small volume of interstitial mobile phase surrounded by the cooling assembly will increase, and thus a sharp elution peak result is expected (Fig. 2.3, right).

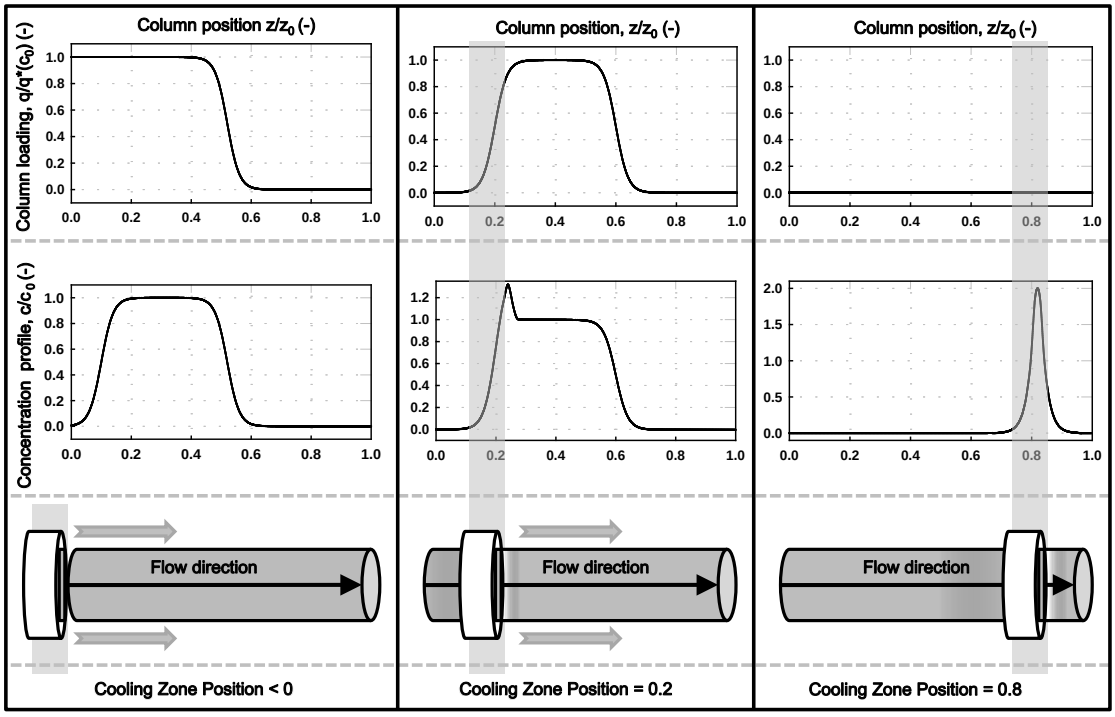

Fig. 2.3 Schematic illustrations of idealised single protein loading (top) and concentration profiles at different stages during batchwise TCZR operation (bottom). The profiles correspond to three discrete z/z_0 positions of the movable cooling zone, i.e. <0, 0.2 and 0.8. The assumptions made are full binding at elevated temperature and no binding at the reduced temperature in the cooling zone.

2.3.6 Thermoresponsive CEX chromatography of LF in the TCZR

The first test conducted with the TCZR described above (Section 2.3.4) was performed using a constant surrounding temperature, Φ_u, of 35 °C, and the lowest possible axial velocity of the cooling zone (v_c) of 0.1 mm/s, which generates a maximum temperature difference of 22.6 °C (i.e. during the cooling zone's progress along the column, parts of the column immediately adjacent to the centre of the cooling assembly were temporarily cooled down to 12.4 °C). The separation column (volume = 2.83 mL) was packed with thermoCEX Sepharose CL-6B matrix (packing factor = 1.2) and u was maintained at 212 cm/h. Using the calculated bed voidage (ε) of 0.31, the interstitial velocity (u_i) at this mobile phase velocity was determined as 682 cm/h. After initial equilibration of the column with 2 CV of 10 mM sodium

phosphate buffer, pH 6.5, 27 CV of a 2 mg/mL suspension of LF (made up in the equilibration buffer) were applied to the column, before washing with a further 5 CV of the same buffer. Thereafter, the cooling zone assembly was moved along the entire column length eight successive times at v_c = 0.1 mm/s, before finally eluting residually bound LF with 5 CV of 10 mM sodium phosphate, PH 6.5, supplemented with 1 M NaCl.

In the second test, the separation column was equilibrated, loaded with LF and washed exactly as described for the first test. Thereafter however, the cooling zone was moved along the whole column six times at different speeds (i.e. at 1.9 mm/s for the first movement, 1.0 mm/s for the second, and at 0.1 mm/s for the remaining movements, 3-6 inclusive), before once again desorbing residually bound LF with a 1 M NaCl step gradient. In these experiments, the different cooling zone velocities employed of 1.9, 1.0 and 0.1 mm/s resulted in maximum temperature difference of ~9, 12.5 and 22.6 °C, respectively.

Fractions generated during the above experiments were subsequently analysed off-line for protein content (see Section 2.3.7).

2.3.7 Analysis

2.3.7.1 Epoxide density measurement

The reactive epoxide group content introduced into Sepharose CL-6B following activation with epichlorohydrin was determined exactly as described by Sundberg and Porath (1974), employing the ring opening reaction of oxiranes with sodium thiosulphate. The epoxy-activated resins (0.5 g, 0.68 mL) was ‘end-over-end’ mixed (1.3 h, RT, 20 rpm) with 1.5 mL of 1.3 M sodium thiosulphate solution of pH 7.0, this reaction results in the release of OH^-, which is followed by titration with 0.1 M HCl. The support’s epoxide density was determined from the amount of HCl required to maintain neutrality.

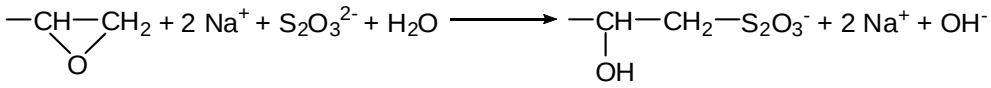

2.3.7.2 FT-IR and ATR-FTIR analysis

FT-IR analysis was employed in two ways, i.e. qualitatively for direct detection of chemical changes introduced into Sepharose CL-6B at various stages during the creation of thermoCEX supports, and quantitatively on liquid samples, in order to determine consumption of ‘NIPAAm + tBAAm’ monomers, and thereby quantify the amount of ‘NIPAAm + tBAAm’ installed on thermoCEX supports. For solid samples, aliquots of aqueous particle suspension were pipetted onto watchglasses and dried in an oven (60 °C, 20h). Small quantities (~3 mg) of dried support samples were then blended with 300 mg of potassium bromide by grinding in agate mortar, until a fine, homogenous powder was produced, before pressing the mixtures into a 13 mm die using a 15 tonne Atlas manual hydraulic press (Model GS15011,

Specac Ltd, Orpington, Kent, UK), producing FT-IR suitable tablets. FT-IR spectra of each tablet were recorded using a Nicolet 380 FT-IR (Nicolet 380, Thermo Fischer Scientific, Waltham, MA, USA) in direct beam mode. Sixty-four scans were averaged to yield spectra at a resolution of 2 cm^{-1}. Attenuated total reflectance FT-IR (ATR FT-IR) was employed for estimation of 'NIPAAm + tBAAm' in liquid samples. Routinely, 150 µl of each solution was applied to the surface of the Smart 53 Orbit diamond accessory of the Nicolet 380 FT-IR, and scanned 64 times at a resolution of 2 cm^{-1} in attenuated total reflection mode. A measurement without any sample in the beam was used as background to keep a relative scale for the adsorption intensity. Background measurements were taken every 0.5 h during sample measurements. NIPAAm, tBAAm and MBAAm give two characteristic peaks in FT-IR, i.e. one at ~1550 cm^{-1} corresponding to N-H bending and another for amide C=O stretching at 1670 cm^{-1}, which is also present in spectra of the AAc monomer. The former N-H bending peak was therefore employed for determination of 'NIPAAm + tBAAm + MBAAm'. The ATR spectrum of standards, i.e. various dilutions of the initial monomer mixtures NIPAAm: tBAAm: AAc: MBAAm (employed in a ratio of 90: 5: 5: 1), were obtained by subtracting the spectrum of pure water from the aqueous solutions spectra. The version 7.3 OMNIC™ DS (Data Security) software (Thermo Fischer Scientific, Waltham, MA, USA), was used as the interface for data collection and processing (interpretations of interferograms and peak area measurements). The area under the N-H bending peak of each spectrum was calculated, keeping the same region and baseline at 1575-1500 cm^{-1} during all the readings, and the combined concentration of 'NIPAAm + tBAAm +

MBAAm' in samples was estimated by reference to standard curves (R^2 > 0.98). The small contribution to this signal from the cross-linking monomer, MBAAm, which accounted for 0.99% of the total monomer concentration and 1.04% of the N-H bending peak amide, was subtracted to give a value for 'NIPAAm + tBAAm'.

2.3.7.3 Gravimetric analysis

Gravimetric analysis was routinely performed on solid supports and on dried residues arising from liquid samples, obtained throughout the different stages of thermoCEX synthesis, and was used to allow determination of support immobilised ACV and copolymer contents, as well as the amount of free copolymer and unreacted monomers in solution at the end of the polymerisation reaction following their separation from one another (detailed below). For solid support measurements, approximately 1 g quantities of suction-drained support samples were accurately weighed in pre-weighed glass crucibles before drying to constant weight in a 60 °C oven (~20 h), cooling to room temperature in a desiccator jar and weighing accurately on an analytical balance. One gram suction-drained gel had a dry weight of 63.2 mg. Post polymer grafting (Section 2.3.2.4), the reaction supernatant and wash solutions were pooled together and evaporated to dryness in a Buchi Rotavapor-RE Rotary Evaporator KRvr-TD-65/45 (Buchi Labortechnik AG, Flawil, Switzerland). The dried residue containing ungrafted free poly(NIPAAm-*co*-tBAAm-*co*-AAc-*co*-MBAAm) and unreacted monomers was resuspended in a small volume of tetrahydrofuran (THF). The free copolymer was then precipitated from solution by the addition of 10 volumes of diethyl

ether. The supernatant fraction containing dissolved monomers was carefully removed, rotary evaporated to dryness, and then redissolved in 100% (v/v) ethanol for ATR FT-IR analysis. The precipitated polymer was subsequently washed with diethyl ether, dried in a 60 °C oven for 20 h and accurately weighed, before finally dissolving in deuterated chloroform ($CDCl_3$) and analysing the relative amounts of NIPAAm and tBAAm from the ^1H NMR spectrum of the polymer in a Bruker AV400 Nuclear Magnetic Resonance (NMR) Spectrometer (Bruker-BioSpin Corporation, Billerica, MA, USA).

2.3.7.4 LCST measurement

The lower critical solution temperature (LCST) of the copolymer was determined in the standard way (Kanazawa et al., 1997; Sakamoto et al., 2004; Ayano et al., 2006a; Maharjan et al., 2009). The copolymer was resuspended at a concentration of 0.5% (w/v) in 10 mM sodium phosphate buffer, pH 6.5, and its optical transmittance at 500 nm was measured at various temperatures in a Cecil CE7500 UV/visible dual beam spectrophotometer (Cecil Instruments Ltd, Cambridge, UK) equipped with a water thermostatted cuvette holder.

2.3.7.5 Ionic capacity analysis

The H^+ exchange capacity of the thermoCEX support was determined by titration according to a procedure supplied by GE Healthcare (method No. 30407; for determination of the ionic capacity of CM Sepharose media).

2.3.7.6 Protein contents determination

Protein contents in samples arising from batch binding and chromatography experiments were determined by UV spectrophotometry at 280 nm in quartz cuvettes in a Lambda 20 UV-vis spectrophotometer (PerkinElmer Analytical Instruments, Shelton, CT, USA) or in a NanoDrop™ 1000 micro-volume UV-vis spectrophotometer (Thermo Fisher Scientific, Wilmington, DE, USA).

2.4 Results and Discussion

In this study, procedures described by Maharjan and co-workers (2009) were improved upon to convert an underivatised beaded cross-linked Sepharose matrix into thermoresponsive cation exchange (thermoCEX) adsorbents featuring surface tethered lightly cross-linked thermoresponsive anionic copolymer chains, and the resulting materials were subsequently employed to demonstrate a new column arrangement (TCZR), specifically designed for thermoresponsive chromatography.

The manufacture of thermoCEX material presented herein differs from that described by Maharjan et al. (2009) in two main respects, i.e. the use of Sepharose CL-6B in place of Sepharose 6 Fast Flow, and more importantly, the markedly different conditions employed for the crucial initial epoxy activation step prior to amine capping and immobilisation of the initiator of polymerisation, ACV (Fig. 2.1). The extent to which these changes impact on

the loading and composition of immobilised poly(NIPAAm-*co*-tBAAm-*co*-AAc-*co*-MBAAm) on the final supports, and the temperature dependent LF binding behaviour, was thoroughly examined, before progressing to dynamic chromatographic experiments with thermally jacketed column and TCZR set ups, primarily, to confirm both the similarity and improvement of the thermoCEX adsorbent detailed herein to that originally described by Maharjan and co-workers (2009), and second, to add further understanding to the concept/mechanisms proposed by the same authors.

2.4.1 Manufacture and characterisation of the thermoCEX adsorbent

For physico-chemical characterisation of support starting material, intermediate supports at every stage of the conversion (Fig. 2.1), pre and post polymerisation reaction supernatants, and the final thermoCEX-CL6B adsorbent itself, we employed a battery of tests (FT-IR, ATR-FTIR, ^{1}NMR, gravimetric measurements and titration based assays for oxirane content and ion exchange capacity). The main findings from these are presented in Fig. 2.4, Fig. 2.5, and Table 2.1, and described in the following text.

FT-IR spectra for dried supports from each stage during fabrication of thermoCEX matrices are shown in Fig. 2.4. All spectra are normalised for peak height at 934 cm^{-1}, as this is characteristic for the 3,6-anhydro moiety of Sepharose (Oza et al., 2010). The spectrum for unmodified Sepharose CL-6B shows peaks corresponding to the functional groups expected of cross-linked agarose, i.e. alkyl CH_2 bending (at 1474, 1419 and 1378 cm^{-1}), alcohol C-O

stretching (1190 and 1159 cm^{-1}) and ether C-O-C stretching (1068 and 1042 cm^{-1}). A pronounced broad peak at 1653 cm^{-1} corresponding to water H-O-H bending is also observed. This peak arises due to the hygroscopic nature of Sepharose, which tends to absorb atmospheric water after being dried.

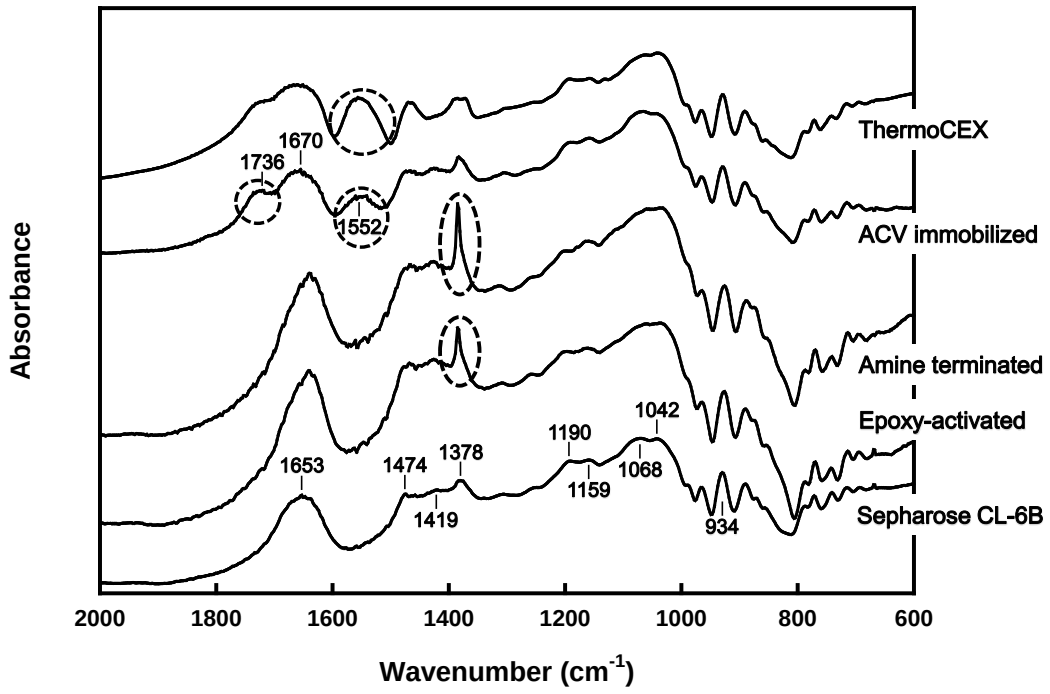

Fig. 2.4 FT-IR spectra recorded at various stages during the conversion of Sepharose CL-6B into thermoCEX adsorbents.

No new peaks were introduced in the Sepharose CL-6B's FT-IR spectrum following activation with epichlorohydrin, but increases in peak heights in the 1474-1378 cm^{-1} region (alkyl, CH2 bend) and areas of peaks at 1068 and 1042 cm^{-1}, were noted. The most striking of these changes, an enhanced peak at 1378 cm^{-1}, is consistent with a rise in alkyl group content arising from additional CH_2 groups of anchored glycidyl functions. Evidence for the introduction of oxirane moieties was tentatively indicated by a less obvious

increase in length of the ‘shoulder’ at 1000-1030 cm^{-1} in the FT-IR spectrum, and was categorically confirmed by independent chemical assay (Table 2.1, 662 µmol/g dried support).

New changes in FT-IR spectrum were not observed following the amine capping of epoxy activated Sepharose CL-6B. Given the relatively low epoxide density, this was not unexpected. Further, the loss of oxirane groups in 1200-1000 cm^{-1} range is likely offset by increases in peak signals corresponding to resulting secondary alcohols (C-O stretch, 1080 cm^{-1}) and amines (C-N stretch, 1200-1025 cm^{-1}). The expected amine N-H bending peak at ca. 1600 cm^{-1} is not clearly seen, and is likely obscured by the broad water peak at 1653 cm^{-1}.

Successful addition of the ACV initiator was confirmed following reaction with ACV, by two striking changes in the FT-IR spectrum, i.e. new peaks at 1736 cm^{-1} (carboxylic acid C=O stretch) and 1552 cm^{-1} (azo N=N stretch and/or amide N-H bend). Some broadening between 1653 cm^{-1} (water H-O-H bending) and 1736 cm^{-1} (carboxylic acid C=O stretch) consistent with the expectation of increased absorbance at ~1670 cm^{-1} corresponding to amide C=O stretching, was also noted. Gravimetric analysis indicated ACV had, following the amine capping step, been coupled to nearly 60% of the initially installed reactive epoxide sites (Table 2.1, 380 µmol/g dried support).

Table 2.1 Comparative chemical characterisation of thermoCEX adsorbents prepared in this study with those reported by Maharjan et al. (2009). See text for details.

Parameter	This work	Maharjan et al. (2009)
Base matrix	Sepharose CL-6B	Sepharose 6 Fast Flow
Immobilised oxirane content (µmol/g dried support)[a]	662	nd
Immobilised ACV content (µmol/g dried support)[b]	380	nd
Immobilised copolymer composition:		
'pNIPAAm + tBAAm' content (µmol/g dried support)[b, c]	4177	2060
pNIPAAm:tBAAm ratio[d]	88:12	92:8
NIPAAm content (µmol/g dried support)	3676	1895
tBAAm content (µmol/g dried support)	501	165
Ion exchange capacity (µmol H^+/g dried support)[e]	469	154
'pNIPAAm + tBAAm + AAc' content (µmol/g dried support)	4646	2204
'NIPAAm:tBAAm:AAc'	79.1:10.8:10.1	85.6:7.4:7.0
% monomer consumed by support:		
NIPAAm + tBAAm + AAc	15.0	6.3
NIPAAm	13.2	6.5
tBAAm	32.5	10.1
AAc	30.4	9.6

Key: Determined by: [a]oxirane ring opening reaction followed by titration (Sundberg and Porath, 1974); [b]gravimetric measurement; [c]ATR-FTIR spectrometry of supernatant samples before and after polymerization reactions, [d]Proton NMR of the ungrafted free copolymer in $CDCl_3$; [e]titration measured at 20 °C.

The spectrum of the thermoCEX activated matrix shows considerable growth of the peak at 1570 cm^{-1} (amide N-H bend), indicating presence of additional amide groups from the grafted copolymer chains (arising from NIPAAm, tBAAm and MBAAm). Peaks at 1736 cm^{-1} (carboxylic acid C=O stretch) and 1670 cm^{-1} (amide C=O stretch) also appear to have grown, indicating that the

amide-containing units from NIPAAM, tBAAm and MBAAm and carboxylic acid-containing units from AAc have both -been successfully grafted in significant amounts.

^{1}H NMR spectra of ungrafted free copolymer in $CDCl_3$ (Fig. 2.5) indicated the successful inclusion of NIPAAm and tBAAm units into the polymer chains. A peak seen at 2.16 ppm corresponds to protons on the carbon α to the carbon of the amide carbonyl group in the NIPAAm and tBAAm monomers, or possibly the carboxylic acid group on AAc. The methyl protons marked ‘A’ and ‘B’ give the characteristic chemical shifts seen at 1.15 and 1.34 ppm, respectively (Spectral Database for Organic Compounds, National Institute of Advanced Industrial Science and Technology, Japan). Comparison of peak heights associated with these ‘A’ and ‘B’ protons (Fig. 2.5) indicated that monomers had been grafted with a NIPAAm to tBAAm ratio of 88: 12 in the ungrafted copolymer. Assuming that the compositions of the free and matrix grafted copolymers are identical, then the ratio of NIPAAm: tBAAm : AAc of the subunits grafted onto the matrix is approximately 79: 11: 10 (Table 2.1). Using the same approach, Maharjan et al. (2009) determined a ‘NIPAAm: tBAAm: AAc’ ratio closer to that of the initial monomer ratio employed in the polymer grafting reaction (i.e. 90: 5: 5) of 86: 7: 7.

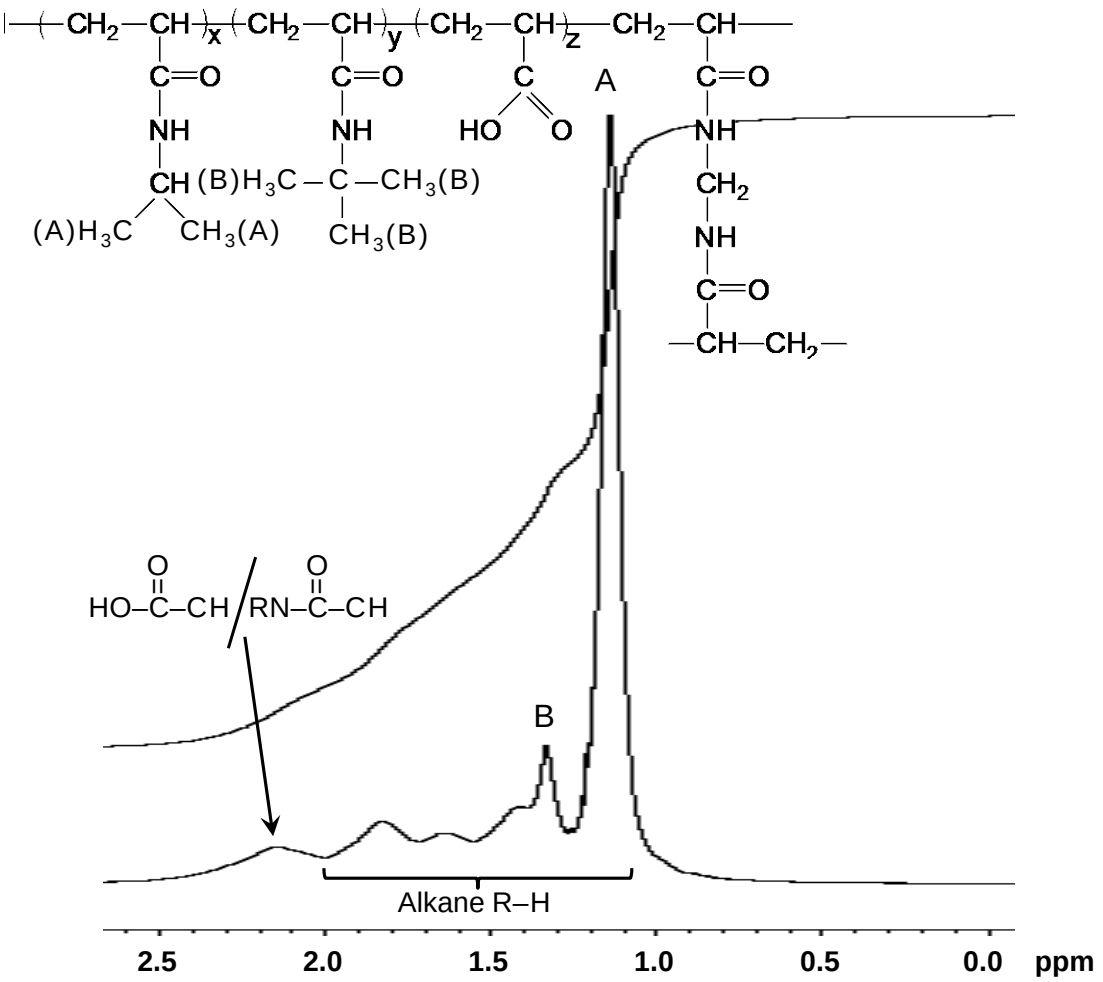

Fig. 2.5 ^{1}H NMR spectrum of free ungrafted copolymer in $CDCl_3$. Peaks corresponding to hydrogen atoms of isopropylacrylamide and *t*-butylacrylamide side chains in the partial structure shown in the upper are indicated by A and B, respectively.

Much higher 'on-support' polymer yields were obtained in the present study cf. Maharjan and co-workers' (2009). Consumption of the individual monomers by the ACV immobilised support was 2- to 3-fold higher (13.2-32.5% cf. 6.5-10.1%; Table 2.1) leading to immobilised NIPAAm, tBAAm and AAc contents of 3676, 501 and 469 µmol/g of thermoCEX support respectively, cf. figures of 1895, 165 and 154 µmol/g reported by Maharjan et al. (2009). The amount of immobilised poly(NIPAAm-*co*-tBAAm-*co*-AAc-*co*-MBAAm) grafted onto ACV

linked Sepharose CL-6B was gravimetrically determined as 67 mg/g suction-drained thermoCEX support, confirming that 12.7% of the total monomers supplied for reaction had been grafted onto the ACV-linked matrix.

The significant differences noted here for copolymer composition and loading (Table 2.1) are unlikely to arise from the use of Sepharose CL-6B in place of Sepharose 6 Fast Flow given the gross similarities shared by these two media, and are instead much more likely to stem from the initial epoxide group density formed in the first step, and its subsequent impact on the immobilised ACV initiator density, and the kinetics and yield of the subsequent polymer grafting reaction.

In our work, we have employed the optimal ECH activation conditions described by Matsumoto and co-workers (1979), i.e. 5% ECH, 0.4 M NaOH, 2 h at 40 °C. The latter introduces high levels of oxirane with minimal cross-linking and is ideally suited for modifying previously cross-linked chromatography media. These conditions routinely yield high and consistent levels of oxirane substitution with various cross-linked Sepharose (650-750 µmol/g dried support) and Superose (850-900 µmol/g dried support) media. In this study, an oxirane density of 662 µmol/g dried matrix was determined using Sepharose CL-6B (Table 2.1). Maharjan et al. (2009) did not report a value for oxirane content of their ECH activated Sepharose 6 Fast Flow support. However, our own measurements performed on ECH activated supports made under the conditions these authors described, yielded a low

oxirane density of 371 µmol/g dried support. The high concentrations of ECH (30%) and alkali (~0.7 M NaOH), coupled with the extended reaction time (21 h) employed by Maharjan et al. (2009), are documented to result in extensive cross-linking of the support and increased hydrolysis of introduced oxirane functions to yield glycerol groups (Porath and Fornstedt, 1970; Porath et al., 1971; L and J.Sundberg, 1972; Lowe and Dean, 1974; Matsumoto et al., 1979).

In view of the similarity of conditions employed for the subsequent amine capping and ACV activation steps prior to graft polymerisation in this and Maharjan and co-workers' study (2009), the likely impact of doubling the initial oxirane content (in this work) is a similar fold increase in the immobilised ACV content. This increased availability of initiator sites can be expected to allow for the generation of a larger number of grafted polymer chains, making a significant contribution to the higher yield seen for our grafting reactions cf. those described by Maharjan et al. (2009).

The polymerisation rate during free radical polymerisation is typically dependent on the square root of the initiator concentration (Eastmond et al., 1976; Odian, 2004), while increased concentrations of initiator have been consistently shown to increase polymerisation yields (Weerts et al., 1989; Jain et al., 2003). The effect of initiator concentration on yield is expected to be particularly pronounced for surface initiated polymerisations which achieve relatively low yields, as in this instance, the rate-slowing effects of polymer

chain viscosity and low monomer concentration do not result in faster, higher initiator concentration polymerisations being ‘pull back’ relative to their lower initiator concentration analogues as they near the end of their polymerisation process.

Grafting of polymer chains on the matrices was accompanied by the generation of significant amounts of free polymer in the supernatant (gravimetrically determined as 27.1% of the total monomers supplied). The presence of this free polymer can be accounted for by two factors in particular: (i) splitting of azo initiator into one immobilised radical and one free radical during initiation (see Fig. 2.1), allowing initiation to occur from molecules free in solution as well as those on the matrix surface; and (ii) radical chain transfer from immobilised polymer chain to free monomer, allowing further initiation from molecules which are free in solution. As the degree to which these two mechanisms occur depends upon the concentration of azo initiators and immobilised radical chains, it can be expected that the approximate 1: 2 ratio of immobilised to free polymer seen for our work (i.e. 1:2) will be similar in Maharjan and co-workers’ study (2009), although the total amount of polymer generated per g of matrix is more than 2-fold higher in our work (i.e. 4646: 2204).

The LCST of the pNIPAAm homopolymer is widely reported as ca. 32 °C (Heskins and Guillet, 1968; Kubota et al., 1990), but can be variably tuned to occur at lower or higher temperatures simply by incorporating various

quantities of hydrophobic or hydrophilic monomers in the pre-polymerisation mix (Hoffman et al., 2000; Maharjan et al., 2008; Yoshimatsu et al., 2012). For example, copolymerisation of NIPAAm with the more hydrophobic tBAAm monomer results in a reduction in LCST (Hoffman et al., 2000; Yoshimatsu et al., 2012), whilst conversely, integrating more hydrophilic monomers has the opposite effect of increasing the LCST (Hoffman et al., 2000). The production of thermoresponsive copolymers possessing ion exchange functionality, while retaining pNIPAAm's LCST can be achieved by balancing the incorporation of charged monomers with ones more hydrophobic than NIPAAm (Kobayashi et al., 2002, 2003; Sakamoto et al., 2004; Ayano et al., 2006a; Maharjan et al., 2009). Fig. 2.6 compares the temperature dependent 'hydrophilic coil-hydrophobic globule' transition of the ungrafted free poly(NIPAAm-*co*-tBAAm-*co*-AAc-*co*-MBAAm) prepared in this work with that produced by Maharjan et al. (2009). Both NIPAAm copolymers exhibit the characteristic sharp decrease in optical transmittance across a relatively narrow temperature range that is expected of polymers exhibiting inverse temperature solubility behaviour, although, the temperature range over which the full phase transition occurs is considerably wider for the copolymer in this work (30-41 °C cf. 28-34 °C, Fig. 2.6); a finding entirely in keeping with the copolymer's lower NIPAAm content (79.1% cf. 85.6%). Despite the differences in NIPAAm content and monomer composition, the temperature at which 50% optical transmittance occurs, i.e. the LCST (Kanazawa et al., 1997; Ayano et al., 2006a; Maharjan et al., 2009), differs by only 2 °C, i.e. 32 °C for the '79.1: 10.8: 10.1' copolymer in this work cf. 30 °C for Maharjan and co-workers' '85.6: 7.4: 7.0' copolymer (2009).

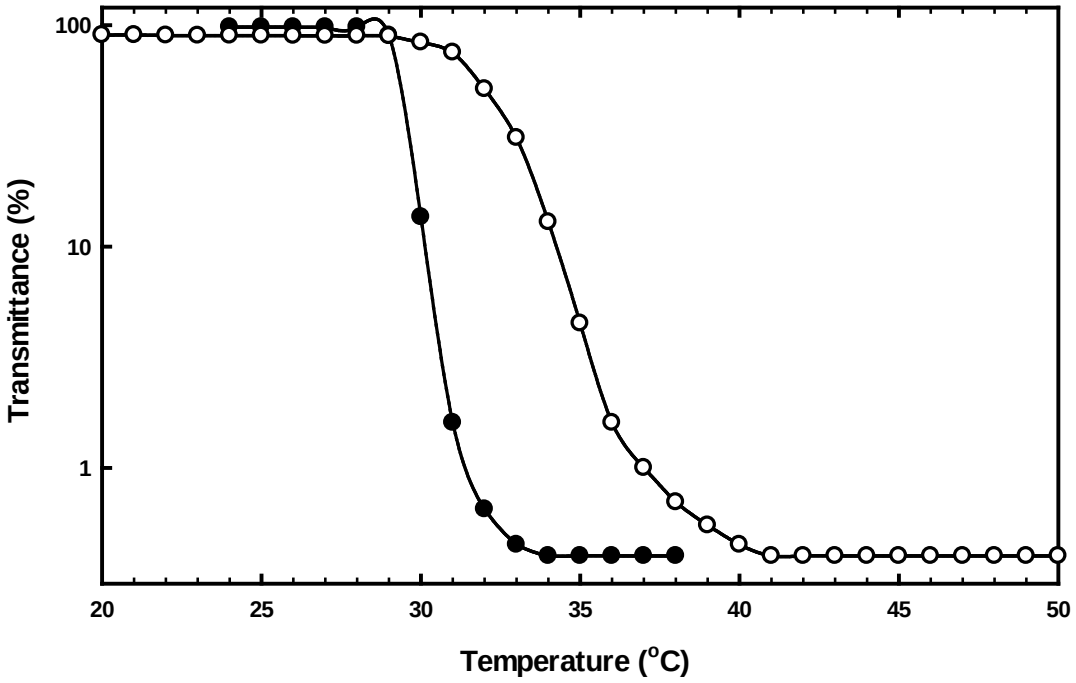

Fig. 2.6 Comparison of temperature-dependent optical transmittance (500 nm) profiles of 0.5% (w/v) solutions of ungrafted free poly(NIPAAm-*co*-tBAAm-*co*-AAc-*co*-MBAAm) prepared in this work (circles, white filled) with that from Maharjan et al.'s (2009) study (circles, black filled).

2.4.2 Temperature dependent batch adsorption of LF on thermoCEX adsorbents

Fig. 2.7a compares the effect of temperature on the adsorption of LF to the thermoCEX adsorbents prepared in this study with Maharjan and co-workers' analogous data (2009) obtained for their adsorbent material. In both cases, and in stark contrast to the solution temperature mediated phase transition behavior exhibited by both free copolymers in Fig. 2.6, incremental increase in temperature from 20 to 50 °C were met with gradual increases in LF binding capacity. In keeping with Maharjan et al.'s hypothesis (2009), at the lowest temperature of 20 °C the copolymer is expected to be fully extended and hydrophilic, and the spacing between neighbouring carboxylic acid moieties in

the immobilised copolymer network is envisaged to be high. Not surprisingly, LF binding capacity is at its lowest value for both thermoCEX supports at this temperature (12 mg/mL – this work; 13 mg/mL – Maharjan et al. (2009)). However, as the temperature is gradually raised from this point, the immobilised copolymer starts to collapse, becoming increasingly hydrophobic and flattening against the surface of the base matrix. In so doing, previously buried negative charges become increasingly exposed and their density per unit surface rises as the distance between them drops. The net effect of these changes in surface hydrophobicity and charge density on the binding of LF, is increased tightness of binding strength and capacity for both thermoCEX adsorbents (Fig. 2.7 a and b and Table 2.1). It is clear however, that the effect of temperature on LF capacity increase is more pronounced for thermoCEX adsorbent made in this work. For this adsorbent, the capacity rises nearly 5-fold from 12 mg/mL at 20 °C to 58 mg/mL at 50 °C, cf. 3.4-fold (13 mg/mL at 20 °C to 44 mg/mL at 50 °C) for Maharjan et al.'s material (2009). Fig. 2.7b shows adsorption isotherms obtained for LF binding to the thermoCEX adsorbents prepared in this work in a 10 mM sodium phosphate buffer, pH 6.5, at temperature of 20, 35 and 50 °C, and Table 2.2 summarises the Langmuir binding parameters fitted to the data sets. At 20 °C LF binding is weak (K_d = 1.66 mg/mL) and of low capacity, (q_{max} = 21.9 mg/mL), but as the temperature is raised, both binding strength and capacity rise significantly; paired values of q_{max} and K_d respectively reaching ~40 mg/mL and 0.83 mg/mL at 35 °C, and ~56 mg/mL and < 0.1 mg/mL at 50 °C. Very similar behavior was noted by Maharjan et al. (2009). However, while binding performance was almost identical at 20 °C (q_{max} = 24 mg/mL, K_d = 1.86 mg/mL; initial slope = 12.9

mL/mL) to that observed herein (Table 2.2), at 50 °C the magnitude of the initial slopes of the isotherms (610 cf. 121 mL/mL) indicates that the thermoCEX adsorbent in this study binds LF > 5 times more tightly than Maharjan and co-workers' material (2009). The much higher copolymer content, increased hydrophobicity and > 3-fold higher charge density on this adsorbent (Table 2.1) are obvious reasons for the observed improvement in LF binding at higher temperatures.

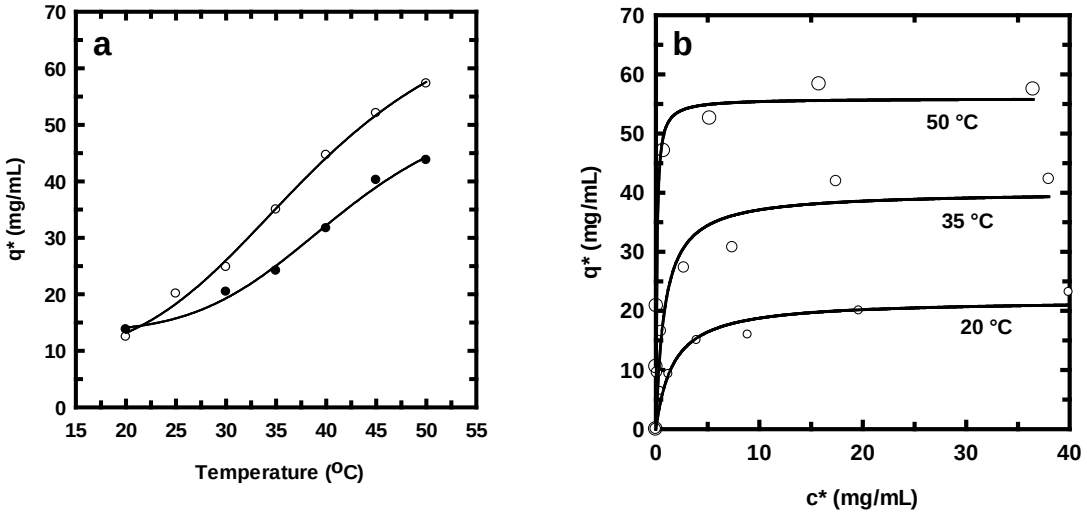

Fig. 2.7 Effect of temperature on the binding of LF on thermoCEX Sepharose CL-6B: (a) illustrates a comparison of the effect of temperature variation on LF adsorption capacity of the thermoCEX material employed in this work with a starting concentration of c_0 = 10 mg/mL (circles, white filled) with that reported in Maharjan and coworkers' (2009) study (c_0 = 5 mg/mL; circles, black filled); and (b) shows equilibrium binding isotherms at 20 °C, 35 °C and 50°C. The solid lines through the data points in (b) represent fitted Langmuir curves with parameters values presented in Table 2.2.

The marked difference in temperature dependent behavior noted above for phase change of the free copolymer and LF binding of the immobilised copolymer, deserves comment. The chain collapse of pNIPAAm based polymers tethered to a surface is generally regarded as very different and

more complex to that in free solution and is influenced by grafting density, architecture and molecular weight of the tethered polymer chains, and overall graft thickness (Zhang and Pelton, 1999; Yim et al., 2003; Mendez et al., 2005; Andersson et al., 2006; Plunkett et al., 2006). The reduced freedom of movement of surface tethered polymer segments within the cross-linked copolymer network results in less abrupt collapse than in free solution (Andersson et al., 2006). At temperatures above LCST, chain collapse occurs less readily for our copolymer in free solution cf. Maharjan and co-workers' (see Fig. 2.6). This apparent disadvantage however, appears to be substantially outweighed in tethered form (Fig. 2.7a), and is most likely due to a combination of higher grafting density, and greater mass/thickness of the attached copolymer graft (Table 2.1). The magnitude of pNIPAAm chain collapse above the LCST is reported to decrease with decreasing grafting density and polymer molecular weight (Plunkett et al., 2006). Further, at low surface coverage thermoresponsive polymer networks are considered to be relatively immobile and confined close to the surface to which they are anchored, but with increasing coverage, the mobility of polymer segments, especially in the outermost regions of the polymer graft, increases (Andersson et al., 2006).

Table 2.2 Langmuir parameters[a] describing the adsorption of LF to thermoCEX Sepharose CL-6B based at 20, 35 and 50 °C.

Temperature (°C)	q_{max} (mg/mL)	K_d (mg/mL)	Initial slope, q_{max}/K_d (mL/mL)
20	21.9 ± 1.4	1.66 ± 0.48	13.2
35	40.2 ± 2.9	0.83 ± 0.34	48.4
50	55.9 ± 2.4	0.09 ± 0.03	621.1

[a] Fig. 2.7b adsorption data were fitted to the Langmuir model.

2.4.3 Chromatography of LF in jacketed columns containing thermoCEX matrix

The temperature-dependent protein sorption behaviour of thermoresponsive ion exchange adsorbents described in this and other work (Kobayashi et al., 2002, 2003; Sakamoto et al., 2004; Ayano et al., 2006a; Kanazawa et al., 2008; Maharjan et al., 2009; Nagase et al., 2010, 2011) makes them attractive prospects for regenerate-free isocratic liquid chromatography, potentially providing viable solutions to issues such as sub-optimal elution/cleaning performance and excessive buffer consumption/waste generation. However, with very few exceptions (Yagi et al., 2008), all reported investigations on thermoresponsive liquid chromatography use conventional fixed-bed columns filled with thermoresponsive adsorbents, and the whole column is tempered by a water bath, a water jacket connected to a water bath, or a column oven (Kanazawa et al., 1997; Teal et al., 2000; Kobayashi et al., 2002; Yoshizako et al., 2002; Ayano et al., 2006b; Maharjan et al., 2009). Typically, protein adsorption takes place at elevated column temperatures, and protein desorption is forced by cooling down the whole column. Using this approach, in combination with thermoresponsive cation exchange supports of similar construction to those employed in this work (i.e. cross-linked beaded 6% agarose matrix grafted with poly(NIPAAm-*co*-tBAAm-*co*-AAc-*co*-MBAAm); Table 2.1), Maharjan and co-workers (2009) reported that: (i) the column's dynamic binding capacity for LF rose from 8 mg/mL at 20 °C to 27 mg/mL at 50 °C (u was not defined); and (ii) following loading at 50 °C, 47% of the adsorbed LF could be recovered simply by lowering the column temperature shift to 20 °C.

Similar results were obtained in this study using packed columns of the higher capacity thermoCEX matrix (Fig. 2.8). A narrower operating temperature range of 42-22 °C (corresponding to 10 °C either side of the free copolymer's LCST; Fig. 2.7a), and mobile phase velocity of 300 cm/h were employed; under these conditions, total dynamic binding capacities of 7.2 and 35.4 mg/mL were determined at the lower and higher temperatures, respectively. In Fig. 2.8a the column was saturated with LF at the lower temperature. A transient increase in column temperature to 42 °C towards the end of washing phase failed to enhance or reduce LF desorption cf. operation at 22 °C, and all of the adsorbed LF was recovered in the subsequent 1 M NaCl elution step. In stark contrast, following LF loading and washing at 42 °C a single cooling transition under binding conditions desorbed 44% of the bound LF (Fig. 2.8b) and multiple transitions (Fig. 2.8c) raised this slightly to 51%. In both of these cases following thermal cycling, most of the residually bound LF was effectively desorbed in the final 1 M NaCl elution step (mass balances closing to 94% and 101%, respectively for Fig. 2.8b and c, respectively). From Fig. 2.8c it is striking to note that LF was only desorbed by cooling (5 steps in all) and further that all four 'hot' transitions promoted a tightening of LF adsorption, in keeping with earlier observations (Fig. 2.7b and Table 2.2).

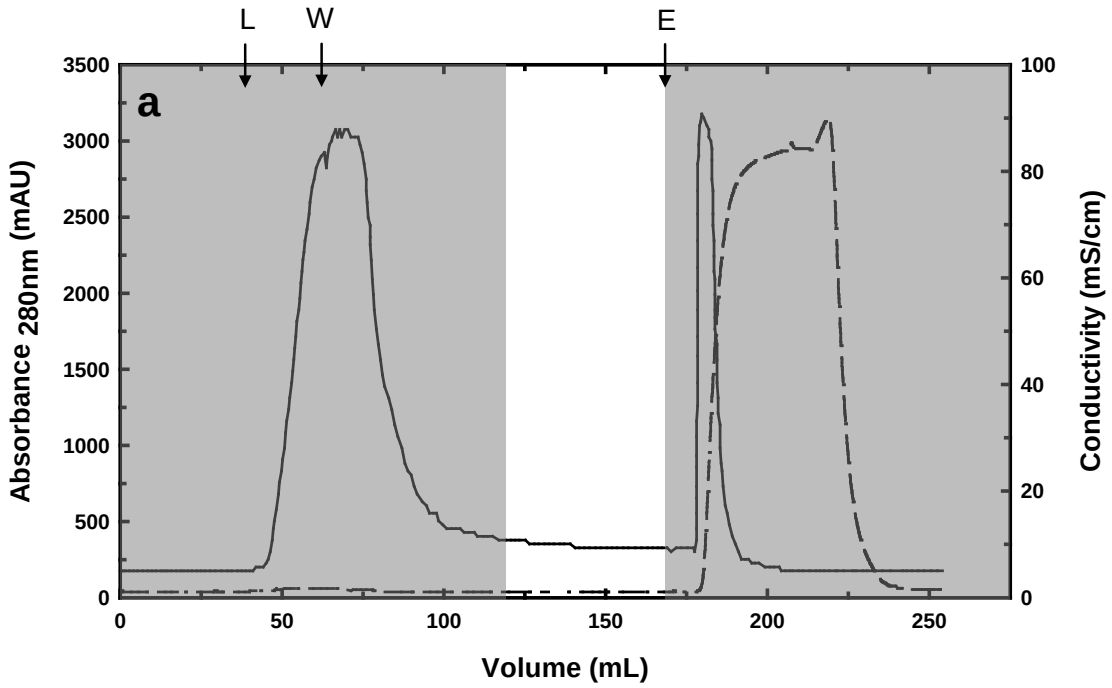
L
W
E
a
Absorbance 280nm (mAU)
Conductivity (mS/cm)
Volume (mL)
0
500
1000
1500
2000
2500
3000
3500
0
20
40
60
80
100
0
50
100
150
200
250

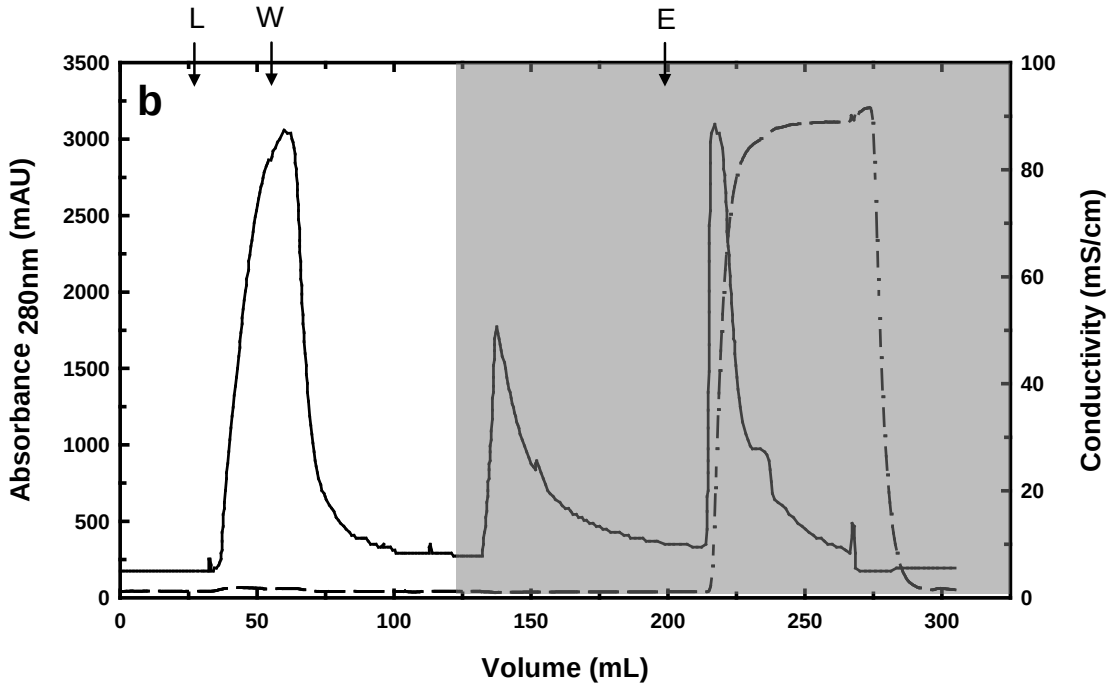
L
W
E
b
Absorbance 280nm (mAU)
Conductivity (mS/cm)
Volume (mL)
0
500
1000
1500
2000
2500
3000
3500
0
20
40
60
80
100
0
50
100
150
200
250
300

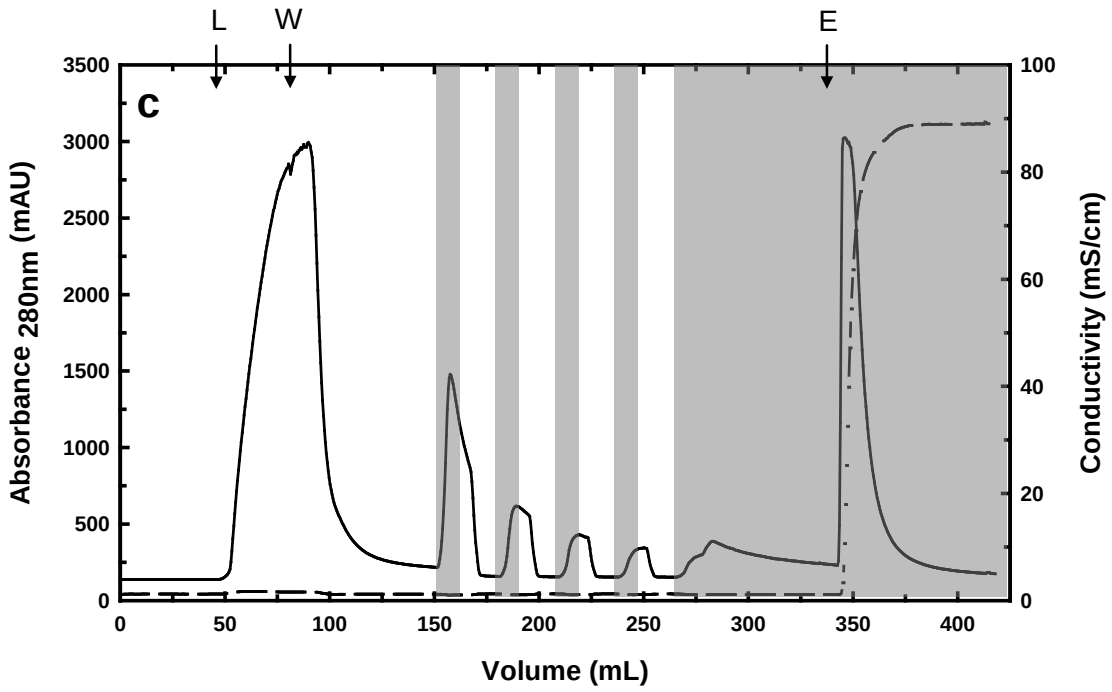

Fig. 2.8 Chromatograms arising from three separate experiments (a-c) conducted with LF and jacketed chromatography columns containing thermoCEX matrix. Columns were saturated with LF at either 42 °C (b and c) or 22 °C (a), and washed at the binding temperature, prior to changing the column and mobile phase temperature once (a and b) or multiple cooling-heating transitions (c). Residual bound LF was subsequently eluted at 22 °C using a 1 M NaCl step gradient. The arrows indicate onset of the loading (L), washing (W) and NaCl mediated elution (E), and the unshaded and shaded grey areas indicate operating temperature of 42 °C and 22 °C, respectively. The solid and dashed lines represent the absorbance and conductivity signals, respectively.

2.4.4 TCZR chromatography of LF

One significant drawback of tempering the entire column is the strong tailing of elution peaks observed (Fig. 2.8b and c), a consequence of the 'weak' conditions typical of isocratic elution. Another disadvantage is that tempering the whole column renders continuous operation impossible, i.e. it permits only batch-wise operation. The TCZR concept proposed earlier (Section 2.3.5 and Fig. 2.3), in which only a small part of the column is cooled via a computer

controlled motor-driven travelling Peltier block arrangement (Fig. 2.2), affords a means of overcoming both of the above issues.

Fig. 2.9 presents the chromatogram arising from the first test of the TCZR system employing thermoCEX adsorbents and LF as the model binding species. With the column held at a temperature of 35 °C, LF was supplied until near saturation of the thermoCEX matrix had been achieved. Following washing with loading buffer, the amount of protein still bound to the support was estimated to be 101.7 mg (equivalent to 27.6 mg/mL). Eight successive temperature-mediated elution steps were then conducted by driving the cooling assembly at its lowest possible axial velocity, v_c, of 0.1 mm/s (corresponding to ~5% of u_i). Nearly 58.9% (59.9 mg) of the previously adsorbed LF was eluted from the column (Table 2.3), and the residually bound LF was subsequently desorbed at 35 °C using equilibration buffer supplemented 1 M NaCl. Striking features of the chromatogram, caused by accumulation of desorbed LF in the narrow travelling cooling zone, are the sharp elution peaks without any peak tailing. The first peak's LF concentration was actually higher than that of the feed. This peak alone accounted for 54.4% of total LF eluted via temperature-mediated elution (i.e. all 8 peaks combined; Table 2.3). Even so, protein was still being eluted in all subsequent cycles (even in the 8th); most likely because of the thermoCEX Sepharose CL-6B matrix's slow intra-particle pore diffusion kinetics. By moving the cooling zone along the separation column, proteins are desorbed with the region of reduced temperature because of the reduced binding affinity under these conditions (Table 2.2). Given that the fluid phase in the resin pores is stagnant

(Tallarek et al., 1999), desorbed proteins must diffuse out of the pores in order to enter the interstitial liquid to be transported by convection towards the column outlet. This step, often identified as the major factor contributing to peak dispersion in liquid chromatography (Tallarek et al., 1999), would also appear to represent a problem for the TCZR chromatography approach. If the time for the diffusion of a previously adsorbed protein out of the pores is longer than that of the moving cooling zone's contact with a given part of the stationary phase, then protein still remaining within the pores in this region will rebind to the support once the cooling zone has passed by and the temperature rises back towards its initial value (i.e. prior to its encounter with the travelling cooling zone; 35 °C in this case). It follows that protein species with longer diffusion paths can eventually be eluted, if multiple movements of the cooling zone are employed.

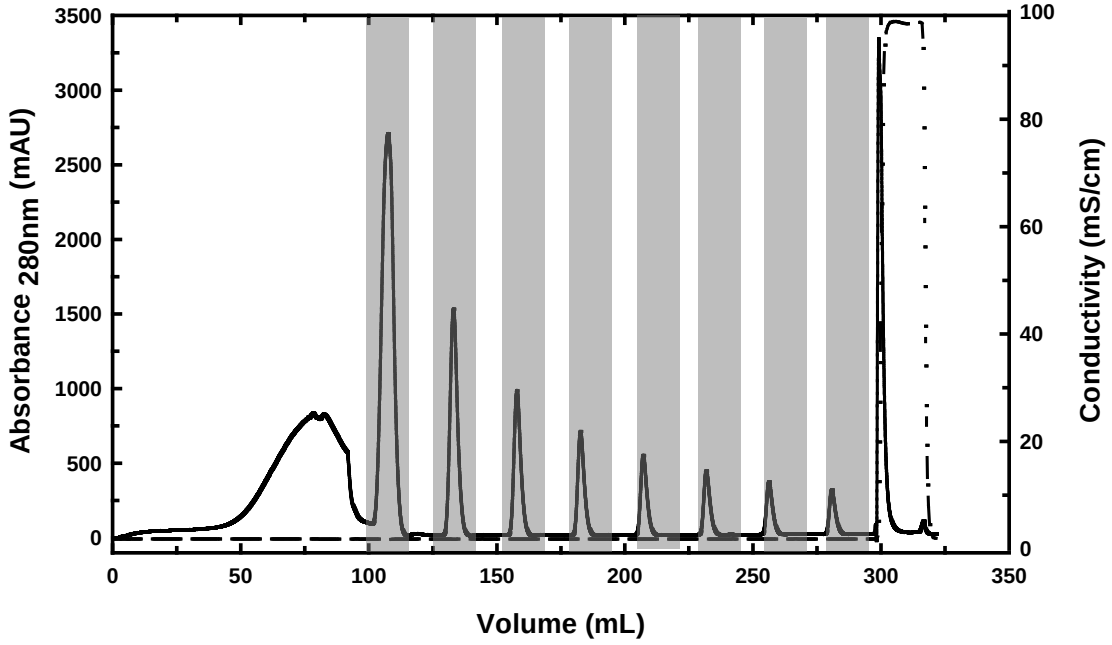

Fig. 2.9 Chromatogram arising from a TCZR test employing eight movements of the cooling zone at a velocity, v_c, of 0.1 mm/s. The unshaded areas indicate column operating temperature of 35 °C, the shaded grey zones indicate movement of the cooling zone. The solid and dashed lines represent the absorbance and conductivity signals, respectively.

The main focus of the second TCZR test (Fig. 2.10) was to examine the impact of varying the ratio of the velocities of the elution front and the cooling zone on chromatographic performance. For this, using identical LF loading, mobile phase velocity and column temperatures to those employed in the first test (Fig. 2.9), the cooling zone was moved along the whole column a total of six times at different speeds. For the first and second movements of the cooling zone, v_c was set at values corresponding to 100% (1.9 mm/s) and ca. 50% (1.0 mm/s) of u_i, and the remaining four movements were conducted at v_c = 0.1 mm/s, i.e. the same as that employed in the first test. It is clear that the 'v_c = 0.1 mm/s' elution incidents in the second test closely resemble those

in the first (compare Fig. 2.9 and Fig. 2.10). For this reason, only the first three movements are considered in the discussion of the influence of v_c on system performance. Clearly, the amount of protein eluted by a single movement of cooling zone increases strongly with decreasing v_c. For example, less than 0.1 mg of LF was eluted from the column at v_c = 1.9 mm/s, increasing to ~3.3 mg at v_c = 1 mm/s, and reaching 29.3 mg at v_c = 0.1 mm/s (Table 2.3). These dramatic differences cannot be attributed to slow pore diffusion alone. A second explanation can be found based on the impact of cooling zone velocity on the minimum temperatures attained within the discrete regions of the column it contacts. At v_c = 1 mm/s the temperature in the cooling zone is ca. 10.1 °C higher than that at v_c = 0.1 mm/s, and thus the eluting power of the cooling zone is considerably reduced.

The main reason, however, for the low performance of the TCZR at the higher cooling zone velocities is likely to be found in the ratio between the v_c and u_i. Examination of the isotherm data (Fig. 2.7 and Table 2.2) confirms that, despite much reduced LF binding affinity at lower temperatures, binding is not completely eradicated. Thus, the velocity of the travelling isocratic elution front is significantly smaller than that of the mobile phase.

In cases where v_c equals u_i or 0.5 u_i, the cooling zone will move faster than the elution front, and thus the elution peak slips back into a region of elevated temperature, and so the protein rebinds.

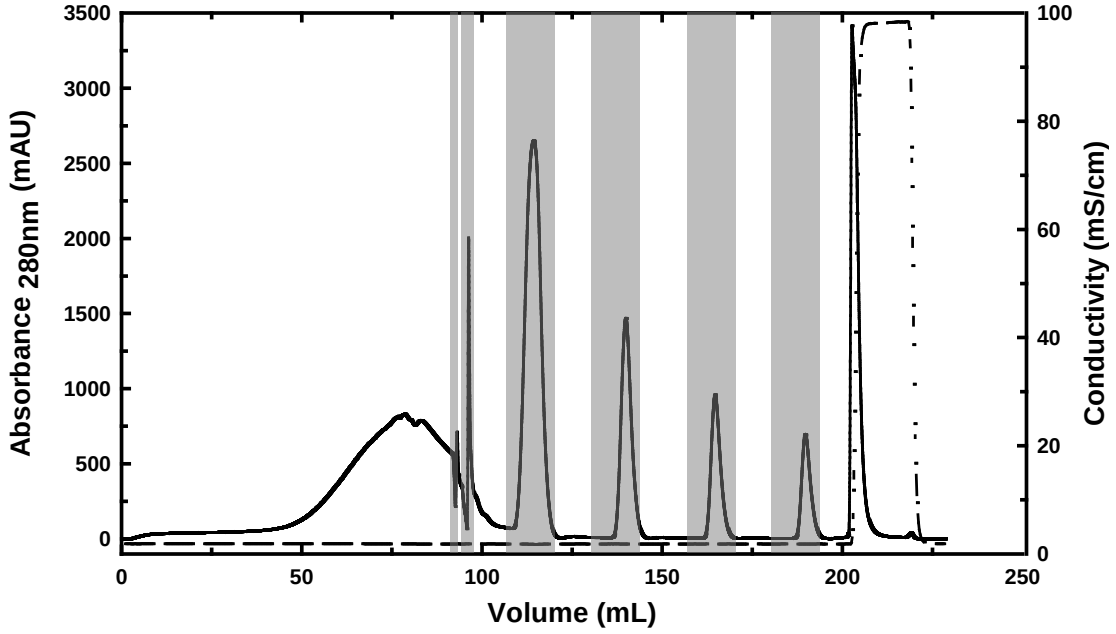

Fig. 2.10 Chromatogram arising from a TCZR test employing six movements of the cooling zone at different velocities, i.e. 1.9 mm/s for the first, 1mm/s for the second and 0.1 mm/s for the subsequent movements. The unshaded areas indicate column operating temperature of 35 °C, the shaded grey zones indicate movement of the cooling zone. The solid and dashed lines represent the absorbance and conductivity signals, respectively.

Table 2.3 LF recoveries from packed beds of thermoCEX adsorbent during multi-cycle TCZR controlled chromatography (see Fig. 2.9 and Fig. 2.10 and text for details). At u = 212 cm/h, u_i was calculated as 682 cm/h (1.89 mm/s).

TCZR test (Figure 2.7)	Temperature mediated elution at v_c = 0.1 mm/s (5% of u_i)									Post elution with	Mass
Step:	1	2	3	4	5	6	7	8	1-8 combined	1 M NaCl @ 35 ^{o}C	balance (%)
LF recovered[a] (%)	32	9.8	5.5	3.7	2.8	2	1.6	1.5	58.9	32.2	91.1

TCZR test (Figure 2.8)	Temperature mediated elution (varying v_c)							Post elution with	Mass
Step:	1	2	3	4	5	6	1-6 combined	1 M NaCl @ 35 ^{o}C	balance (%)
v_c (mm/s):	1.9	1.0	0.1	0.1	0.1	0.1			
v_c as % of u_i	100	53	5.3	5.3	5.3	5.3			
LF recovered[a] (%)	0.1	3	27	8.8	5	3.3	47.2	38	85.2

2.5 Conclusions

An integrated approach to temperature-controlled chromatography, comprising copolymer modified beaded agarose adsorbents and a novel travelling cooling zone reactor (TCZR) arrangement, is described in this study. Published procedures for transforming underivatised cross-linked Sepharose matrices into thermoresponsive cation exchange (thermoCEX) adsorbents, featuring surface tethered lightly cross-linked thermoresponsive anionic copolymer chains (Maharjan et al., 2009), were substantially improved upon. The resulting adsorbent materials displayed superior temperature regulated LF binding performance, i.e. identical low affinity binding at 20 °C, but much higher affinity at higher temperature, which conferred dual operational advantages during temperature-controlled chromatography, namely the use of a reduced temperature for LF adsorption (42 cf. 50 °C), whist still retaining a capacity advantage of > 30% (35.4 mg/mL at 42 °C cf. 27 mg/mL at 50 °C). ThermoCEX adsorbents were subsequently employed to demonstrate the new TCZR arrangement, one specifically designed for temperature-controlled chromatography. As the cooling zone travelled along the column, LF, previously adsorbed on the stationary phase at 35 °C, was desorbed in the form of sharp, concentrated peaks. Intra-particle diffusion of desorbed protein out of the pores of the support and the ratio between the velocities of the cooling zone and mobile phase were identified as the main parameters affecting the TCZR's performance. The use of thermoresponsive adsorbents with smaller particle diameters (*in nuce* shorter diffusion paths) or, better still, appropriately functionalised monolithic chromatography media (not subject to diffusion-controlled mass transfer) are possible routes to better TCZR system

performance. The adaptation of the TCZR system for continuous liquid chromatography is also envisaged to bring added benefits, as in this instance protein loading and elution would occur concurrently within different regions of the TCZR.

Despite the significant improvements in thermoresponsive anionic copolymer loading and operational performance noted here, further advances in support functionalisation are required, principally to: (i) raise protein binding capacity (the H^+ exchange and LF binding capacities of the thermoCEX matrix in this work were less than half those of CM Sepharose Fast Flow); (ii) improve desorption efficiency; and (iii) lower the operating temperature range. The current design, combining thermoresponsive and charged monomers within the same polymeric chains or network, is unlikely to deliver temperature-sensitive ion exchange adsorbents possessing charge densities and protein binding capacities similar to those commercial ion exchangers, whilst simultaneously retaining desirable thermoresponsive properties. Uncoupling ‘thermoresponsiveness’ from ‘charge’ may be the solution, and could conceivably be achieved by grafting thermoresponsive chains directly into the surfaces of commercial high capacity ion exchangers. Finally, in order to extend the applicability of temperature-controlled chromatography to the separation of proteins less thermally stable than LF, temperature transitions should ideally take place at lower temperatures using appropriately functionalised media. With surface grafted polymers based on NIPAAm, this can be achieved by increasing the content of hydrophobic monomers such as tBAAm (Hoffman et al., 2000; Maharjan et al., 2008; Yoshimatsu et al., 2012).

Alternatively, newer non-NIPAAm PEG based versions with even better properties (Lutz and Hoth, 2006; Lutz et al., 2006; Magnusson et al., 2008) invite investigation.

3 Integrated system for temperature-controlled fast protein liquid chromatography. II. Optimised thermoresponsive cation exchange adsorbents and 'single column continuous operation'

3.1 Abstract

Continued advance of a new temperature-controlled chromatography system, comprising a column filled with thermoresponsive stationary phase and a travelling cooling zone reactor (TCZR), is described. Nine copolymer grafted thermoresponsive cation exchangers (thermoCEX) with different balances of thermoresponsive (*N*-isopropylacrylamide), hydrophobic *(N-tert*-butylacrylamide) and negatively charged (acrylic acid) units were fashioned from three cross-linked agarose media differing in particle size and pore dimensions. Marked differences in grafted copolymer composition on finished supports were sourced to base matrix hydrophobicity. In batch binding tests with lactoferrin, maximum binding capacity (q_{max}) increased strongly as a function of charge introduced, but became increasingly independent of temperature, as the ability of the tethered copolymer networks to switch between extended and collapsed states was lost. ThermoCEX formed from Sepharose CL-6B ('A2'), Superose 6 prep grade ('B2') and Superose 12 prep grade ('C1') under identical conditions displayed the best combination of thermoresponsiveness ($q_{max,50°C}$ / $q_{max,10°C}$ ratios of 3.3, 2.2 and 2.8 for supports 'A2', 'B2' and 'C1' respectively) and lactoferrin binding capacity ($q_{max,50°C}$ ~56, 29 and 45 mg/mL for supports 'A2', 'B2' and 'C1' respectively),

and were selected for TCZR chromatography. With the cooling zone in its parked position, thermoCEX filled column were saturated with lactoferrin at a binding temperature of 35 °C, washed with equilibration buffer, before initiating the first of 8 or 12 consecutive movements of the cooling zone along the column at 0.1 mm/s. A reduction in particle diameter (‘A2’ ➞ ‘B2’) enhanced lactoferrin desorption, while one in pore diameter (‘B2’ ➞ ‘C1’) had the opposite effect. In subsequent TCZR experiments conducted with thermoCEX ‘B2’ columns continuously fed with lactoferrin or ‘lactoferrin + bovine serum albumin’ whilst simultaneously moving the cooling zone, lactoferrin was intermittently concentrated at regular intervals within the exiting flow as sharp uniformly sized peaks. Halving the lactoferrin concentration in the feed to 0.5 mg/mL, slowed acquisition of steady state, but increased the average peak concentration factor from 7.9 to 9.2. Finally, continuous TCZR mediated separation of lactoferrin from bovine serum albumin was successfully demonstrated. While the latter’s presence did not affect the time to reach steady state, the average lactoferrin mass per peak and concentration factor both fell (respectively from 30.7 to 21.4 mg and 7.9 to 6.3), and lactoferrin loss in the flowthrough between elution peaks increased (from 2.6 to 12.2 mg). Fouling of the thermoCEX matrix by lipids conveyed into the feed by serum albumin is tentatively proposed as responsible for the observed drops in lactoferrin binding and recovery.

3.2 Introduction

Today, liquid chromatography is universally recognised as a supremely effective and practical bioseparation tool (Goheen and Gibbins, 2000; Asenjo

and Andrews, 2009). There are a multitude of reasons for this, but perhaps the two most important are the technique's adaptability to analytical and preparative separation tasks (Guiochon, 2002) and the availability of a huge variety of differently functionalised chromatographic supports affording orthogonal separation mechanisms (Venkatramani and Zelechonok, 2003; Shi et al., 2004). In typical adsorption chromatography, defined amounts of a given feed solution, containing a single target component and multiple contaminants, are loaded onto a fixed-bed of adsorbent contained in a chromatography column. While the target component adsorbs, to be recovered in a later dedicated elution step by changing the chemical composition of the mobile phase, contaminant species either flow through the column unhindered, or alternatively are washed out in a subsequent washing step and/or during elution procedures. In addition to modifying the mobile phase's chemical composition, physical parameters can also be manipulated to influence protein adsorption to and desorption from chromatographic supports; the most popular of these being temperature, especially in the case of Hydrophobic Interaction Chromatography, HIC (Hjerten, 1973; Haidacher et al., 1996; J.A. Queiroz, C.T. Tomaz, 2001; Muca et al., 2009a, 2009b). According to the Gibbs-Helmholtz equation, an increase in temperature exerts an influence similar to that imposed by raising the cosmotropic salt content in the mobile phase during HIC, which leads to enhanced protein adsorption affinity (J.A. Queiroz, C.T. Tomaz, 2001). However, the relatively small differences in working capacity, even across temperature differentials as high as 40 °C, makes HIC adsorbents unattractive materials for purely temperature mediated liquid chromatography. The anchoring of 'smart' temperature–

sensitive polymers or ‘smart’ thermoresponsive polymers onto chromatography supports offers a potential means of overcoming this drawback.

Smart thermoresponsive polymers are ones that exhibit inverse temperature solubility behaviour, i.e. they are water-soluble at low temperature and insoluble at high temperature, above a critical temperature known as the lower critical solution temperature (LCST) (Taylor and Cerankowski, 1975). The most studied smart thermoresponsive polymer by far is poly(*N*-isopropylacrylamide) or pNIPAAm (Heskins and Guillet, 1968; Kubota et al., 1990; Schild, 1992), and it’s successful and broad application within biomedicine and biotechnology is extensively documented (Galaev and Mattiasson, 1999; Hoffman and Stayton, 2004; Matsuda et al., 2007; Maharjan et al., 2008). pNIPAAm undergoes a sharp reversible ‘hydrophilic coil – hydrophobic globule’ phase transition in water at a LCST of 32–34 ºC (Heskins and Guillet, 1968; Kubota et al., 1990). A large body of work on endowing chromatographic packing materials with temperature switchable behaviour, through their modification with e.g. pNIPAAm or pNIPAAm copolymers, has appeared since the 1990s (Kanazawa et al., 1996; Hoshino et al., 1998; Maharjan et al., 2009; Müller et al., 2013; Terefe et al., 2014). Most of this has involved modification of small pored inorganic or hydrophobic (polystyrene based) chromatography supports for use in analytical separations of small biomolecules (especially steroids). In stark contrast, very little has been done on the modification of softer macroporous media for preparative separations of much larger macromolecules, such as proteins

(Maharjan et al., 2009; Müller et al., 2013; Terefe et al., 2014). Maharjan et al. (2009) and subsequently we (Müller et al., 2013) grafted lightly cross-linked networks of poly(*N*-isopropylacrylamide-*co*-*N*-tert-butylacrylamide-*co*-acrylic acid) into the surfaces of cross-linked agarose supports to produce thermoresponsive cation exchangers (hereafter abbreviated to thermoCEX). In tests with the thermally robust protein lactoferrin (LF) and jacketed columns of thermoCEX media, LF previously adsorbed at a higher temperature could be desorbed by lowering the mobile phase and column temperature.

To exploit thermoresponsive chromatography media more effectively, we invented a bespoke column arrangement (Müller et al., 2013), the so-called Travelling Cooling Zone Reactor (TCZR). TCZR chromatography employs a vertically held stainless steel walled column filled with thermoresponsive stationary phase and a computer-controlled motor-driven Peltier cooling device (the travelling cooling zone, TCZ) surrounding a discrete zone of the column (Fig. 3.1). In standard operation, a protein feed is administered to the column at an elevated temperature. On completion of the loading phase, the column is irrigated with an equilibration buffer whilst simultaneously moving the TCZ along the full length of the separation column (multiple times) in the direction of the mobile phase, and at a velocity lower than that of the interstitial fluid. With each TCZ arrival at the end of the column, a sharp concentrated protein peak appears in the exiting flow, which can be collected by means of a fraction collector.

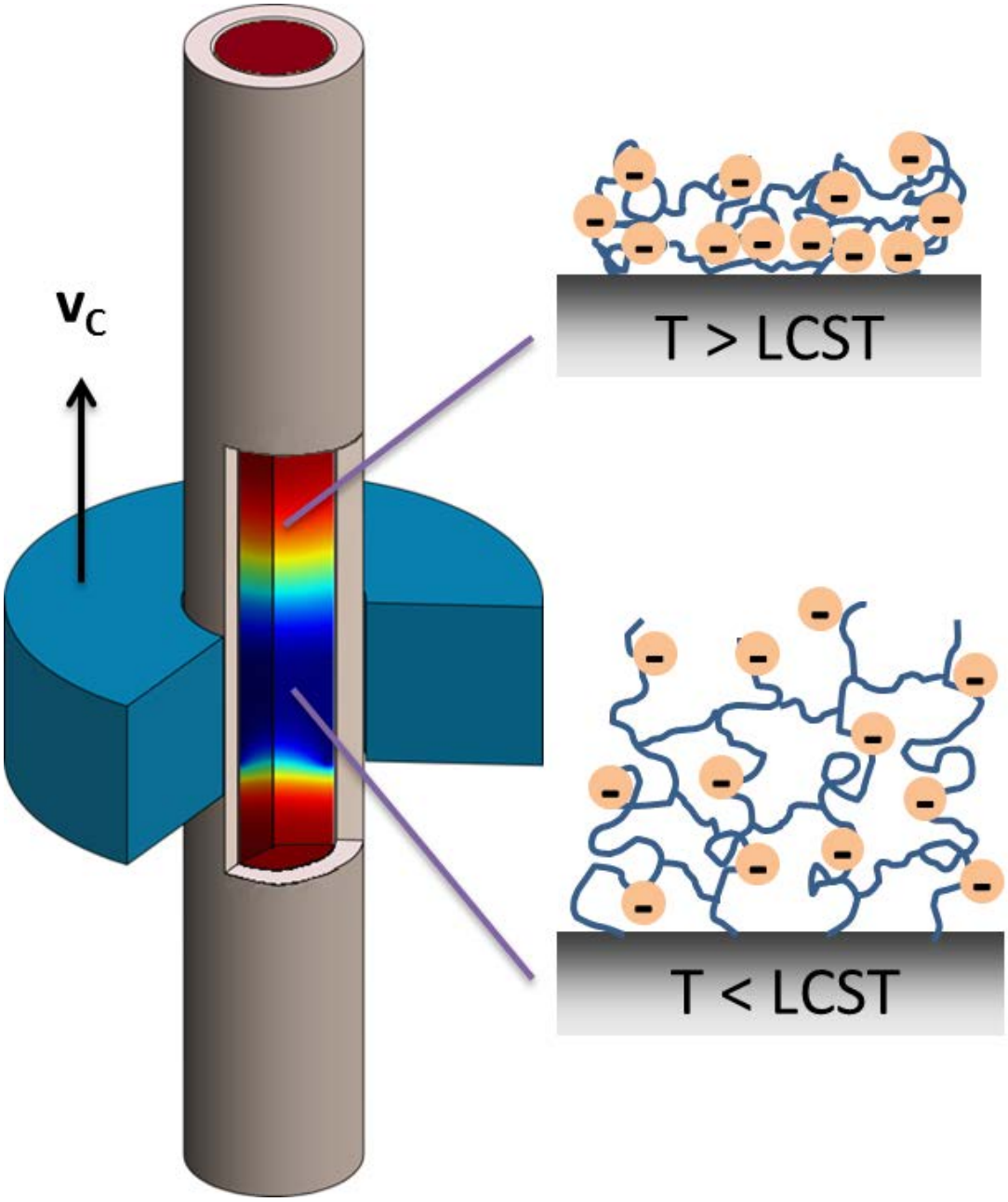

Fig. 3.1 Schematic illustration of the TCZR principle. A stainless steel column filled with thermoresponsive copolymer modified chromatographic media is contained in a temperature-controlled environment at a value above the copolymer's LCST. At this temperature (indicated by red) the grafted thermoresponsive copolymer network exists in a collapsed and highly charged state (top right) that affords high protein binding affinity. For elution a motor-driven Peltier cooling device, the travelling cooling zone or TCZ (shown as a turquoise ring), is moved along the column's full length at a velocity (v_c) lower than that of the mobile phase. Within the cooled zone (shown in blue) generated by the TCZ travels along the column, the tethered thermoresponsive copolymer expands, the charge density drops (bottom right) and bound protein detaches from the support surfaces and is carried away in the exiting mobile phase.

In this second follow up study, we push the boundaries of the TCZR chromatography concept further. From 3 different agarose base matrices, we construct and fully characterise 9 thermoCEX media varying in particle size, pore diameter, and copolymer composition, and subsequently identify, from batch adsorption and batch mode TCZR chromatography, the thermoCEX variant best suited for operation in TCZR modified columns. We then demonstrate, for the first time, how TCZR can be operated in continuous mode, to accumulate and concentrate a model binding protein (LF), and then separate the same target molecule from a simple protein mixture.

The schematic illustration of temperature measurement in the separation column under real operating conditions is shown is Fig. 3.2. A long, thin, wire-like thermocouple (Type J) was stuck to a fishing line. The string was then attached to special fasteners and clamped in the separation column used later, so that the probe was fixed to the tip of the thermocouple in a central position of the column and without contact with the inner column wall. The thermocouple was coupled to a digital temperature meter Tastotherm® MP2001 for temperature recording. The column was then filled with a viscous solution 40% (w/w) polyethylene glycol 35000 in water, the cooling zone was moved along the column from top to bottom at pre-defined temperature settings. Furthermore, the temperature zone was also moved to the position of probe at high speed and the temperature development was also recorded over time in order to determine the kinetics of heat transfer.

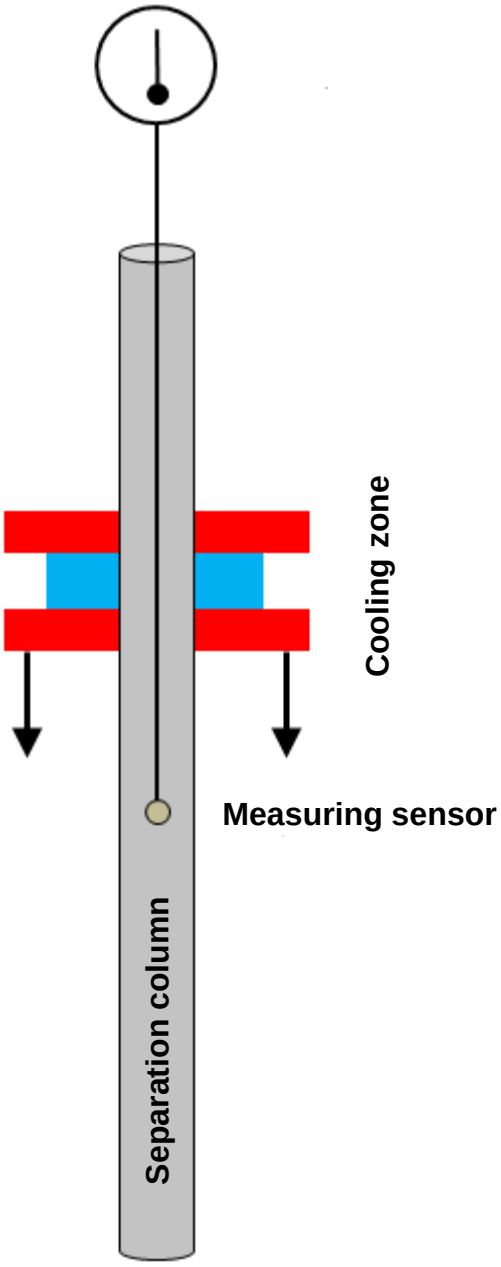

Fig. 3.2 Schematic demonstration of temperature measurement within the separation column. (taken from the thesis of Dr Tobias Müller, 2013)

3.3 Experimental

3.3.1 Materials

The base matrices, Sepharose CL-6B (Cat. no. 170160-01, Lot no. 10040943), Superose 6 prep grade (Cat. no. 17-0489-01, Lot. no. 10037732) and Superose 12 prep grade (Cat. no.17-0536-01, Lot. no. 10057699) were all supplied by GE Healthcare Life Sciences (Little Chalfont, Bucks, UK). The chemicals, *N*-isopropylacrylamide (Cat. no. 415324, 97%; NIPAAm), *N*-*tert*-butylacrylamide (Cat. no. 411779, 97%; *t*-BAAm), acrylic acid (Cat. no. 147230, anhydrous, 99%, AAc), 2-ethoxy-1-ethoxycarbonyl-1,2-dihydroquinoline (Cat. no. 149837, ≥99%; EEDQ), 4,4′-azobis(4-cyanovaleric acid) (Cat. no. 11590, ≥98%; ACV), *N,N*-dimethylformamide (Cat. no. 270547, >99.9%; DMF), *N*,*N*′-methylenebisacrylamide (Cat. No. 146072, 99%; MBAAm), epichlorohydrin (Cat. no. E1055, 99%; ECH), tetrahydrofuran (Cat. no. 34865, >99%; THF), diethyl ether (Cat. no. 309966, >99.9%), sodium borohydride (Cat. no. 71321, >99%) and sodium hydroxide (Cat. no. S5881, anhydrous, >98%) were obtained from Sigma-Aldrich Company Ltd (Poole, Dorset, UK). Absolute ethanol (Cat. no. E/0650DF/17, 99.8+%) and ammonia solution (Cat. no. A/3280/PB15, AR grade, 0.88 S.G., 35%) were acquired from Fisher Scientific UK Ltd (Loughborough, Leics, UK), and bottled oxygen-free nitrogen gas was supplied by the British Oxygen Co Ltd (Windlesham, Surrey, UK). Bovine whey lactoferrin (MLF-1, Lot. No. 12011506, ~96%) was a gift from Milei GmbH (Leutkirch, Germany), and bovine serum albumin (BSA, Cat. No. A7906, lyophilised powder, ≥98% by agarose gel electrophoresis) and ‘Blue Dextran MW 2,000,000’ (Cat. No. D-5751) were purchased from

Sigma-Aldrich. Di-sodium hydrogen phosphate (Cat. no. 4984.1, dihydrate, ≥99.5%) was from Carl Roth GmbH + Co. KG (Karlsruhe, Germany). Disodium hydrogen phosphate (dihydrate, ≥99.5%) and sodium chloride (ACS reagent, ≥99.5%) were supplied by Carl Roth or Sigma-Aldrich, and citric acid monohydrate (≥99%) and Coomassie Brilliant Blue R250 (C.I. 42660) were from Merck Millipore (Darmstadt, Germany). Pre-cast 15% mini-PROTEAN® TGX™ gels and Precision Plus Protein™ All Blue Standards were supplied by Bio-Rad Laboratories Inc. (Hercules, CA, USA). All other chemicals not stated above were from Sigma-Aldrich or Merck Millipore. The water used in all experiments was deionised and purified using a Milli-Q Ultrapure system (Merck Millipore, Darmstadt, Germany.

3.3.2 Preparation of the thermoCEX media used in this work

For detailed descriptions of the procedures involved in the four step conversion of underivatised beaded agarose chromatography supports into thermoCEX media, the reader is referred to our previous study (Müller et al., 2013). Exactly the same methods were applied here to three different beaded agarose starting materials (i.e. Sepharose CL-6B, Superose 6 prep grade and Superose 12 prep grade; see Table 3.1 and Table 3.2). The first three steps of the conversion, i.e. epoxy activation, amine capping and immobilisation of the ACV radical initiator were identically performed, but in the fourth and final ‘graft from’ polymerisation step the initial AAc monomer concentration entering reactions with ACV anchored supports was systematically varied between 25 and 150 mM (equivalent to 2.5 to 13.5% of the total monomer

concentration), whilst maintaining fixed concentrations of all other monomers, i.e. 900 mM NIPAAm, 50 mM tBAAm, and 10 mM of the cross-linking monomer, MBAAm. For point of comparison, the AAc concentration used in our previous study (Müller et al., 2013) was 50 mM (corresponding to ~5% of the total monomer composition).

3.3.3 Batch adsorption experiments with LF

In batch binding tests, portions of settled thermoCEX matrices (0.1 mL), previously equilibrated with 10 mM sodium phosphate buffer, pH 6.5, were mixed with 0.5 mL aliquots of varying initial LF concentration (c_0 = 1 – 15 mg/mL made up in the same buffer) and incubated at 10, 20, 35 or 50 °C with shaking at 1000 rpm in a Thermomixer Comfort shaker (Eppendorf, Hamburg, Germany) for 1 h. After an additional 0.5 h at the selected temperature without shaking, the supernatants were carefully removed and analysed for residual protein content (see 3.3.5 Analysis). The equilibrium loadings on supports (q^*) were computed from the differences in initial (c_0) and equilibrium (c^*) bulk phase protein concentrations, and the resulting q^* vs. c^* data were subsequently fitted to the simple Langmuir model (Eq 2.1), where q_{max} and K_d are respectively, the maximum protein binding capacity of the support and the dissociation constant. Data fitting was performed by SigmaPlot® software version 12.5 (Systat Software Inc., San Jose, CA, USA) using the least squares method.

3.3.4 TCZR chromatography experiments

All chromatographic experiments were conducted using Travelling Cooling Zone Reactors (TCZRs) connected to ÄKTA Purifier UPC 10 or Explorer 100 Air chromatography workstations (GE Healthcare, Uppsala, Sweden). For detailed descriptions of the TCZR arrangement, the reader is referred to our recent study (Müller et al., 2013). A brief, but necessary description of the workings of the system is given here. The TCZR set-up features four components, i.e. (i) a temperature controlled box housing, (ii) the thermoresponsive stationary phase contained in (iii) a stainless steel walled (1 mm thick) fixed-bed column (length = 10 cm; internal diameter = 6 mm; volume = 2.83 mL), and (iv) a movable assembly of copper blocks and Peltier elements surrounding a small discrete zone of the column. The whole cooling unit can be moved up or down the column's length via a ball bearing guided linear motorised axis, and by adjusting the Peltier elements, the centre of the assembly can be cooled down by >20 °C. In all of the work described here, the constant surrounding temperature was 35 °C, and the velocity of the TCZ assembly (v_c) was the lowest attainable in the system (0.1 mm/s), generating a maximum temperature difference of 22.6 °C corresponding to a minimum temperature in the centre of the column of 12.4 °C extending across 2 cm of column length.

3.3.4.1 Batch mode TCZR chromatography of LF

LF (c_f = 2 mg/mL) in an equilibration buffer of 10 mM sodium phosphate, pH 6.5 was continuously applied to beds of thermoCEX media (packing factor = 1.2) until almost complete breakthrough had been achieved in each case (i.e.

c/c_f approaching 1). At this point the LF saturated columns were then washed with 5 CVs of equilibration buffer, before moving the TCZ assembly multiple times (8 times in the case of thermoCEX-CL6B and thermoCEX-S6PG, and 12 times for thermoCEX-S12PG) along the full separation column's length at its minimum velocity of 0.1 mm/s, generating a minimum temperature in the centre of the column of 12.4 °C (Müller et al., 2013). On completion of TCZ's last movement residually bound LF was dislodged from the columns using a 1 M NaCl step gradient. Constant mobile phase velocities of 30 mL/h for the small particle sized Superose based thermoCEX media, or 60 mL/h for the larger Sepharose CL-6B derived thermoCEX adsorbent, were employed, giving rise to interstitial velocities for the packed columns of thermoCEX-S6PG, thermoCEX-S12PG and thermoCEX-CL6B of 0.70 mm/s, 0.84 mm/s and 1.89 mm/s respectively. The percentages of LF in each of collected peaks were calculated by dividing the LF mass eluted in each by the total mass of LF recovered in all of the elution peaks.

3.3.4.2 Continuous TCZR chromatography

In continuous chromatography experiments, feeds of LF (c_f = 0.5 or 1 mg/mL) or 'LF + BSA' (1 mg/mL of each) in 10 mM sodium phosphate equilibration buffer were continuously fed at a temperature of 35 °C, and interstitial velocity of 0.74 mm/s on to a column filled with thermoCEX-S6PG. During the first 2 h of operation the TCZ remained in its parking position above the separation column, by which point the protein loading front had approached ~75% of the column's length. At this stage slow constant movement of the TCZ along the column was initiated resulting in the first elution peak. At the applied velocity

(v_c = 0.1 mm/s) the TCZ travelled down the column at less than a seventh the rate of the interstitial mobile phase velocity. On reaching the base of the column, some ~20 minutes later, the elution peak left the column, and the TCZ was once again moved, at high speed, to its parking position above the column. Seven further movements of the TCZ along the column's length were conducted in each experiment at regular 80 minute intervals, i.e. after 200, 280, 360, 440, 520, 600 and 680 minutes had elapsed. During the continuous application of the TCZR system, desorbed proteins were fractionated after every movement of the TCZ. The fractionation started when the UV adsorption at 280 nm in the effluent showed values above 100 mAu. The protein peaks were collected and the protein concentration was determined. Residual bound protein finally was eluted by an increase to 1 M of sodium chloride in the mobile phase. The concentration factor ($CF_{Peak,i}$) of every single protein peak *i* was determined by dividing the protein peak concentration by the feed concentration (Eq 3.1):

$$CF_{Peak,i} = \frac{c_{Peak,i}}{c_f} \qquad \text{Eq 3.1}$$

where $c_{Peak,i}$ is the peak concentration of the respective fractionated protein peak. An averaged concentration factor (*CF*) was determined by calculating the average of the peak concentration factors when a steady-state was reached (Eq 3.2):

$$CF = \frac{\sum CF_{Peak,i}}{j} \qquad \text{Eq 3.2}$$

where *j* is the number of fractionated protein peaks in a steady-state. By multiplying the protein concentration of the fractions and the fraction volume, the eluted protein mass could be calculated.

3.3.5 Analysis

The battery of methods employed to characterise the various thermoCEX adsorbents prepared in this work, including all intermediates in their manufacture, are summarised briefly below and described in detail elsewhere (Müller et al., 2013).

3.3.5.1 Epoxide density measurement

Reactive epoxide contents introduced by activation with epichlorohydrin were determined as described by Sundberg and Porath (1974).

3.3.5.2 FT-IR and ATR-FTIR analysis

For qualitative FT-IR analysis of solid supports, oven dried samples (~3 mg) were mixed with potassium bromide (300 mg), ground down to a fine powder and hydraulically pressed (15 tonne) into tablet form. Each tablet was subjected to 64 scans (averaged at a resolution of 2 cm^{-1}) in a Nicolet 380 FT-IR (Thermo Fisher Scientific, Waltham, MA, USA) in direct beam mode. Quantitative estimation of 'NIPAAm + tBAAm' consumption by supports during grafting reactions, by monitoring changes in area of the characteristic peak for N-H bending (1575 –1500 cm^{-1}), was performed on liquid samples (150 µL)

applied directly to the surface of the Nicolet 30 FT-IR's Smart 53 Orbit diamond accessory. The samples were scanned 64 times at a resolution of 2 cm^{-1} in attenuated total reflectance mode (ATR FT-IR).

3.3.5.3 Gravimetric analysis

Gravimetric analyses was used to determine the immobilised ACV and copolymer contents on solid supports and also of dried residues recovered from liquid samples, to allow determination of free ungrafted copolymer content and unreacted monomers remaining in solution post-grafting. Free copolymers were separated from unreacted monomers by rotary evaporating to dryness, resuspending in tetrahydrofuran, precipitating with diethyl ether and oven drying, and unreacted monomers remaining in the supernatants were recovered by rotary evaporating to dryness.

3.3.5.4 NMR analysis

The relative amounts of NIPAAm and tBAAm in ungrafted copolymers were obtained by proton NMR spectroscopic analysis of $CDCl_3$ dissolved samples using a Bruker AV400 NMR Spectrometer (Bruker-BioSpin Corporation, Billerica, MA, USA). 'NIPAAm:tBAAm' ratios (Table 3.1 and Table 3.2) were computed from characteristic chemical shifts in ^1H NMR spectra at 1.15 ppm and 1.34 ppm for two strong methyl proton peaks arising from the NIPAAm and tBAAm side chains respectively (Maharjan et al., 2009; Müller et al., 2013).

3.3.5.5 LCST measurement

Full temperature dependent ‘coil–globule’ transition profiles and lower critical solution temperature (LCST) values for ungrafted copolymers were obtained by monitoring the optical transmittance (at λ = 500 nm) of test solutions (0.5% w/v copolymer in 10 mM sodium phosphate, pH 6.5) in a Cecil CE7500 UV/visible dual beam spectrometer equipped with a water thermostatted cuvette holder.

3.3.5.6 Ionic capacity analysis

H^+ exchange capacities of supports were determined by titration using GE Healthcare’s method for determination of the ionic capacity of CM Sepharose media (No. 30407). The void volumes of packed beds of thermoCEX media were determined by SEC of Blue Dextran (50 µL, 1 mg/mL) under non binding conditions, using an equilibrating and mobile phase of 50 mM Tris-HCl, pH 7.5 supplemented with 100 mM KCl.

3.3.5.7 Protein contents determination

The protein content in samples was spectrophotometrically assayed at a wavelength of 280 nm either off-line during batch binding experiments using a NanoDrop® ND-1000 Spectrophotometer (Thermo Fisher Scientific, Waltham, MA, USA) or quartz cuvettes in a Lambda 20 UV-vis spectrophotometer (PerkinElmer Analytical Instruments, Shelton, CT, USA), or on-line during chromatographic investigations using ÄKTA chromatography workstations operated under Unicorn™ software (GE Healthcare, Uppsala, Sweden).

3.3.5.8 SDS-PAGE analysis

The composition of fractions generated during continuous TCZR chromatographic separation of LF and BSA was examined by reducing SDS-PAGE (Laemmli, 1970) in 15% (w/v) pre-cast polyacrylamide gels in a Mini-Protean® Tetracell electrophoresis system (Bio-Rad Laboratories, Hercules, CA, USA). After electrophoresis, gels were stained with 0.1% (w/v) Coomassie Brilliant Blue R250, dissolved in 40% (v/v) ethanol and 10% (v/v) acetic acid) for 1 h at room temperature, and were subsequently destained at the same temperature in a solution composed of 7.5% (v/v) acetic acid and 10% (v/v) ethanol. The LF and BSA contents were determined by densitometric analysis of scanned TIFF images of appropriately loaded Coomassie Blue stained gels following electrophoresis. The images were captured with an HP ScanJet C7716A flat bed scanner (Hewlett-Packard Company, Palo Alto, CA, USA) at a resolution of 2400 dpi, and analysed using ImageJ software (Schneider et al., 2012).

3.4 Results and Discussion

3.4.1 Concept of single-column continuous TCZR chromatography

Schematic concentration and loading profiles within the TCZR fitted column are illustrated in Fig. 3.3 for the various operation phases. These are characterised by different positions of the TCZ relative to the column. The profiles at three different positions of the TCZ are shown, i.e.: (i) outside the column (Fig. 3.3a); and after travelling (ii) a quarter (Fig. 3.3b) and (iii) three-

quarters (Fig. 3.3c) of the separation column's length. When the TCZ is parked 'outside' (Fig. 3.3a), the whole column is operated at an increased temperature (T_B). Protein is continuously loaded and binds to the adsorbent. In keeping with the binding strength of the protein to the support at T_B, sharp concentration and loading fronts of the protein propagate through the system at a constant velocity, v_{pf} (Eq 3.3):

$$v_{pf} \cong \frac{u_i}{1+\frac{1-\varepsilon_b}{\varepsilon_b}\frac{\partial q}{\partial c}} \qquad \text{Eq 3.3}$$

Here, v_{pf} is a function of the slope of the isotherm, $\frac{\partial q}{\partial c}$, the interstitial fluid velocity, u_i, and the phase ratio between the solid and liquid phases expressed by the bed voidage, ε, of the column packing.

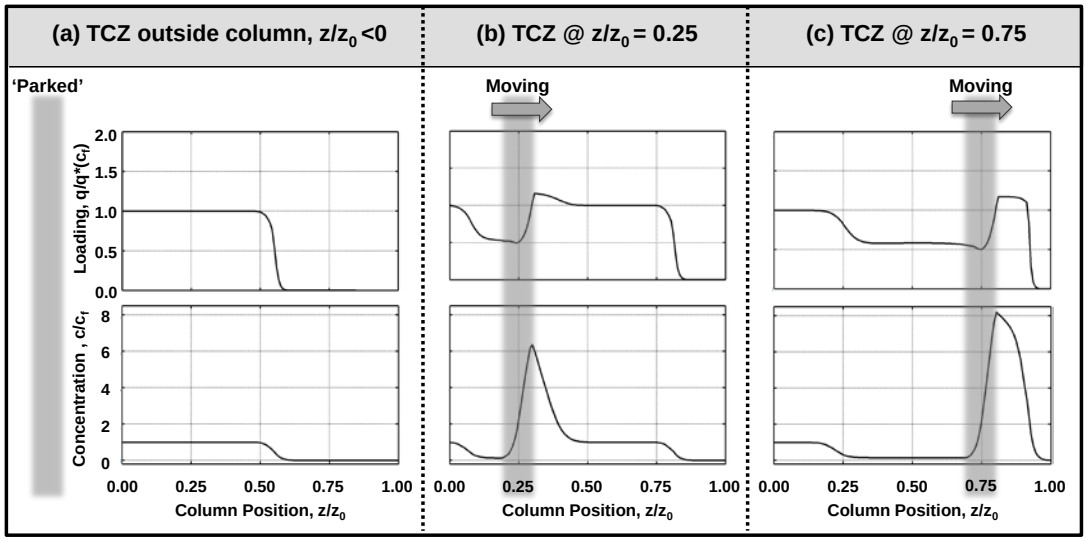

Fig. 3.3 Schematic illustrations of single protein loading (top) and concentration (bottom) profiles at different stages during TCZR operation. The profiles correspond to three discrete z/z_0 positions (<0, 0.25, 0.75) of the TCZ illustrated by the grey shaded vertical bars, i.e.: (i) parked outside the separation column resulting in conventional operation with slowly progressing concentration and loading profiles; (ii) shortly after initiation of TCZ movement, where a sharp concentration peak evolves just ahead of the TCZ; and (iii) as the TCZ nears the end of its journey along the column. At this point, in addition to further protein accumulation within the elution peak, new loading and concentration profiles arising from constant feed flow at the column inlet become clearly visible.

When the TCZ starts to move along the column, previously bound protein desorbs at the front of the zone, resulting in a strong increase in mobile phase protein concentration (Fig. 3.3b, lower trace). Because the TCZ's velocity (v_c) is slower than that of the mobile phase (i.e. $v_c < u_i$), the flow transports the desorbed protein further along the column into the adjacent region, which is still at the elevated temperature, T_B. At T_B, this increased protein concentration leads to a corresponding rise in the local protein loading at this point within the column. When, sometime later, the constantly moving TCZ reaches this 'protein-laden' part of the column, its action desorbs the bound protein, resulting in an even larger surge in mobile phase protein concentration. In essence, what results within the column, provided that mass transfer limitations are small, are sharp concentration and loading waves formed in front of the moving TCZ. The concentration of adsorbing species will be much higher than that in the feed, and protein loading closely approaches the maximum capacity of the adsorbent. With progressive movement of the TCZ along the column more and more protein is desorbed at its front, to continuously supply the immediately flanking high temperature (T_B) region ('over-travelled' column section) with an increasing protein challenge (Fig. 3.3c. lower trace). Given that the adsorbent's protein binding capacity cannot be exceeded (Fig. 3.3c, upper trace) the protein concentration wave broadens (Fig. 3.3c, lower trace).

Closer scrutiny of the plots in Fig. 3.3 reveals further noteworthy features of the TCZR principle highlighted as follows:

1. When the rate of progress of the feed concentration front along the column is slower than that of the TCZ, an increasingly wide region of low protein loading and concentration forms in the TCZ's wake (compare Fig. 3.3b & Fig. 3.3c). The extent of reduction in protein loading and concentration, and therefore in effect the operational working capacity of the TCZR, are determined by the TCZ's efficiency in eluting the adsorbed protein.

2. When the protein wave cresting the TCZ reaches the column outlet, protein elutes in high concentration. In the meantime, the protein feed is continuously applied at the other end of the column (inlet), protein loading of the front section of the column attains equilibrium with the feed, and once this loaded section reaches ~70% of the column length, another movement of the TCZ is initiated, giving rise to a second elution peak, and so on and so forth.

3. Thus, by careful selection of both the velocity of the TCZ and the timing between successive movements of the device, a quasi-stationary state operation should be attained, where similar concentration and protein loading profiles are generated before every movement of the TCZ. This confers unique capabilities on the TCZR system, namely the possibility of continuously loading protein at one end of column whilst simultaneously desorbing previously bound protein from the other, in a single-column installation without need of additional steps of regeneration and/or equilibration.

3.4.2 Manufacture and characterisation of thermoresponsive CEX adsorbents

Three types of beaded cross-linked agarose matrices (Sepharose CL-6B, Superose 6 prep grade and Superose 12 prep grade) differing in particle diameter, agarose content and pore size (see Table 3.1and Table 3.2) were fashioned into thermoCEX adsorbents in four successive steps, i.e. epoxide activation, amine capping, ACV initiator immobilisation and graft-from polymerisation using improved protocols detailed previously (Müller et al., 2013). The initial composition of monomers entering the final copolymer grafting step was systematically varied to create families of thermoCEX materials with different balances of thermoresponsive, hydrophobic and charged building blocks in the copolymers anchored to their exteriors and lining their pores. The resulting thermoCEX adsorbents and intermediates in their manufacture (both supports and reaction liquors) underwent rigorous qualitative and quantitative physicochemical analysis prior to use.

FT-IR spectra obtained during the stepwise conversion of Superose 6 prep grade into the thermoCEX-S6PG adsorbent family are shown in Fig. 3.4. Identical sets of spectra were obtained with Superose 12 prep grade and Sepharose CL-6B subjected to the same procedures. During the various steps, the expected peaks previously assigned in converting Sepharose CL-6B into a thermoresponsive cation exchanger (Müller et al., 2013), were also observed during the manufacture of the Superose based thermoCEX media in this work. Of special note are: (i) the growth in peak heights between 1474 and 1378 cm^{-1} in the spectrum of epoxy-activated S6PG due to increased

alkyl group content, consistent with incorporation of glycidyl moieties into S6PG; (ii) sharpening and growth of the signal at 1378 cm^{-1} following amination of epoxy-activated S6PG, likely arising from diminished flexibility, and therefore reduced variance in the vibrational frequency of the CH_2 groups in the backbone; (iii) the appearance of two new peaks in the FTIR spectrum of ACV immobilised S6PG (1736 cm^{-1} for carboxylic acid C=O stretching, and 1552 cm^{-1} for azo N=N stretching and/or amide N-H bending); the growth of (iv) amide N–H bending (1570 cm^{-1}) and amide C=O stretching (1670 cm^{-1}) contributions from incorporated NIPAAm, tBAAm and MBAAm units, and (v) of carboxylic acid C=O stretching (1736 cm^{-1}), arising from the presence of AAc in the grafted copolymer on the thermoCEX supports; and finally that (vi) despite marked differences in the compositions of grafted copolymers on thermoCEX supports ‘B1’-‘B4’ (see Table 3.2), their FTIR spectra appear identical.

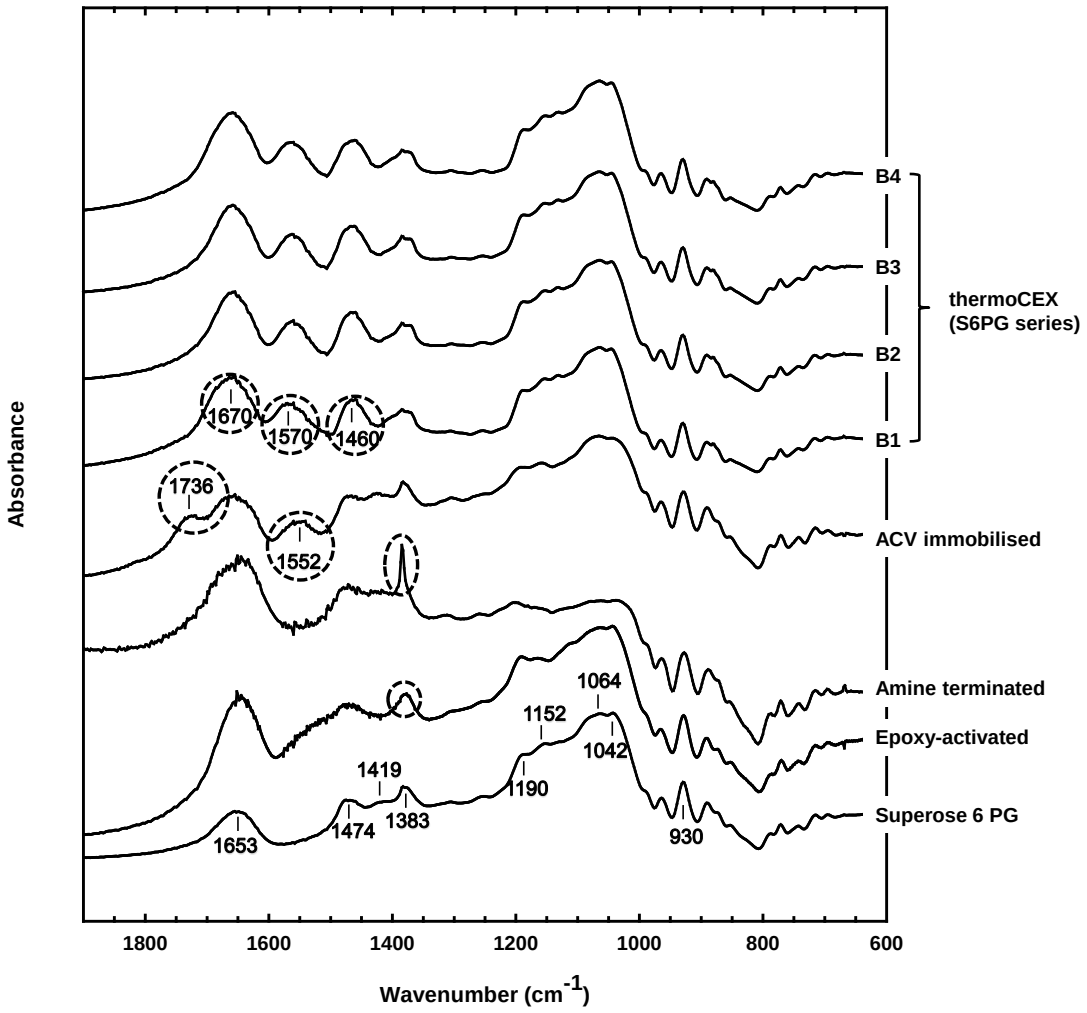

Fig. 3.4 FT-IR spectra during the fabrication of thermoCEX-S6PG supports (B1-B4) characterised in Table 3.2. All spectra are normalised for peak height at the 'fingerprint' wavenumber for agarose of 934 cm^{-1} characteristic of 3,6 anhydro moiety (Oza et al., 2010), and functional groups expected of cross-linked agarose (Oza et al., 2010; Müller et al., 2013) are identified on the spectrum for Superose 6 prep grade.

Analysis of the immobilised copolymer compositions of Sepharose CL-6B and Superose based thermoCEX (Table 3.1 and Table 3.2 respectively) illustrates marked differences. Under identical reaction conditions, unique monomer consumption preferences appear to be displayed by the different ACV-coupled supports. Compare supports 'A2', 'B2' and 'C1' for example. When normalised against the initial monomer composition entering polymerisation

reactions with ACV immobilised supports, ACV-immobilised Sepharose CL-6B consumed tBAAm and AAc roughly equally (32.5% *cf.* 30.4%), and ~2.4 times more readily than NIPAAm (13.2%); by contrast, ACV-coupled S6PG consumed tBAAm (33.5%) in >1.8 fold preference to both AAc (19.0%) and NIPAAm (18.7%), whereas ACV-linked S12PG consumed tBAAm (39.2%) ~1.5 and ~2.2 fold more readily than AAc (25.4%) and NIPAAm (17.6%) respectively. Thus, despite the higher initial epoxide density (878 µmol/g) driving increased ACV immobilisation (568 µmol/g) and ~1.4 fold higher mass of grafted copolymer, the ionic capacity of the thermoCEX-S6PG was 38% lower than that on thermoCEX-CL6B (i.e. 293 *cf.* 469 µmol/g dried support), whereas its NIPAAm and tBAAm contents had both increased (by 42% and 3% respectively). We observed this phenomenon previously during fabrication of thermoCEX adsorbents fashioned from ostensibly very similar cross-linked 6% agarose media, and suggested that differences were likely linked to the epoxide densities introduced in the first synthetic step, rather than to subtle chemical disparities between the two base matrices (Müller et al., 2013). Based on findings in this study with 15 support materials, i.e. 9 finished thermoCEX and 6 intermediates in their manufacture (Table 3.1 and Table 3.2), we no longer believe this to be the case. Though sharing agarose backbones, and being subjected to identical polymer modification reactions, it appears here that differences in proprietary modification (principally cross linking) of the base matrix starting materials (Porath et al., 1971; Andersson et al., 1985, 1998; Lindgren, 1986; Pernemalm et al., 1987) influence the initial epoxy activation level, subsequent immobilised initiator density, loading and composition of grafted copolymer of the finished thermoCEX adsorbents.

Sepharose CL-6B is prepared by first reacting Sepharose 6B with 2,3-dibromopropanol under strongly alkaline conditions and then desulphating post cross-linking, by reducing alkaline hydrolysis, to give a cross-linked matrix with high hydrophilicity and very low content of ionisable groups (Andersson et al., 1985, 1998). In the manufacture of Superose media, cross-linking to confer rigidity occurs in two stages, i.e. initial priming reaction with a cocktail of long-chain bi- and poly- functional epoxides in organic solvent, followed by cross-linking via short-chain bi-functional cross-linkers conducted in aqueous solvent (Andersson et al., 1985; Pernemalm et al., 1987). Superose media are thus less hydrophilic than Sepharose CL supports, and it is this fundamental difference that likely: (i) contributes to the 30 – 50% greater number of immobilised oxiranes introduced into Superose matrices (Table 3.2, 878 µmol/g for S6PG, 1018 µmol/g for S12PG) by epichlorohydrin activation (step 1) under identical conditions *cf.* Sepharose CL-6B (Table 3.1, 662 µmol/g); leads in turn (ii) both to higher immobilised ACV contents (568 and 611 µmol/g for S6PG and S12PG respectively *cf.* 380 µmol/g for Sepharose CL-6B) and elevated grafted polymer yields (6005 ± 68 µmol/g for ThermoCEX-Superose adsorbents *cf.* 4675 ± 97 µmol/g for ThermoCEX-CL6B); and (iii) significantly higher incorporation of the charged AAc monomer into the grafted copolymers on ThermoCEX-CL6B *cf.* ThermoCEX adsorbents fashioned from Superose media across all AAc input concentrations during grafting (see Table 3.1and Table 3.2).

Table 3.1 Characterisation of the Sepharose CL-6B based thermoCEX supports prepared and used in this work. See text for details.

Parameter	ThermoCEX-CL6B			
Support ID (symbol)	A1	A2	A3	A4
Base matrix	Sepharose CL-6B (lot 10061497)			
Particle size distribution	45 – 165 µm (98%)			
Globular protein fractionation range, M_r	$1 \times 10^4 – 4 \times 10^6$ Da			
Step 1 Immobilised oxirane content (µmol/g dried support) [a]	662			
Step 3. Immobilised ACV content (µmol/g dried support) [b]	380			
Step 4. Free monomers entering reaction:				
'NIPAAm: tBAAm: AAc' (mM)	900: 50: 25	900: 50: 50	900: 50: 100	900: 50: 150
'NIPAAm: tBAAm: AAc' ratio	90:5:2.5	90:5:5	90:5:10	90:5:15
Immobilised copolymer composition of thermoCEX support:				
'pNIPAAm + tBAAm' content (µmol/ g dried support) [b,c]	4227	4177	4131	3974
pNIPAAm: tBAAm ratio[d]	90:10	88:12	85:15	81:19
NIPAAm content (µmol/ g dried support)	3804	3676	3511	3219
tBAAm content (µmol/ g dried support)	423	501	620	755
Ion exchange capacity (µmol H^+/ g dried support)[e]	330	469	582	811
'pNIPAAm + tBAAm + AAc' content (µmol/ g dried support)	4557	4646	4713	4785
'NIPAAm: tBAAm: AAc' ratio	83.5: 9.3: 7.2	79.1: 10.8: 10.1	74.5: 13.2: 12.3	67.3: 15.8: 16.9
% monomer consumed by support:				
NIPAAm + tBAAm + AAc	15.1	15.0	14.5	14.1
NIPAAm	13.7	13.2	12.6	11.6
tBAAm	27.4	32.5	40.2	49.0
AAc	42.8	30.4	18.9	17.5

Key: Determined by: [a]oxirane ring opening reaction followed by titration [Sundberg and Porath, 1974]; [b]gravimetric measurement; [c]ATR-FTIR spectrometry of supernatant samples before and after polymerisation reactions, [d]Proton NMR of the ungrafted free copolymer in $CDCl_3$; [e]titration measured at 20 °C.

Table 3.2 Characterisation of the Superose 6 and 12 prep grade based thermoCEX supports prepared and used in this work. See text for details.

Parameter	ThermoCEX-S6PG				ThermoCEX-S12PG
Support ID	B1	B2	B3	B4	C1
Base matrix	Superose 6 PG (lot 10037732)				Superose 12 PG (lot 10057699)
Particle size distribution	20 – 40 µm (83%)				20 – 40 µm (88%)
Globular protein fractionation range, M_r	$5 \times 10^3 – 5 \times 10^6$ Da				$1 \times 10^3 – 3 \times 10^5$ Da
Step 1 Immobilised oxirane content (µmol/g dried support) [a]	878				1018
Step 3. Immobilised ACV content (µmol/g dried support) [b]	568				611
Step 4. Free monomers entering reaction:					
'NIPAAm: tBAAm: AAc' (mM)	900: 50: 25	900: 50: 50	900: 50: 100	900: 50: 150	900: 50: 50
'NIPAAm: tBAAm: AAc' ratio	90:5:2.5	90:5:5	90:5:10	90:5:15	90:5:5
Immobilised copolymer composition of thermoCEX support:					
'pNIPAAm + tBAAm' content (µmol/ g dried support) [b,c]	5745	5733	5659	5641	5495
pNIPAAm: tBAAm ratio[d]	92:8	91:9	87:13	84:16	89:11
NIPAAm content (µmol/ g dried support)	5285	5217	4923	4738	4891
tBAAm content (µmol/ g dried support)	460	516	736	903	604
Ion exchange capacity (µmol H^+/ g dried support)[e]	268	293	382	416	391
'pNIPAAm + tBAAm + AAc' content (µmol/ g dried support)	6013	6026	6041	6057	5886
'NIPAAm: tBAAm: AAc' ratio	87.9: 7.6: 4.5	86.6: 8.5: 4.9	81.5: 12.2: 6.3	78.2: 14.9: 6.9	83.1: 10.3: 6.6
% monomer consumed by support:					
NIPAAm + tBAAm + AAc	19.9	19.5	18.6	17.8	19.1
NIPAAm	19.0	18.7	17.6	17.0	17.6
tBAAm	29.8	33.5	47.7	58.5	39.2
AAc	34.8	19.0	12.4	9.0	25.4

Key: Determined by: [a]oxirane ring opening reaction followed by titration [Sundberg and Porath, 1974]; [b]gravimetric measurement; [c]ATR-FTIR spectrometry of supernatant samples before and after polymerization reactions, [d]Proton NMR of the ungrafted free copolymer in $CDCl_3$; [e]titration measured at 20 °C.

The temperature dependent phase transition behaviour of ungrafted free copolymer solutions emanating from various grafting reactions with ACV-immobilised Sepharose CL-6B and Superose prep grade are compared in Fig. 3.5. Fig. 3.5a and Fig. 3.5b display the raw transmittance vs. temperature profiles, and Fig. 3.5c examines the wider impact of NIPAAm replacement on the LCST and full transition temperature ranges of the copolymers.

In accord with literature reports (Heskins and Guillet, 1968; Kubota et al., 1990; Schild, 1992), the LCST at 50% optical transmittance ($T_{50\%}$) for the 'smart' homopolymer pNIPAAm was 32.3 °C and sharp transition from fully extended 'hydrophilic coil' ($T_{90\%}$) to fully collapsed 'hydrophobic globule' ($T_{0.4\%}$) occurred between 31 and 35 °C (dashed line traces in Fig. 3.5a-c). Copolymerising NIPAAm with more hydrophobic monomers leads to a reduction in the LCST (Hoffman et al., 2000; Yoshimatsu et al., 2012), whereas incorporation of more hydrophilic species increases it (Hoffman et al., 2000). Here, simultaneous low level substitution of AAc and tBAAm into pNIPAAm's backbone ('A1', 'B1' & 'C1') at the expense of 12.1 to 16.9% of its NIPAAm content (Table 3.1 & Table 3.2), had the effect of lowering the LCST (by 1.4 °C for 'A1', 2.3 °C for 'B1', 1.5 °C for 'B2' and 0.9 °C for 'C1') and broadening the transition temperature range in both directions (i.e. 28.3 to 36.7 °C for 'A1', 26.5 to 34.8 °C for 'B1', 26.5 to 37.7 °C for 'B2', and 28.5 to 36.8 °C for 'C1'). With mounting NIPAAm replacement ('A3', 'A4', 'B3', 'B4'), smart thermoresponsive behaviour became increasingly compromised. For example, the LCST for the '67.3:15.8:16.9' copolymer (Fig. 3.5c, 'A4') reached

36.6 °C and temperature range over which full ‘coil – globule’ transition range extended >25 °C, i.e. from 20.5 to 46 °C.

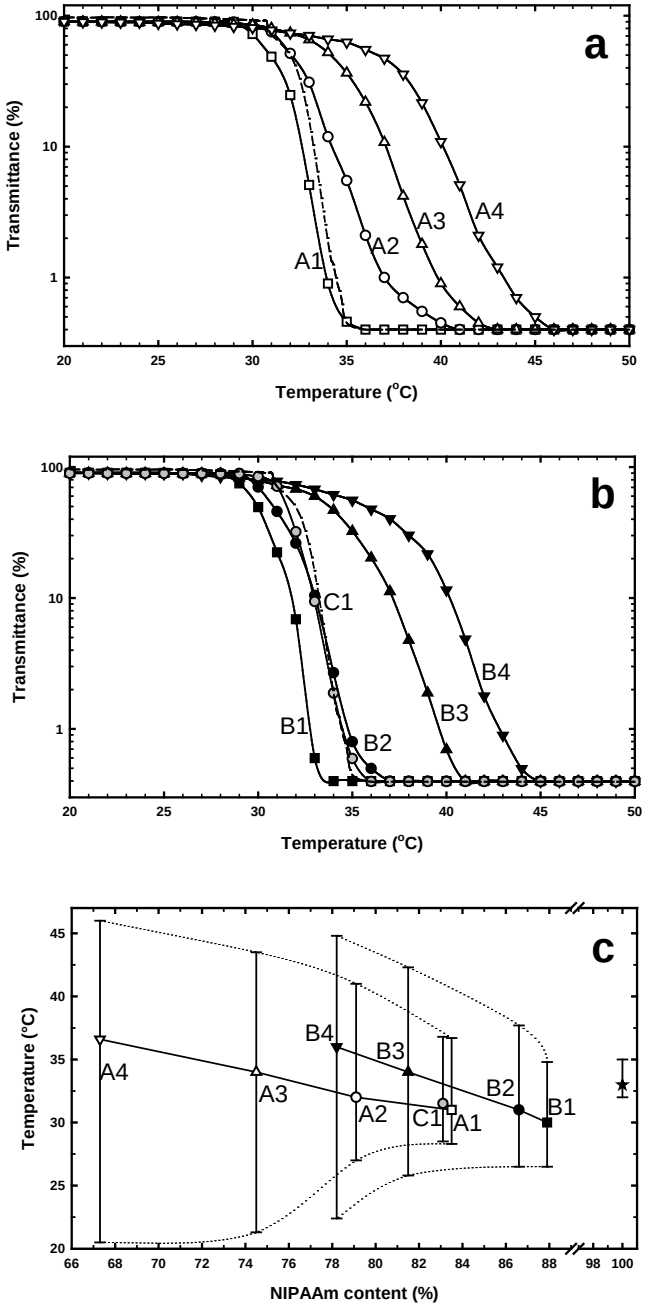

Fig. 3.5 Optical transmittance (500 nm) vs. temperature profiles for 0.5% (w/v) solutions of ungrafted free poly(NIPAAm-*co*-tBAAm-*co*-AAc-*co*-MBAAm) arising during fabrication of (a) Sepharose CL-6B and (b) Superose based thermoCEX supports (detailed in Table 3.1 and Table 3.2), and (c) the influence of NIPAAm content on temperature transition behaviour of the copolymers. The symbols in ‘c’ indicate the determined LCST values at 50% transmittance ($T_{50\%}$), capped bars define the temperature range over which phase transition occurred, and the lower dotted and upper dashed lines respectively delineate the temperatures at which full collapse ($T_{0.4\%}$) and extension ($T_{90\%}$) of the copolymer chains occurred. Key: pNIPAAm (★); Sepharose CL6B series (A1 – □, A2 – ○, A3 – △, A4 – ▽); Superose series (B1 – ■, B2 – ●, B3 – ▲, B4 – ▼, C1 – ●).

3.4.3 Temperature dependent adsorption of LF on thermoCEX adsorbents

The optimum condition for an effective thermoresponsive adsorbent is one where the binding of a given target is strongly temperature dependent; in the ideal case being effectively switched ‘on’ (powerful adsorption) and ‘off’ (no adsorption) by a small change in bulk phase temperature across the LCST of the thermoresponsive copolymer. In practice this has not been achieved, i.e. the sharp ‘coil – globule’ transitions observed in free solution are not mirrored by protein binding vs. temperature plots (Maharjan et al., 2009; Müller et al., 2013). The collapse and extension of surface-anchored thermoresponsive copolymer chains is considerably more constrained (Andersson et al., 2006) and complex (Andersson et al., 2006; Plunkett et al., 2006; Müller et al., 2013) than that of the free untethered species. As a consequence, changes to the binding interface in response to a thermal trigger are gradual in nature.

The effect of temperature on the maximum LF adsorption capacity (q_{max}) for all nine thermoCEX supports is illustrated in Fig. 3.6 a & b. In all cases, q_{max} rose linearly with increase in temperature over the examined range (10 – 50 °C), as the tethered copolymer networks gradually transitioned from predominantly hydrophilic and fully extended low charge density states (Fig. 3.3, bottom right) to increasingly flattened, hydrophobic and highly charged ones (Fig. 3.3, top right), as the distance between neighbouring charged AAc units within the collapsed copolymer decreased and previously shielded/buried negative charges became exposed (Maharjan et al., 2009). However, the degree of thermoresponsiveness exhibited varied significantly

between and within each thermoCEX family, and a clear trend emerged. For the least substituted supports in the Sepharose CL-6B and Superose 6PG thermoCEX families, i.e. 'A1' (Fig. 3.6a, Table 3.1) and 'B1' (Fig. 3.6b, Table 3.2), LF binding capacity was strongly temperature dependent ('$q_{max,\ 50°C}$ / $q_{max,\ 10°C}$' ratios of 2.2 for 'A1' & 3.3 for 'B1'), but low ($q_{max,50°C}$ values of <22 mg/mL for 'B1' and <27 mg/mL for 'A1'). With increasing NIPAAm replacement by hydrophobic tBAAm and negatively charged AAc monomers (➞'A2'➞'A3'➞'A4', Fig. 3.6a; ➞'B2'➞'B3'➞'B4'; Fig. 3.6b), LF binding increased dramatically ($q_{max,\ 50°C}$ rising to ~52 mg/mL for 'B4' and ~83 mg/mL for 'A4'), but became increasingly temperature independent ('$q_{max,\ 50°C}$ / $q_{max,\ 10°C}$' ratios of 1.06 for 'A4' & 1.1 for 'B4'), as the ability of the tethered copolymers to transition between extended and collapsed states was lost. ThermoCEX supports with moderate levels of NIPAAm replacement, i.e. 'A2', 'B2' & 'C1', displayed the best combination of thermoresponsiveness and LF binding capacity (i.e. reasonable $q_{max,\ 50°C}$ and low $q_{max,10°C}$ values), and were therefore selected for further study.

For all nine thermoCEX adsorbents, the ion exchange capacity rises with increased temperature (Fig. 3.6 c & d), which means the electrostatic interaction between adsorbents and LF is stronger at higher temperature. A possible explanation is that the negative charges of tethered polymer chains become more exposed due to the conformation change of immobilised copolymer from hydrophilic coil to hydrophobic globule with the temperature increases across the LCST.

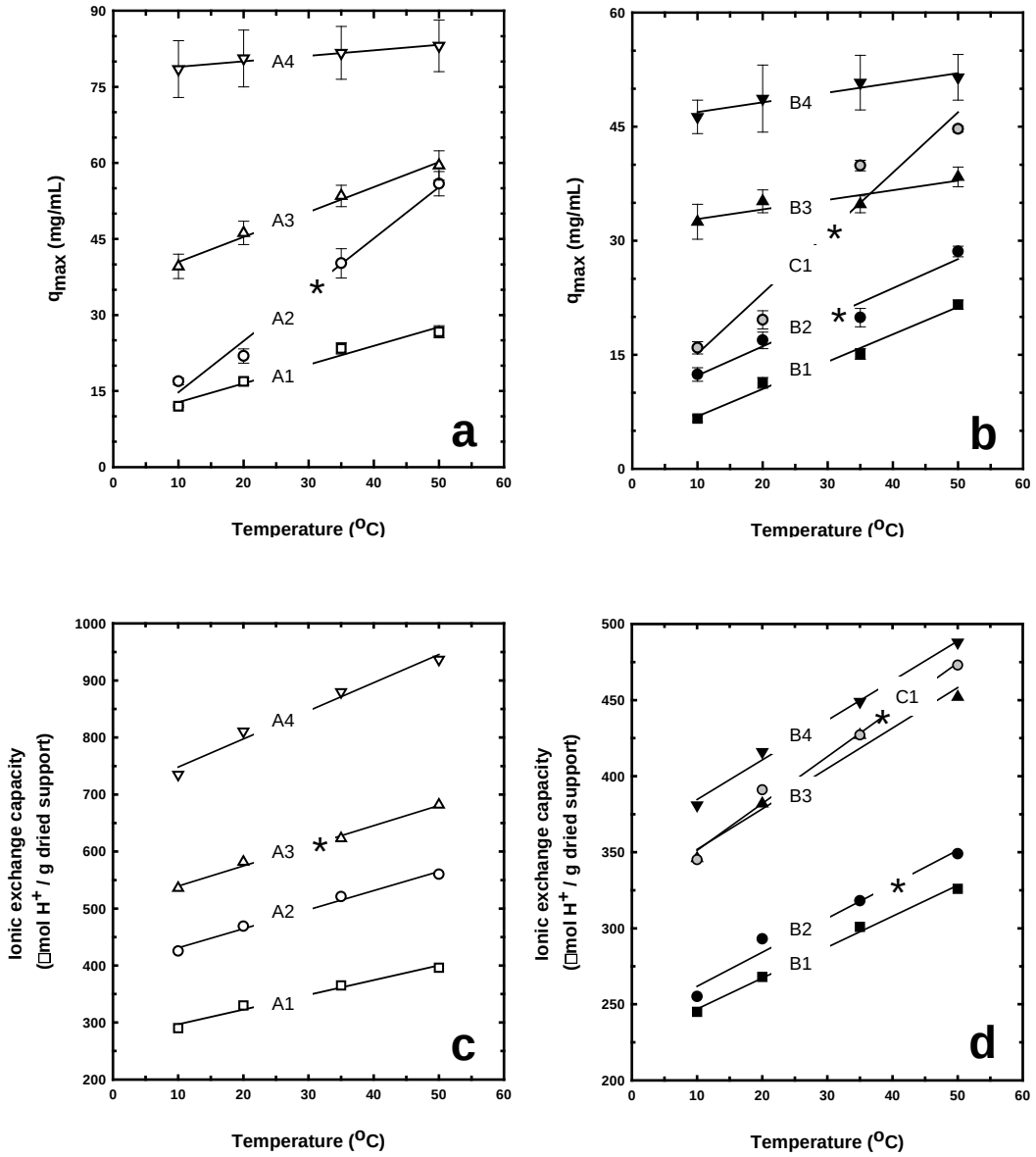

Fig. 3.6 Effect of temperature on the maximum LF adsorption capacity (q_{max}) on (a) thermoCEX-CL6B supports (open circles) and (b) thermoCEX-S6PG (filled black circles) and thermoCEX-S12PG (filled grey circles); and effect of temperature on the ionic capacity of (c) thermoCEX-CL6B supports (open circles) and (d) thermoCEX-S6PG (filled black circles) and thermoCEX-S12PG (filled grey circles). The asterisks next to supports A2, B2 and C1 indicate those initially selected for TCZR chromatography. The solid lines represent linear fits to the data.

Fig. 3.7 shows adsorption isotherms obtained for the binding of LF to these at different temperatures, and Table 3.3 presents the fitted Langmuir parameters. At the lowest temperature of 10 °C, the binding of LF to all three thermoCEX adsorbents is rather weak (K_d values between 0.82 and 4.8 mg/mL) and of low capacity (q_{max} values <17 mg/mL), but as the temperature is gradually stepped up, the tightness and capacity of LF sorption rise strongly. At the highest temperature of 50 °C, the paired values for q_{max} and tightness of binding (initial slope, q_{max}/K_d) are 55.9 mg/mL and 621 for support 'A2', 28.6 mg/mL and 168 for 'B2', and 44.7 mg/mL and 213 for support 'C1' (Table 3.3). An identical pattern of behaviour in response to temperature (between 20 and 50 °C) was noted previously by Maharjan et al. (2009) for a thermoCEX support fashioned out of Sepharose 6 FF. The ranking of static LF binding performance of this family of thermoCEX supports of 'Sepharose CL-6B > Superose 12 prep grade > Superose 6 prep grade > Sepharose 6 FF' (initial slope values at 50 °C of 621, 213, 168 and 120 respectively) is not correlated with mass of copolymer attached (respectively 4177, 5495, 5733, 2060 µmol/g dried support), nor the tBAAm content (respectively 501, 604, 516, 165 µmol/g dried support), but rather with the support's intrinsic ionic capacity (i.e. 469 µmol > 391 µmol > 293 µmol > 154 µmol H^+/g dried support).

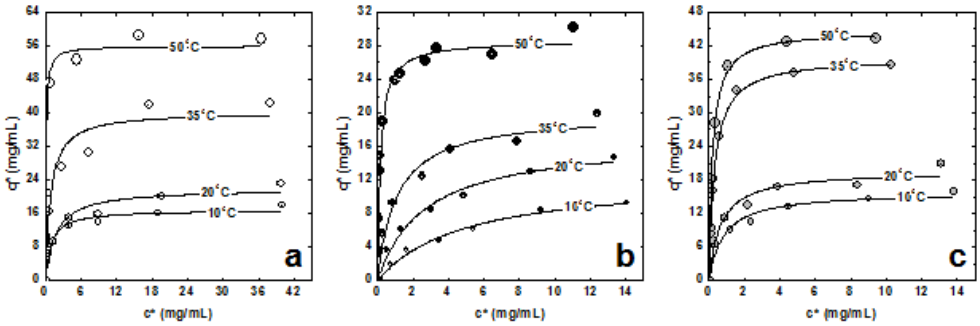

Fig. 3.7 Equilibrium isotherms for the adsorption of LF to thermoCEX supports initially selected for TCZR chromatography (Fig. 3.8) A2 (a), B2 (b), and C1 (c) at 10, 20, 35 and 50 °C. The solid lines through the data points represent fitted Langmuir curves with parameter values presented in Table 3.3.

Table 3.3 Langmuir parameters[a] describing the adsorption of LF at 10, 20, 35, 50 °C to three different thermoCEX media prepared under identical conditions using a common initial 'NIPAAm: tBAAm: AAc' ratio of '90: 5: 5' (Table 3.1 and Table 3.2)

Support (ionic capacity)	Temperature (˚C)	q_{max} (mg/mL)	K_d (mg/mL)	Initial slope, q_{max}/K_d
thermoCEX-CL6B A2 (40.7 µmol H^+/mL)	10	16.9 ± 0.7	0.93 ± 0.19	18.2
	20	21.9 ± 1.4	1.66 ± 0.48	13.2
	35	40.2 ± 2.9	0.83 ± 0.34	48.4
	50	55.9 ± 2.4	0.09 ± 0.03	621.1
thermoCEX-S6PG B2 (25.4 µmol H^+/mL)	10	12.4 ± 0.9	4.79 ± 0.83	2.6
	20	16.9 ± 1.1	2.63 ± 0.52	6.4
	35	19.9 ± 1.2	1.09 ± 0.26	18.3
	50	28.6 ± 0.7	0.17 ± 0.02	168.2
thermoCEX-S12PG C1 (34.8µmol H^+/mL)	10	15.9 ± 0.8	0.82 ± 0.20	19.39
	20	19.6 ± 1.2	0.65 ± 0.20	30.2
	35	39.9 ± 0.7	0.32 ± 0.03	124.7
	50	44.7 ± 0.4	0.21 ± 0.01	212.9

[a]Fig. 3.7 adsorption data were fitted to the Langmuir model.

Fig. 3.8 compares chromatographic profiles arising from batch TCZR chromatography of LF on fixed beds of three thermoCEX manufactured under identical conditions from cross-linked agarose base matrices differing in particle diameter and pore size (see Table 3.1 and Table 3.2), i.e. thermoCEX-CL6B 'A2' (Fig. 3.8a), thermoCEX-S6PG 'B2' (Fig. 3.8b) and thermoCEX-S12PG 'C1' (Fig. 3.8c). A striking similarity is instantly evident,

namely that every movement of the TCZ results in a sharp LF elution peak. Of greater importance, however, are the differences. Following 8 movements of the TCZ along beds of the thermoCEX-CL6B 'A2' (Fig. 3.8a) and thermoCEX-S6PG 'B2' (Fig. 3.8b), the percentages of eluted LF recovered in peaks '*a*' to '*h*' combined were practically the same, i.e. 64.6% of that initially bound for thermoCEX-CL6B 'A2' *cf.* 67.1% for thermoCEX-S6PG 'B2'. But whereas just over half (54.4%) of the thermally eluted LF from all 8 peaks ('*a* – *h*') was recovered by the first movement of the TCZ (peak '*a*') along the thermoCEX-CL6B 'A2' column (Fig. 3.8a), peak '*a*' accounted for more three-quarters (76.6%) of the combined thermally eluted LF (*a* – *h* inclusive) from thermoCEX-S6PG 'B2' (Fig. 3.8b). Twelve movements of the TCZ were employed during TCZR chromatography on thermoCEX-S12PG 'C1'. In this case, eluted LF recovered in peaks '*a* – *l*' was just 58.3%, and the first movement of the TCZ accounted for only 17.5% of combined thermally eluted LF ('*a* – *l*').

Achieving significantly higher LF desorption with a single movement of the TCZ, i.e. approaching the 100% level, would require the absence of both mass transport limitations and LF binding at the minimum column temperature of 12.4 °C. Clearly, neither condition applies. Inspection of Fig. 3.7 and Table 3.3 confirm that LF is still able to bind to the thermoCEX media at 10 °C albeit weakly, thus at 12.4 °C in the TCZR system some LF will inevitably remain bound. Further, evidence of significant limitations on mass transport during TCZR mediated elution (though noticeably less marked for thermoCEX-S6PG 'B2') is provided by the observation that LF elution continued up to and

including the last TCZ movement for all three matrices (Fig. 3.8). Because the total amounts of LF eluted on approaching equilibrium (after 8 movements of the TCZ) were essentially the same for thermoCEX-CL6B ‘A2’ and thermoCEX-S6PG ‘B2’, the lower LF binding strength of thermoCEX-S6PG ‘B2’ cannot adequately explain its improved LF recovery following the first TCZ movement (peak ‘*a*’ in Fig. 3.8 a & b). Instead, differences in particle size and pore diameter (highlighted in Table 3.1 and Table 3.2) manifested in form of pore diffusion limitation, likely account for the significant disparity in % LF desorption observed following the first TCZ movement along packed beds of the three different thermoCEX media, i.e. 76.6% for thermoCEX-S6PG ‘B2’ *cf.* 54.4% for thermoCEX-CL6B ‘A2’ *cf.* 17.5% for thermoCEX-S12PG ‘C1’.

Consider the case of a target protein adsorbed close to the centre of a thermoCEX support particle. If such a species is to be desorbed by the temperature change effected by the TCZ, it must diffuse out of the support particle’s pores and into the mobile phase to be eluted from the column. However, should the time required for this diffusion process be greater than the TCZ’s contact time with the region of the column where the support resides, the target protein will re-adsorb en route and hence will not contribute to the elution peak. The advantage of smaller adsorbent particle diameters and adequately large pores for TCZR application with protein adsorbates is therefore clear. Smaller particles dictate shorter diffusion paths, while large pores provide less of an impediment to mass transfer of large macromolecules (Langford et al., 2006). This combination leads to reduced times for the diffusion process, culminating practically in fewer numbers of

movements of the TCZ to achieve a desired target desorption yield, and is displayed best in this work by the Superose 6 prep grade based thermoCEX matrix.

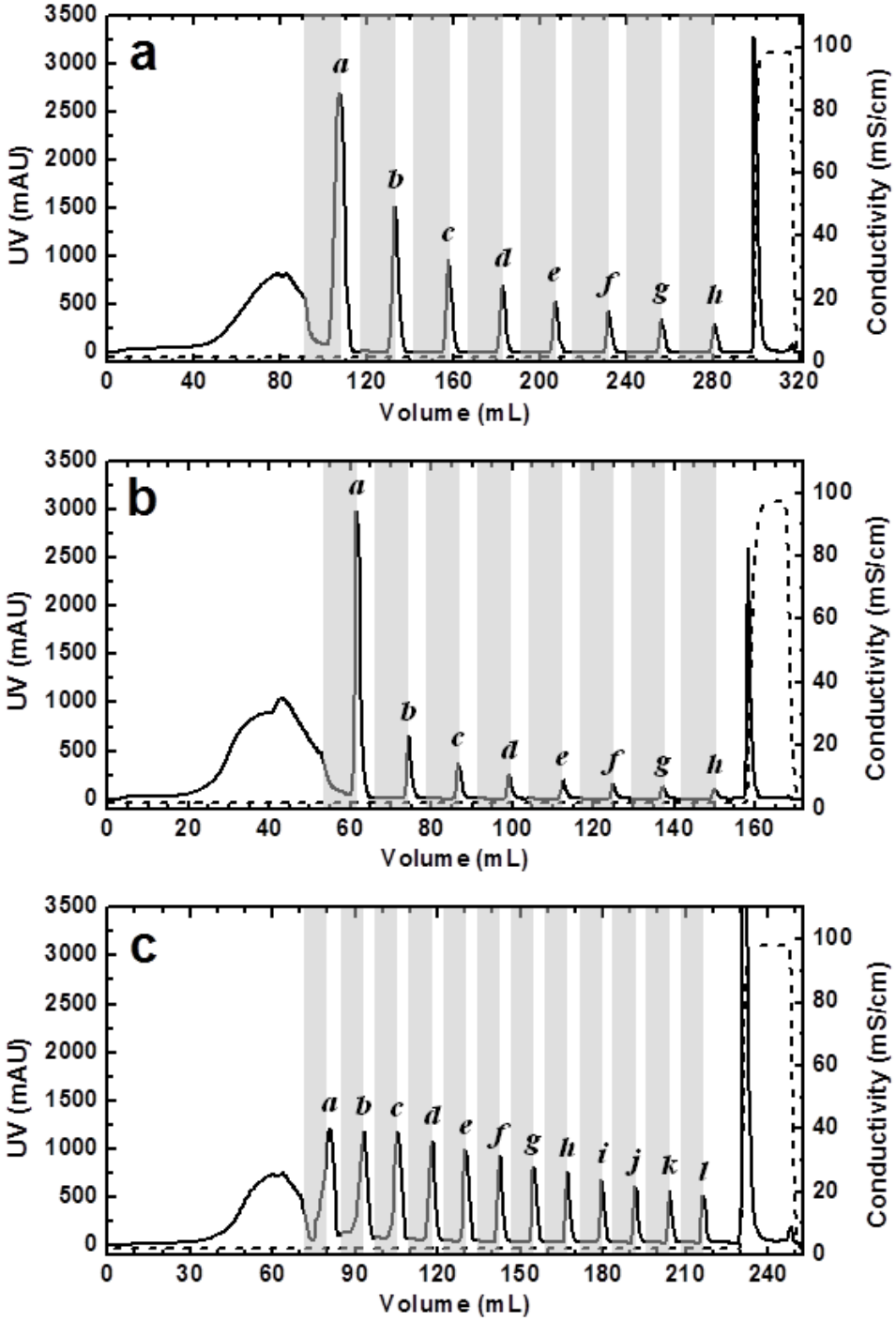

Fig. 3.8 Chromatograms arising from TCZR tests conducted with thermoCEX supports A2 (a), B2 (b) and C1 (c), employing multiple movements of the TCZ at a velocity, v_c, of 0.1 mm/s. Columns were saturated with LF (c_f = 2 mg/mL) and washed at the binding temperature (35 °C) prior to initiating the first of eight (a & b) or twelve (c) sequential movements of the TCZ. Unshaded regions indicate column operation at a temperature of 35 °C with the TCZ in its 'parked' position. Grey shaded zones indicate the periods when the TCZ moves along the column. The solid and dashed lines represent the absorbance and conductivity signals respectively.

3.4.4 Continuous protein accumulation experiments

In our first series of continuous TCZR chromatography experiments, the influence of the target protein concentration (c_f) on total system performance during continuous feeding and 8 movements of the TCZ along the column was examined using LF as the model binding component and thermoCEX-S6PG 'B2' as the column packing material. Chromatograms corresponding to continuous feeding of LF at 0.5 mg/mL and 1 mg/mL are shown in Fig. 3.9 a & b respectively. In both cases, residual bound LF not desorbed by the TCZ was eluted after the last movement by raising the mobile phase's ionic strength.

Visual comparison of the 8 individual eluted peaks (*a* – *g*) within each chromatogram suggests a certain time is required before the profiles and peak areas become uniform (i.e. 4 movements at c_f = 0.5 mg/mL and 3 movements at c_f = 1 mg/mL), and the quantitative analysis in Table 3.4 confirms this. Quasi-stationary states are effectively reached from peaks '*d*' (c_f = 0.5 mg/mL) and '*c*' (c_f =1 mg/mL) onwards, where the mass of LF eluted in each peak remains essentially constant (i.e. 14.2 ± 2.1 mg and 30.7 ± 1.3 mg for the low and high LF feed concentrations respectively) and small traces of LF are lost in the flowthrough between successive individual elution peaks (i.e. averages of 1.5 and 2.6 mg for low and high LF feed conditions respectively). The observation that steady state was reached later, when feeding the lower strength LF feed, merits explanation. Attaining a quasi-stationary condition is only possible after the TCZ has completed its transit and the protein loading across the full column length approaches equilibrium. Under such circumstances, the amount of protein temporarily loaded at the elevated

temperature T_B, (with the TCZ parked outside, Fig. 3.3a) will be constant. From this it follows that raising the protein concentration in the feed should speed the acquisition of a steady state.

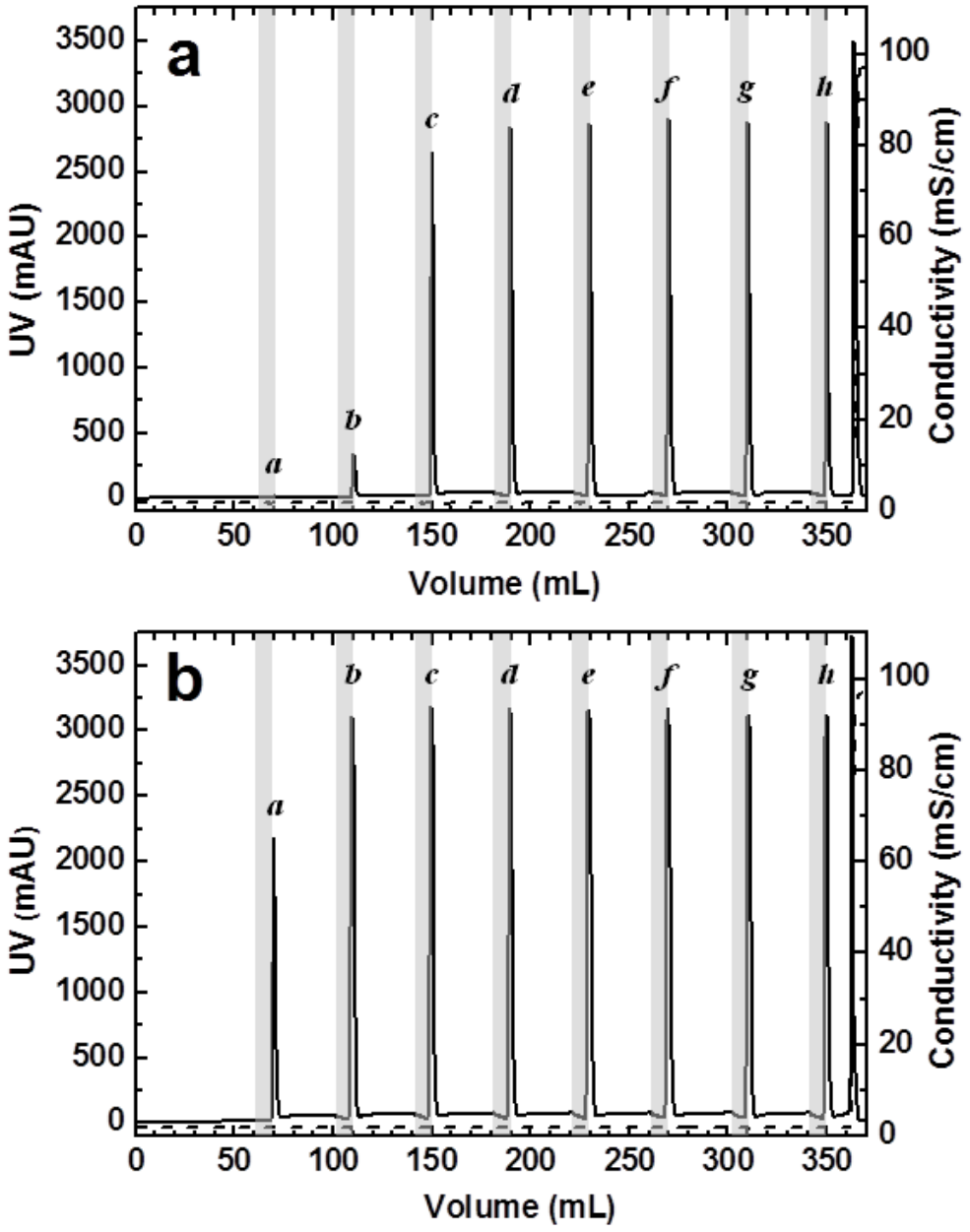

Fig. 3.9 Chromatograms arsing from TCZR tests conducted with thermoCEX support B2 employing eight movements of the TCZ at a velocity, v_c, of 0.1 mm/s. The columns were continuously supplied with LF at concentrations c_f of (a) 0.5 mg/mL and (b) 1.0 mg/mL. Unshaded regions indicate column operation at a temperature of 35 °C with the TCZ 'parked'. Grey shaded zones indicate the periods when the TCZ moves along the column. The solid and dashed lines represent the absorbance and conductivity signals respectively.

Another important parameter influenced by the protein concentration in feed is averaged concentration factor, *CF*, (Eq 3.2) attainable during steady state operation. The *CF* reached 9.2 at c_f = 0.5 mg/mL (Fig. 3.9a), but dropped to 7.9 on increasing the LF concentration in the feed twofold (Fig. 3.9b). An explanation for the slight reduction in *CF* with increasing LF concentration can be found in the isotherm describing LF adsorption to thermoCEX-S6PG 'B2' at 35 °C (Fig. 3.7b); i.e. isotherm starts to become non-linear between 0.5 and 1 mg LF per mL.

Table 3.4 LF contents in peaks *a* – *h* obtained following eight sequential movements of the cooling zone during continuous feeding of LF (c_f = 0.5 and 1 mg/mL) to a column filled with the thermoCEX-S6PG B2 matrix (see Table 3.2)

LF concentration in feed (mg/mL)	LF content (mg) in peak:							
	a	*b*	*c*	*d*	*e*	*f*	*g*	*h*
0.5	0.0	1.46	10.5	12.3	13.4	14.5	17.8	13.2
1.0	7.54	28.9	31.3	31.2	31.4	30.6	31.7	28.1

3.4.5 Continuous separation of a binary protein mixture

The ability of TCZR to function continuously having been established (Fig. 3.9, Table 3.4), the next step was to test TCZR's feasibility to not only accumulate and concentrate a single target protein, but to continuously separate it from a protein mixture. For this we employed a simple binary protein mixture consisting 1 mg/mL LF and 1 mg/mL BSA in a 10 mM sodium phosphate pH 6.5 buffer. At this pH the binding species LF carries an overall cationic charge, whereas the BSA is negatively charged. The experiment was conducted in a similar manner to the LF accumulation study reported above (Section 3.4.4, Fig. 3.9), and Fig. 3.10 shows the chromatogram obtained. Shortly after applying the protein mix to the column, the UV signal stepped steeply to ~350 mAU where it remained (first flowthrough pooled 'a') until directly after the first

of 8 individual movements of the TCZ (highlighted by shaded grey bars). Each TCZ movement led immediately to a sharp (>2750 mAU) symmetrical elution peak, and the UV signal of the flowthrough between each temperature mediated elution peak rapidly returned to roughly constant threshold of ~500 mAU. Following the 8th TCZ motion, residually bound protein was desorbed from the column by a step change in ionic strength (S).

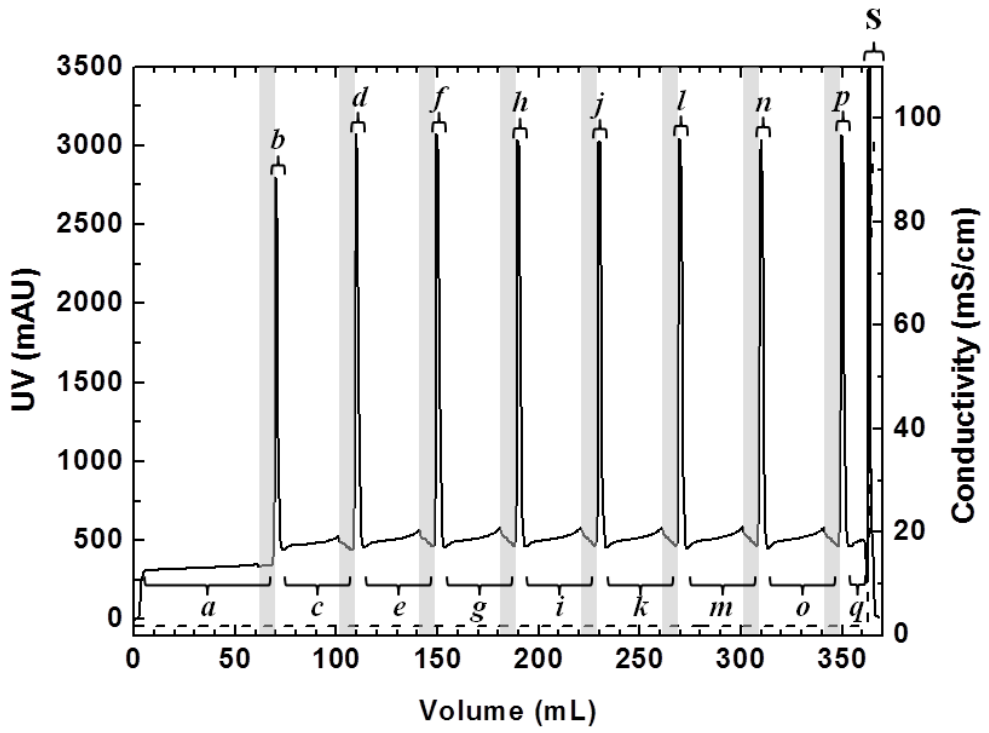

Fig. 3.10 Chromatogram arising from TCZR test conducted with thermoCEX support B2 during continuous feeding of a binary protein mixture (1 mg/mL LF + 1 mg/mL BSA) and movement of the TCZ at a velocity, v_c, of 0.1 mm/s. Unshaded regions indicate column operation at a temperature of 35 °C with the TCZ 'parked'. Grey shaded zones indicate the periods when the TCZ moves along the column. The solid and dashed lines represent the absorbance and conductivity signals respectively. SDS-PAGE analysis of pooled flowthrough (*a, c, e, g, i, k, m, o & q*); peak (*b, d, f, h, j, l, n & p*) and salt-stripped (S) fractions are shown in Fig. 3.11.

SDS-PAGE analysis of the feed (F), pooled flowthrough (*c*, *e*, *g*, *i*, *k*, *m*, *o* & *q*), peak (*b*, *d*, *f*, *h*, *j*, *l*, *n* & *p*) and salt-stripped (S) fractions corresponding to the chromatogram in Fig. 3.10 is presented in Fig. 3.11. Commercial BSA and LF

were employed in this work, and neither protein was subjected to further purification prior to use. Thus, the binary 'LF+BSA' mixture used actually contained many additional species present in trace quantities. Cation exchange chromatography had been employed as the main purification step for the ~96% pure LF, and all but one contaminant species observable in Fig. 3.11(esp. noticeable in pool 'S') emanates from this preparation. Only two species within the BSA preparation are observed in Coomassie Blue stained electrophoretograms following SDS-PAGE, i.e. the 66.4 kDa monomer accounting for >98% of the BSA content, and a much lower intensity 130.5 kDa dimer contaminant. The intensities of the lower migrating BSA monomer and upper dimer species remain constant across all flowthrough and peak fractions indicating their continued presence in the mobile phase throughout the run. The early UV signal surge to 350 mAU in Fig. 3.10 (flowthrough pool '*a*') is primarily due to breakthrough of BSA (see Fig. 3.11, only a small percentage of the feed's LF is noted in pool '*a*'); the sharp strong peaks, on the other hand, arise from the accumulation on and subsequent temperature mediated elution of LF along with small traces of numerous contaminants of the LF preparation (Fig. 3.11) from the adsorbent bed. The increase in UV signal from 350 mAU for the flowthrough pool '*a*' to 500 mAU for all inter peak flowthroughs (pools *c*, *e*, *g*, *i*, *k*, *m*, *o*, & *q*) is due to LF leakage. The addition of 1 mg/mL BSA to the 1 mg/mL LF feed did not disturb the time taken to attain quasi-stationary state; in both cases this was reached from the third peak on (compare Fig. 3.9b and Fig. 3.10). However, the average eluted LF mass per peak and concentration factors were significantly lower (i.e. 21.4 mg *cf.* 30.7 mg & *CF* = 6.3 *cf.* 7.9), and the loss of LF in the flowthrough between

successive elution peaks was much higher (12.2 *cf.* 2.6 mg). Nevertheless, the mean purity of LF in eluted peaks was ~86%.

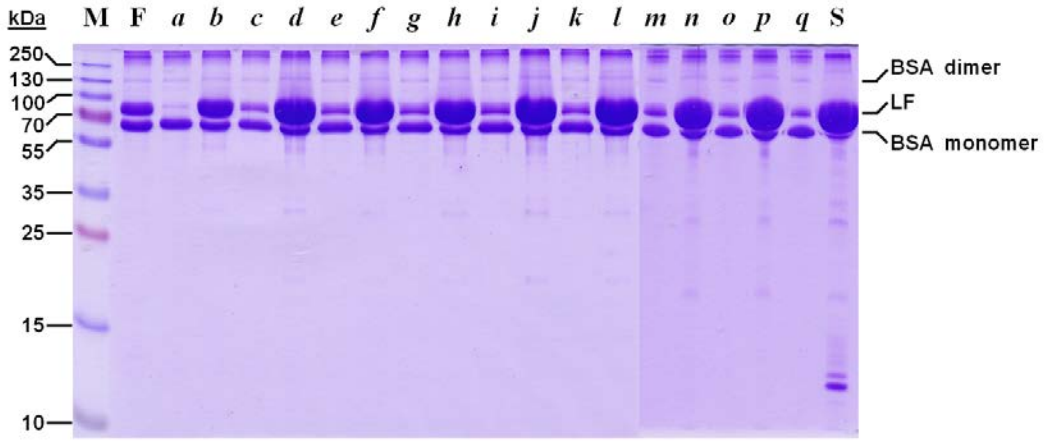

Fig. 3.11 Reducing SDS 15% (w/v) polyacrylamide gel electrophoretogram corresponding to the chromatogram shown in Fig. 3.10. Key: molecular weight markers (M); feed (F); flowthrough fractions (*a, c, e, g, i, k, m, o & q*); peak fractions (*b, d, f, h, j, l, n & p*) and salt-stripped fraction (S).

Reasons for impaired LF recovery in the presence of BSA are presently unclear. The presence of small amounts of BSA in the NaCl stripped pool 'S' (Fig. 3.11) illustrates that a tiny fraction of applied BSA had been adsorbed sufficiently strongly to resist desorption by 8 movements of the TCZ. The occurrence of BSA in the strip fraction 'S' and unbound fractions (pools *a*, *c*, *e*, *g*, *i*, *k*, *m*, *o*, & *q*) raises the possibility of two or more distinct BSA species, i.e. those that electrostatically repelled, and others that bind strongly and possibly unfold and spread on the thermoCEX matrix at 35 °C. Such a scenario could occur were the distribution of exposed hydrophobic and charged monomers within the collapsed copolymer non-uniform, such that highly hydrophobic clusters or islands are created occupying a few percent of the overall binding surface. In this instance a slight drop in the adsorbent's LF binding capacity, but not in its LF binding affinity, would be anticipated.

A more satisfactory explanation for the reduction in both LF binding strength and capacity in the presence of BSA is fouling of binding interface by the lipids it carries. Long-chain free fatty acids (FFAs) are found in many bioprocess liquors (e.g. fermentation broths), but their influence on fouling of chromatography media and membrane units has gone largely ignored owing to their low concentrations and poor solubility (Brinck et al., 2000; Jin et al., 2010). Serum albumin's principal role *in vivo* is to bind otherwise insoluble long-chain fatty acids released into the blood from adipose cells and transport them within circulating plasma, and the effectiveness with which it binds FFAs is highlighted by the fact that the solution concentration of a given long-chain FFA can be increased as much 500 fold in its presence (Spector et al., 1969). To date, most chromatographic studies with BSA have employed commercial preparations substantially pure with respect to protein, but not free of lipids. Procedures for delipidation of serum albumin usually involve extraction with organic phases at elevated temperatures or sorption of free fatty acids (FFAs) onto activated charcoal at elevated temperature under acidic–neutral conditions (Chen, 1967; Spector et al., 1969). Under the operating conditions employed here, i.e. mobile phase of pH 6.5, temperature of 35 °C, FFA binding to BSA is weak (Chen, 1967) and FFA solubility is comparatively high (Brinck et al., 2000); it is conceivable that FFAs bind to and foul the copolymer binding surface, thereby reducing both the adsorbent's binding affinity and occupancy for LF.

3.5 Conclusions

The fabrication and detailed characterisation of porous beaded thermoCEX adsorbents varying in particle size, pore dimensions and grafted poly(*N*-isopropylacrylamide-*co*-*N*-tert-butylacrylamide-*co*-acrylic acid) composition has been done for two main reasons, i.e. to (i) challenge an earlier hypothesis (Müller et al., 2013) that intra-particle diffusion of desorbed protein out of the support pores is the main parameter affecting TCZR performance; and (ii) identify an effective adsorbent customised for TCZR chromatography. ThermoCEX matrices with moderate levels of NIPAAm replacement (by *N*-tert-butylacrylamide and acrylic acid) displayed the best combination of thermoresponsiveness and LF binding capacity. Head-to-head batch TCZR chromatography tests with LF and three such materials confirmed the advantage of small particles with adequately sized pores, namely faster diffusion leading to fewer numbers of TCZ movement to attain a set desorption yield.

Chromatographic separations of proteins are typically performed in batch mode requiring sequential steps of equilibration, loading, washing elution and regeneration. Unless fully optimised, a common feature is inefficient use of the separation medium. The switch from batch to continuous operation promises several advantages, key of which is more efficient utilisation of the bed (Lay et al., 2006). Several continuous chromatography formats have been developed and applied for the separation of biomacromolecules thus far, including Continuous Annular Chromatography (Giovannini and Freitag, 2002), Continuous Radial Flow Chromatography (Lay et al., 2006), Simulated Moving

Bed in various guises (Andersson and Mattiasson, 2006; Park et al., 2006; Palani et al., 2011), and Periodic Counter-current Chromatography (Godawat et al., 2012). The new addition described here, Continuous Travelling Cooling Zone Reactor Chromatography, employs a single column operated isocratically. The simplicity of its configuration notwithstanding the main benefits over batchwise operation include reduced solvent and buffer component usage, time savings and increased productivity. The continuous steady state accumulation on and regular cyclic elution of the thermostable basic protein, LF, from a fixed bed of a thermoresponsive cation exchange adsorbent in the form of sharp uniformly sized peaks has been demonstrated in this work. The time required to reach quasi steady state operation and the degree of concentration attained on TCZ mediated elution appear inversely related to the concentration of LF being continuously supplied to the bed. The addition of the non-binding species, BSA, to the LF feed had unexpectedly deleterious effects on lactoferrin accumulation and recovery; the latter being tentatively attributed to fouling of the thermoCEX matrix by lipids carried into the feed by serum albumin. No evidence of temperature induced protein unfolding during TCZR chromatography was observed in the current study, but it remains a potential problem, especially for more thermolabile proteins. Non-NIPAAm based thermoresponsive polymers tuned to transition at lower temperatures should mitigate this concern (Li et al., 2013; Müller et al., 2013).

Currently, the primary limiters on TCZR system throughput come from the necessary use of low flow rates – a direct consequence of the prevailing mass transfer limitations. In the present example the sorbate, LF, must diffuse into

and back out of individual thermoCEX adsorbent beads within a period of ~3 minutes. A small particle diameter combined with sufficiently large pores is necessary in this instance (hence Superose 6 prep grade's superiority over Sepharose CL-6B and Superose 12 prep grade), and the magnitude of the interstitial fluid velocity is practically constrained to ~1 mm/s (i.e. ~10 times the TCZ's minimum speed of 0.1 mm/s). It should be possible to overcome the above issues by using thermoresponsive adsorbents fashioned from either more pressure tolerant smaller uniformly sized support particles with similar pore dimensions, or monolithic materials (Peters et al., 1997; Li et al., 2013; Nagase et al., 2013). Future work on TZCR will explore this tenet.

Instead of simply increasing the column diameter of TCZR due to heat transfer issue, a design of multiple small columns (maximum inner diameter could be reached to 2 cm) nested in a common cooling block could be a possibility for scale-up of TCZR (see the layout in Fig. 7.6).

4 Integrated system for temperature-controlled fast protein liquid chromatography. III. Poly(ethylene glycol) based thermoresponsive cation exchange adsorbents in TCZR chromatography

4.1 Abstract

Following the successful integrated approach of comprising NIPAAm grafted thermoCEX adsorbents and the new TCZR arrangement, another more cost-effective and environmentally friendly thermoresponsive polymer – poly(ethylene glycol) (PEG) is introduced to substitute NIPAAm for the preparation of a new type of thermoCEX-PEG support in this study. FT-IR, gravimetry and chemical assays allowed precise determination of the adsorbent's copolymer composition and loading. In static binding studies with LF, the binding affinity and maximum adsorption capacity of thermoCEX-PEG adsorbents increased smoothly with temperature increased across the LCST, however, the magnitude of $q_{max,\ 50\ °C}$ of thermoCEX-PEG adsorbents is much less than that of thermoCEX supports produced in our previous studies (i.e. $q_{max,50°C}$ of thermoCEX-PEG-S6PG D2 , thermoCEX-CL6B A2, and thermoCEX-S6PG B2 are 19.8, 55.9 and 28.6 mg/mL respectively). Consequently, the 'adsorption-desorption' performance of thermoCEX-PEG adsorbent 'D2' in the TCZR has also been found worse than that of thermoCEX supports 'A2' and 'B2'. Only 36.9% of the lactoferrin bound at 35 °C can be recovered via 8 successive movements of the cooling zone at a velocity of 0.1 mm/s; and only 34.4% of the recovered protein was eluted in

the first peak. Testing of more monomers compositions for the polymerisation and substitution of AAc with alternative anionic monomers are two optional approaches to improve the 'adsorption-desorption' behaviour of thermoCEX-PEG adsorbents in future works.

4.2 Introduction

As the representative of smart temperature-sensitive or thermoresponsive polymers, poly(*N*-isopropylacrylamide) or pNIPAAm which processes a LCST around 32 °C has been most studied and successful widely applied within biomedicine and biotechnology fields in last three decades (Heskins and Guillet, 1968; Kubota et al., 1990; Schild, 1992; Galaev and Mattiasson, 1999; Hoffman and Stayton, 2004; Matsuda et al., 2007; Maharjan et al., 2008). In stark contrast, studies and applications of another more cost-effective and environmentally friendly polymer (Duncan, 2003) – poly(ethylene glycol) (PEG) has attracted much less attention so far. One of the main reasons for this is likely to be the LCST of each individual macromonomer in PEG families is different due to various lengths of their PEG side chains, and more importantly, not suitable for the in vivo applications (i.e. poly(2-(2-Methoxyethoxy) ethyl methacrylate) (pMEO_2MA) displays a LCST in water around 28 °C, and poly(oligo (ethylene glycol) methacrylate) (pOEGMA) exhibits a LCST in water around 90 °C, respectively) (Han et al., 2003; Lutz and Hoth, 2006). However, the lower LCST of pMEO_2MA is precisely the significant advantage for us to take into the LF 'adsorption and desorption' studies with thermoresponsive adsorbents. For the copolymer of p(MEO_2MA-*co*-OEGMA), although the LCST can be tuned via adjustment of the ratio of

MEO_2MA to OEGMA ((Lutz and Hoth, 2006), Table 4.1), we only employed MEO_2MA as the thermoresponsive monomer in this study to prepare thermoCEX-PEG adsorbents.

Table 4.1 LCST of copolymer of OEGMA and MEO_2MA (Lutz and Hoth, 2006)

[OEGMA]/[MEO_2MA]	LCST (°C)
100:0	90
30:70	59
20:80	49
15:85	44
10:90	39
8:92	37
5:95	32
0:100	28

It has been confirmed via our previous studies that the advantage of small adsorbent particle diameters and adequately sized pores leads to reduced times for the diffusion process, culminating practically in fewer numbers of movements of the TCZ to achieve a desired target desorption yield, and is displayed best performance, consequently, Superose 6 prep grade was employed as the base matrix for preparation of thermoCEX-PEG adsorbents in this study because our main focus is on the support's behaviour of protein 'adsorption-desorption' with TCZR due to it's advantages (i.e. generating sharp concentrated elution peaks without tailing effects) compared to conventional system, which rely on cooling the whole column to effect elution.

The preparation and characterisation of thermoCEX-PEG adsorbents were first described. Subsequently, we examine the static LF binding capacity with the thermoCEX-PEG-S6PG supports families (i.e. 'D1', 'D2' and 'D3'), and then apply the identified optimal adsorbent 'D2' into TCZR arrangement in

order to explore the dynamic LF ‘adsorption-desorption’ performance tuned via temperature.

4.3 Experimental

4.3.1 Materials

Bovine whey lactoferrin (MLF-1, Cat. no. 12011506, ~96%) was received as a gift from Milei GmbH (Leutkirch, Germany). Superose 6 prep grade (Cat. no. 17-0489-01, Lot. no. 10037732) was obtained from GE Healthcare Life sciences (Little Chalfont, Bucks, UK). The chemicals, 2-(2-Methoxyethoxy) ethyl methacrylate (Cat. no. 447927, 95%, MEO_2MA), acrylic acid (Cat. no. 147230, anhydrous, 99%, AAc), 2-ethoxy-1-ethoxycabonyl-1,2-dihydroquinoline (Cat. no. 149837, ≥99%; EEDQ), 4,4’-azobis(4-cyanovaleric acid) (Cat. no. 11590, ≥98%; ACV), *N,N*-dimethylformamide (Cat. no. 270547, >99.9%; DMF), *N,N’*-methylenebisacrylamide (Cat. no. 146072, 99%; MBAAm), epichlorohydrin (Cat. no. E1055, 99%; ECH), tetrahydrofuran (Cat. no. 34865, >99%; THF), diethyl ether (Cat. no. 309966, >99.9%), sodium borohydride (Cat. no. 71321, >99%) and sodium hydroxide (Cat. no. S5881, anhydrous, >98%) were purchased from the Sigma-Aldrich Company Ltd (Poole, Dorset, UK), whereas absolute ethanol (Cat. no. E/0650DF/17, 99.8+%) and ammonia solution (Cat. no. A/3280/PB15, AR grade, 0.88 S.G., 35%) were acquired from Fisher Scientific UK Ltd (Loughborough, Leics, UK), di-sodium hydrogen phosphate (Cat. no. 4984.1, dihydrate, ≥99.5%) was from Carl Roth GmbH+Co.KG (Karlsruhe, Germany), and bottled oxygen-free

nitrogen gas was supplied by the British Oxygen Co Ltd (Windlesham, Surrey, UK).

4.3.2 Preparation of thermoCEX-PEG-S6PG adsorbents

Depended on the results from Chapters 2 & 3, Superose 6 prep grade was chosen as base matrix in this study due to the better static and dynamic protein ‘adsorption-desorption’ performance with it’s smaller particle diameters and adequately sized pores. The methods used to convert underivatised Superose 6 prep grade supports into PEG modified thermoresponsive cation exchange matrices (thermoCEX-PEG-S6PG) involve four successive steps – epoxide activation, amine capping, initiator immobilisation and ‘graft from’ polymerisation. These are detailed below and summarised schematically in Fig. 4.1.

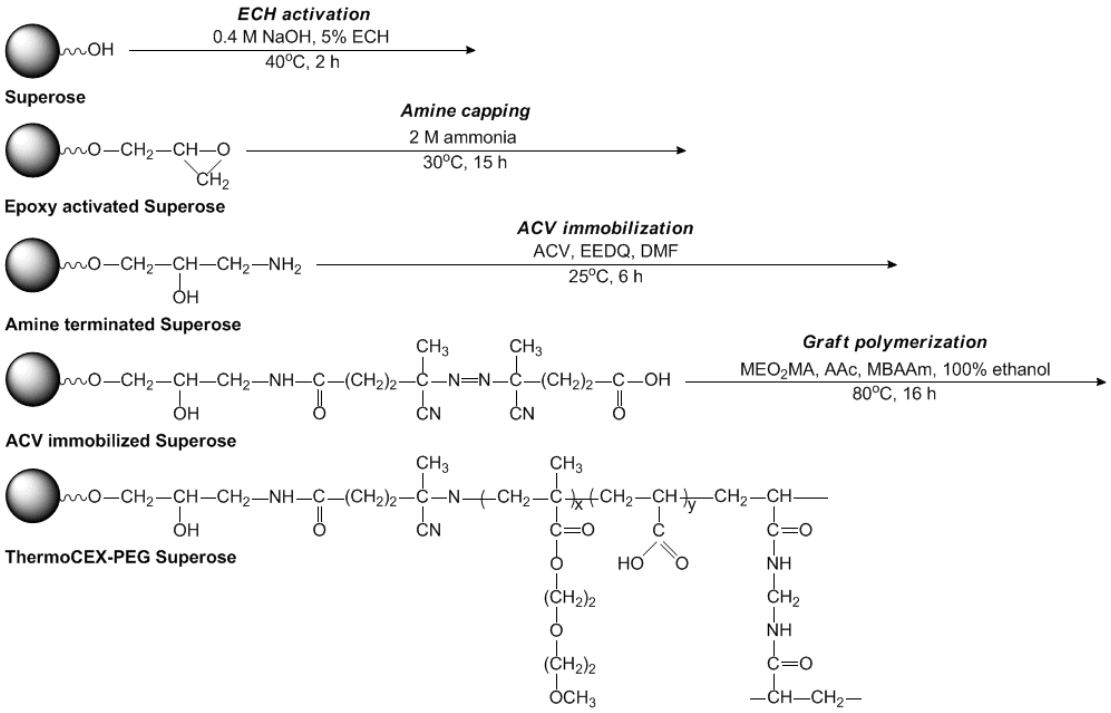

Fig. 4.1 Schematic illustration of steps involved in converting Superose 6 prep grade into thermoCEX-PEG-S6PG adsorbents (see text for details)

4.3.2.1 **Epoxy activation** (Matsumoto et al., 1979)

Washed suction-drained Superose 6 prep grade (50 g, 68 mL) were mixed with 85 mL of water in 250 mL Pyrex® conical flasks and 40 mL of 2 M NaOH before placing in a 40 °C shaking water bath (Julabo SW22, Labortechnik GmbH, Seelbach, Germany) reciprocating at 150 rpm for 0.5 h. Ten millilitres of ECH (99%) was then added to a final concentration of ~5% (v/v), and reaction was allowed to proceed at 40 °C with shaking for an additional 2 h. The resulting epoxy-activated supports were washed copiously with water under vacuum.

4.3.2.2 Amine capping

After washing, the oxirane groups of epoxy-activated Superose 6 prep grade were reacted and capped with ammonium ions using a procedure adapted from Hermansson et al. (1992). The support (47.5 g, 61 mL) were resuspended as a ~57% (v/v) slurry with 50 mL of 2 M ammonium hydroxide. After incubating overnight (~20 h) at ~30 °C with shaking at 150 rpm, the amine-terminated supports were recovered, washed exhaustively at room temperature with water in a sintered glass filter under vacuum, and then stored in 20% (v/v) ethanol at 4 °C until required.

4.3.2.3 Initiator immobilisation

The radical initiator ACV was coupled to amine-terminated Superose 6 prep grade using a modified version of Maharjan and co-workers' procedure (2009), one adapted from methods originally applied to aminated silica matrices (Kanazawa et al., 1997; Yakushiji et al., 1999; Sakamoto et al., 2004; Ayano et al., 2006a), employing EEDQ as the condensing agent. Amine-terminated supports were washed sequentially with 5 volumes each of 50%, 75% and 100% (v/v) ethanol. For each wash, the supports were mixed 'end-over-end' (0.25 h, RT, 35 rpm) on a Stuart Scientific SB1 tube rotator (Bibby Scientific Ltd, Stone, Staffs, UK), before recovering by vacuum filtration and resuspending in the next wash solution in the series. Subsequently, the drained supports (45 g, 52 mL) were resuspended with 145 mL of DMF containing 75 mM ACV and 150 mM EEDQ. While housed in a zipper-locked inflatable glove box (AtmosBag, Sigma-Aldrich, UK), nitrogen gas was bubbled through the support slurries, before tightly sealing the reaction flasks

with suba-Seal® rubber stoppers (Sigma-Aldrich, UK) and transferring to a shaking (150 rpm) water batch for 6 h of reaction at ~25 °C. The ACV coupled matrices were recovered from reaction solvent by vacuum filtration and then washed by end-over-end mixing (0.33 h, RT) and recovered by vacuum filtration, first with 5 volumes of DMF and subsequently with 5 volumes of absolute ethanol.

4.3.2.4 Graft from polymerisation of poly(MEO_2MA-*co*-AAc-*co*-MBAAm)

In this work, MEO_2MA was used as thermoresponsive monomer, and AAc was employed as anionic monomer. Three different compositions of monomers (MEO_2MA: AAc = 95: 2.5/5/10) were selected in order to identify the optimal monomers ratio for preparation of thermoCEX-PEG-S6PG adsorbents (see details in Table 4.2). The surface of ACV-Superose 6 prep grade were grafted with an immobilised lightly cross-linked (i.e. MBAAm as 1% of the total monomers) copolymer network of poly(MEO_2MA-*co*-AAc-*co*-MBAAm). The method employed in this work was essentially that described by Maharjan et al (2009), with minor modifications to pre and post washing regimes and reaction conditions. Suction-dried ACV-linked Superose 6 prep grade (25 g, 31 mL) was sequentially washed with 125 mL aliquots of 20%, 50%, 75% and 100% (v/v) ethanol in cycles of resuspension, 'end-over-end' mixing (0.33 h, RT, 20 rpm) and vacuum filtration. Subsequently, the supports were resuspended with 125 mL of ethanol containing the monomers MEO_2MA (950 mM) and AAc (25 mM/ 50 mM/ 100 mM), and the cross-linking monomer MBAAm (9.75 mM/ 10 mM/ 10.50 mM), before transferring to the environment

of a glove box and bubbling nitrogen gas through the reaction slurries. After 0.5 h the reaction flasks were tightly stoppered, and placed in a shaking water bath operated at 150 rpm and 80 °C for 16 h. The reaction mixtures were cooled to room temperature and the poly(MEO_2MA-*co*-AAc-*co*-MBAAm) grafted supports were recovered by vacuum filtration, before successively cycling through a descending ethanol concentration wash series (100%, 75%, 50%, 20%, v/v) and then with water. Each cycle involved mixing the support with 5 volumes of the appropriate solvent (0.33 h, RT, 20 rpm), followed by vacuum filtration. After the final wash, the polymer grafted supports were resuspended with 20% (v/v) ethanol and stored at 4 °C until required. The washes were retained for subsequent analysis (see Section 4.3.5).

4.3.3 Batch adsorption experiments with LF

For batch binding tests, pure LF solutions of defined concentrations (c_0 = 1-15 mg/mL) were prepared in 10 mM sodium phosphate pH 6.5. Aliquots (0.9 mL) of these LF solutions were added to 0.1 mL volumes of settled thermoCEX-PEG-S6PG supports before mixing at various temperatures between 10 and 50 °C, for 1 h with shaking (1000 rpm, Thermomixer Comfort shaker, Eppendorf, Hamburg, Germany). After an additional 0.5 h at the selected incubation temperature without shaking, the supernatants were analysed for residual protein content (see Section 4.3.5). The protein bound to the supports was determined from the difference between the protein concentration in the starting binding solution and the supernatant after binding, and where appropriate the data were fitted to the Langmuir Equation 2.1, where q^* and c^* represent the equilibrium concentrations of adsorbed and

liquid-phase protein respectively; q_{max} is the maximum protein binding capacity of the support; and K_d is the dissociation constant. Data were fitted to the model using the x^2 minimisation procedure of SigmaPlot software version 12.5 (Systat Software Inc, CA, USA).

4.3.4 ThermoCEX-PEG-S6PG supports chromatography of LF in the batchwise TCZR

The first test conducted with the TCZR was performed using a constant surrounding temperature, Φ_u, of 35 °C, and the lowest possible axial velocity of the cooling zone (v_c) of 0.1 mm/s, which generates a maximum temperature difference of 22.6 °C (i.e. during the cooling zone's progress along the column, parts of the column immediately adjacent to the centre of the cooling assembly were temporarily cooled down to 12.4 °C). The separation column (volume = 2.83 mL) was packed with thermoCEX-PEG-S6PG matrix (packing factor = 1.2) and u was maintained at 106 cm/h. Using the calculated bed voidage (ε) of 0.42, the interstitial velocity (u_i) at this mobile phase velocity was determined as 252 cm/h. LF (c_f = 2 mg/mL) in an equilibration buffer of 10 mM sodium phosphate, pH 6.5 was continuously applied to beds of thermoCEX-PEG media (packing factor = 1.2) until almost complete breakthrough had been achieved (i.e. c/c_f approaching 1). At this point the LF saturated column was then washed with 5 CVs of equilibration buffer. Thereafter, the cooling zone assembly was moved along the entire column length eight successive times at v_c = 0.1 mm/s, before finally eluting residually bound LF with 5 CV of 10 mM sodium phosphate, pH 6.5, supplemented with 1 M NaCl.

In the second test, the separation column was equilibrated, loaded with LF and washed exactly as described for the first test. Thereafter however, the cooling zone was moved along the whole column five times at different speeds (i.e. at 1.9 mm/s for the first movement, 1.0 mm/s for the second, and at 0.1 mm/s for the remaining movements, 3-5 inclusive), before once again desorbing residually bound LF with a 1 M NaCl step gradient. In these experiments, the different cooling zone velocities employed of 1.9, 1.0 and 0.1 mm/s resulted in maximum temperature difference of ~9, 12.5 and 22.6 °C, respectively.

Fractions generated during the above experiments were subsequently analysed off-line for protein content (see Section 4.3.5).

4.3.5 Analysis

4.3.5.1 Epoxide density measurement

The reactive epoxide group content introduced into Superose 6 prep grade following activation with epichlorohydrin was determined exactly as described by Sundberg and Porath (1974). The epoxy-activated resins (0.5 g, 0.64 mL) was ‘end-over-end’ mixed (1.3 h, RT, 20 rpm) with 1.5 mL of 1.3 M sodium thiosulphate solution of pH 7.0, results in the release of OH^- due to ring opening of oxiranes, which is followed by titration with 0.1 M HCl. The

support's epoxide density was determined from the amount of HCl required to maintain neutrality.

4.3.5.2 FT-IR and ATR-FTIR analysis

FT-IR analysis was employed in two ways, i.e. qualitatively for direct detection of chemical changes introduced into Superose 6 prep grade at various stages during the creation of thermoCEX-PEG-S6PG supports, and quantitatively on liquid samples, in order to determine consumption of MEO_2MA monomer, and thereby quantify the amount of MEO_2MA installed on thermoCEX-PEG-S6PG supports. For solid samples, aliquots of aqueous particle suspension were pipetted onto watchglasses and dried in an oven (60 °C, 20 h). Small quantities (~3 mg) of dried support samples were then blended with 300 mg of potassium bromide by grinding in agate mortar, until a fine, homogenous powder was produced, before pressing the mixtures into a 13 mm die using a 15 tonne Atlas manual hydraulic press (Model GS15011, Specac Ltd, Orpington, Kent, UK), producing FT-IR suitable tablets. FT-IR spectra of each tablet were recorded using a Nicolet 380 FT-IR (Nicolet 380, Thermo Fischer Scientific, Waltham, MA, USA) in direct beam mode. Sixty-four scans were averaged to yield spectra at a resolution of 2 cm^{-1}. Attenuated total reflectance FT-IR (ATR FT-IR) was employed for estimation of MEO_2MA in liquid samples. Routinely, 150 µl of each solution was applied to the surface of the Smart 53 Orbit diamond accessory of the Nicolet 380 FT-IR, and scanned 64 times at a resolution of 2 cm^{-1} in attenuated total reflection mode. A measurement without any sample in the beam was used as background to keep a relative scale for the adsorption intensity. Background measurements

were taken every 0.5 h during sample measurements. MEO_2MA and AAc give one characteristic peak in FT-IR, i.e. at ~1760 - 1690 cm^{-1} corresponding to carboxylic acid C=O stretching was employed for determination of 'MEO_2MA + AAc'. The ATR spectrum of standards, i.e. various dilutions of the initial monomer mixtures MEO_2MA: AAc: MBAAm (employed in a ratio of 95: 2.5/5/10: 0.975/1/1.05), were obtained by subtracting the spectrum of pure water from the aqueous solutions spectra. The version 7.3 OMNIC™ DS (Data Security) software (Thermo Fischer Scientific, Waltham, MA, USA), was used as the interface for data collection and processing (interpretations of interferograms and peak area measurements). The area under the C=O stretching peak of each spectrum was calculated, keeping the same region and baseline at 1765-1600 cm^{-1} during all the readings, and the combined concentration of 'MEO_2MA + AAc + MBAAm' in samples was estimated by reference to standard curves (R^2 > 0.98). The contributions to this signal from the anionic monomer, AAc, which accounted for 2.50, 5.0 and 9.4% (corresponding to the three different compositions of monomers employed in polymerisation step, see Section 4.3.2.4), and the cross-linking monomer, MBAAm, which accounted for 0.99% of the total monomer concentration, were subtracted to give a value for MEO_2MA.

4.3.5.3 Gravimetric analysis

Gravimetric analysis was routinely performed on solid supports and on dried residues arising from liquid samples, obtained throughout the different stages of thermoCEX-PEG-S6PG synthesis, and was used to allow determination of support immobilised ACV and copolymer contents, as well as the amount of

free copolymer and unreacted monomers in solution at the end of the polymerisation reaction following their separation from one another (detailed below). For solid support measurements, approximately 1 g quantities of suction-drained support samples were accurately weighed in pre-weighed glass crucibles before drying to constant weight in a 60 °C oven (~20 h), cooling to room temperature in a desiccator jar and weighing accurately on an analytical balance. Post polymer grafting (Section 4.3.2.4), the reaction supernatant and wash solutions were pooled together and evaporated to dryness in a Buchi Rotavapor-RE Rotary Evaporator KRvr-TD-65/45 (Buchi Labortechnik AG, Flawil, Switzerland). The dried residue containing ungrafted free poly(MEO_2MA-*co*-AAc-*co*-MBAAm) and unreacted monomers was resuspended in a small volume of tetrahydrofuran (THF). The free copolymer was then precipitated from solution by the addition of 10 volumes of diethyl ether. The supernatant fraction containing dissolved monomers was carefully removed, rotary evaporated to dryness, and then redissolved in 100% (v/v) ethanol for ATR FT-IR analysis. The precipitated polymer was subsequently washed with diethyl ether, dried in a 60 °C oven for 20 h and finally accurately weighed.

4.3.5.4 LCST measurement

The lower critical solution temperature (LCST) of the copolymer was determined in the standard way (Kanazawa et al., 1997; Sakamoto et al., 2004; Ayano et al., 2006a; Maharjan et al., 2009). The copolymer was resuspended at a concentration of 0.5% (w/v) in 10 mM sodium phosphate buffer, pH 6.5, and its optical transmittance at 500 nm was measured at

various temperatures in a Cecil CE7500 UV/visible dual beam spectrophotometer (Cecil Instruments Ltd, Cambridge, UK) equipped with a water thermostatted cuvette holder.

4.3.5.5 Ionic capacity analysis

The H^+ exchange capacity of the thermoCEX-PEG-S6PG support was determined by titration according to a procedure supplied by GE Healthcare (method No. 30407; for determination of the ionic capacity of CM Sepharose media) at 10, 20, 35 and 50 °C respectively in order to explore the influence of various temperatures on resin's ionic capacity.

4.3.5.6 Protein contents determination

Protein contents in samples arising from batch binding and chromatography experiments were determined by UV spectrophotometry at 280 nm in quartz cuvettes in a Lambda 20 UV-vis spectrophotometer (PerkinElmer Analytical Instruments, Shelton, CT, USA).

4.4 Results and Discussion

In order to prepare thermoCEX-PEG-S6PG, MEO_2MA was employed as thermoresponsive monomer, and AAc was continuously selected as anionic monomer. Through three different compositions of monomers (MEO_2MA: AAc = 95: 2.5/5/10), the thermoCEX-PEG-S6PG support 'D2' which with the optimal combination of thermoresponsiveness and LF binding capacity has

been identified via a battery of analyses, and subsequently applied in TCZR batchwise arrangement for detailed investigation.

4.4.1 Manufacture and characterisation of thermoCEX-PEG-S6PG

A series of analyses (FT-IR, ATR FT-IR, gravimetric measurements and titration based assays for oxirane content and ion exchange capacity) were employed in this study for exploring the physico-chemical characterisation of supports starting material, intermediate supports at every stage of the conversion (Fig. 4.1), pre and post polymerisation reaction supernatants, and the final thermoCEX-PEG-S6PG. The main results from these are illustrated in Fig. 4.2, and Table 4.2.

The thermoCEX-PEG-S6PG supports ID (i.e. ‘D1’, ‘D2’ and ‘D3’) refer to the resins prepared with different initial monomers compositions (detailed information see Table 4.2). Fig. 4.2 illustrates the detailed FT-IR spectra for dried resins from each stage synthesis of thermoCEX-PEG-S6PG matrices. All spectra are normalised for peak height at 934 cm^{-1}, as this is characteristic for the 3,6-anhydro moiety of Sepharose (Oza et al., 2010). The detailed description of FT-IR spectra for Superose 6 prep grade, epoxy-activate Superose 6 prep grade, aminated Superose 6 prep grade and ACV initiated Superose 6 prep grade has been mention previously (see Section 3.4.2).

The spectra of thermoCEX-PEG-S6PG series (‘D1’, ‘D2’ and ‘D3’) display considerable increase of peak heights in the regions of 1190 – 1120 cm^{-1}, and also 1280 – 1250 cm^{-1}, due to the contribution from carboxylic acid, ester and ether C-O stretch. A series of new or increased peaks between 1500 – 1350 cm^{-1} were noted, which are corresponding to the alkane C-H bending of introducing AAc and MBAAm into the final supports. It is not surprisingly that the peak at 1552 cm^{-1} is disappeared in thermoCEX-PEG-S6PG series due to the loss of azo N=N stretch during the polymerisation. A pronounced growth at the peak of 1736 cm^{-1} (C=O stretch) indicates the successful addition of MEO_2MA in significant amounts.

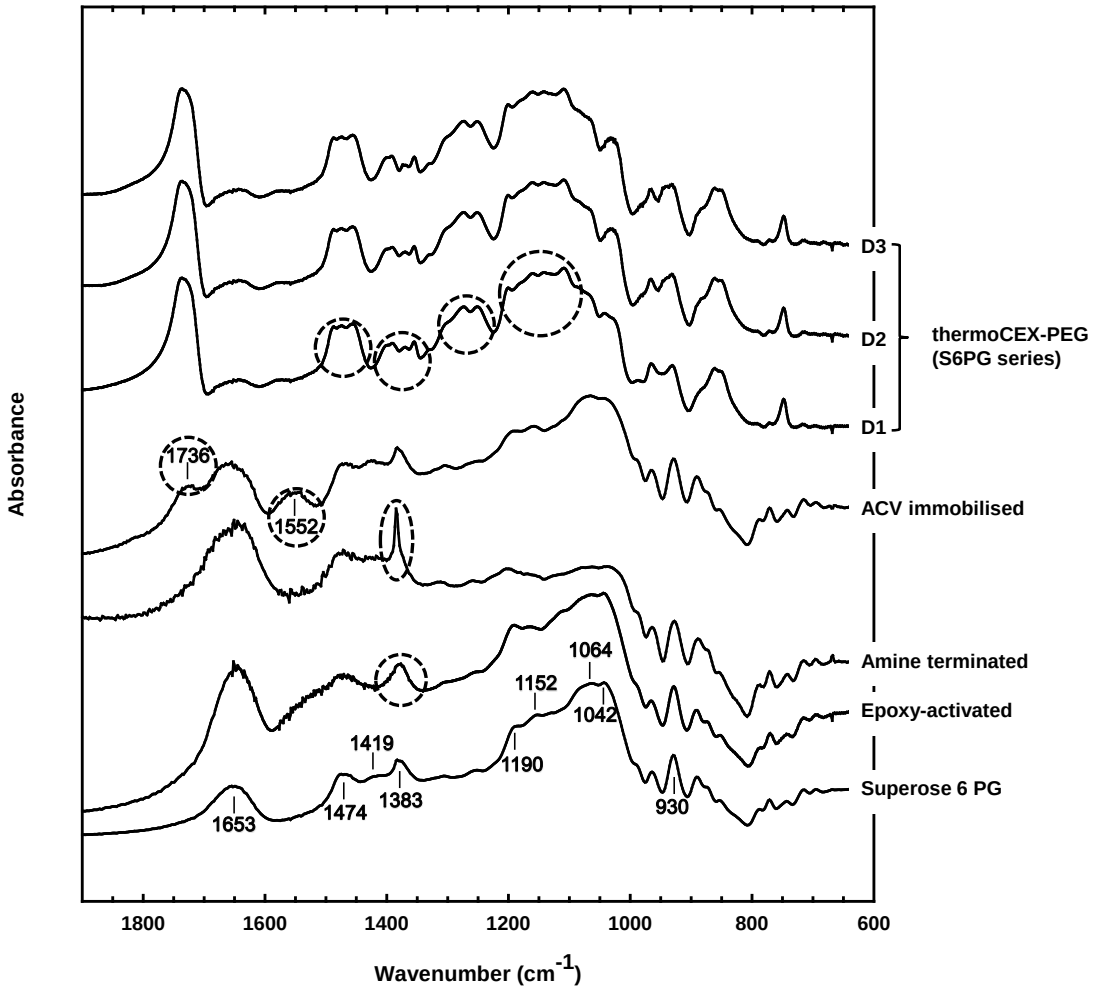

Fig. 4.2 FT-IR spectra recorded at various stages during the conversion of Superose 6 prep grade into thermoCEX-PEG adsorbents series.

Table 4.2 Characterisation of the Superose 6 PG based thermoCEX-PEG supports prepared and used in this work. See text for details.

Parameter	ThermoCEX-PEG-S6PG		
Support ID (symbol)	D1	D2	D3
Base matrix		Superose 6 PG (lot 10037732)	
Particle size distribution		20 – 40 µm (83%)	
Globular protein fractionation range, M_r		$5 \times 10^3 – 5 \times 10^6$ Da	
Step 1 Immobilised oxirane content (µmol/g dried support) [a]		878	
Step 3. Immobilised ACV content (µmol/g dried support) [b]		568	
Step 4. Free monomers entering reaction:			
'MEO_2MA: AAc' (mM)	950: 25	950: 50	950: 100
'MEO_2MA: AAc' ratio	95:2.5	95:5	95:10
Immobilised copolymer composition of thermoCEX support:			
'MEO_2MA' content (µmol/ g dried support) [b,c]	2037	1945	1914
Ion exchange capacity (µmol H^+/ g dried support)[d]	122	233	283
'MEO_2MA + AAc' content (µmol/ g dried support)	2159	2178	2197
'MEO_2MA: AAc' ratio	94.3:5.7	89.3:10.7	87.1:12.9
% monomer consumed by support:			
MEO_2MA + AAc	7.6	7.5	7.2
MEO_2MA	7.3	7.0	6.9
AAc	16.7	16.0	9.7

Key: Determined by: [a]oxirane ring opening reaction followed by titration [Sundberg and Porath, 1974]; [b]gravimetric measurement; [c]ATR-FTIR spectrometry of supernatant samples before and after polymerisation reactions; $_3$; [d]titration.

The temperature dependent phase transition behaviour of ungrafted free copolymer solutions arising from the polymerisation with ACV-immobilised Superose 6 prep grade are compared in Fig. 4.3. Fig. 4.3a illustrates the raw transmittance against temperature profiles, and Fig. 4.3b explores the wider impact of MEO_2MA replacement on the LCST and full transition temperature ranges of the copolymers.

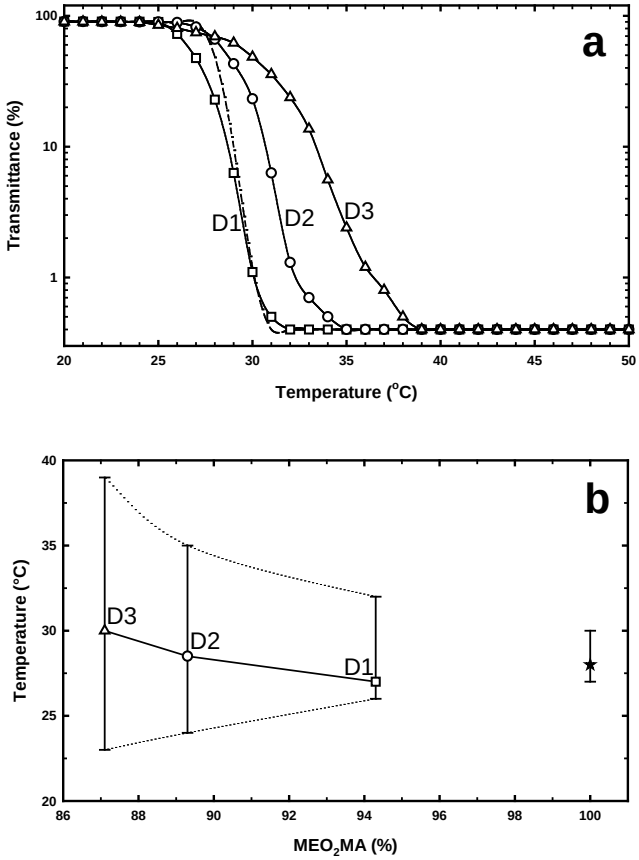

Fig. 4.3 Optical transmittance (500 nm) vs. temperature profiles for 0.5% (w/v) solutions of ungrafted free poly(MEO_2MA-*co*-AAc-*co*-MBAAm) arising during fabrication of (a) Superose 6 prep grade based thermoCEX-PEG-S6PG supports (detailed in Table 4.2), and (b) the influence of MEO_2MA content on temperature transition behaviour of the copolymers. The symbols in 'b' indicate the determined LCST values at 50% transmittance ($T_{50\%}$), capped bars define the temperature range over which phase transition occurred, and the lower dotted and upper dashed lines respectively delineate the temperatures at which full collapse ($T_{0.4\%}$) and extension ($T_{90\%}$) of the copolymer chains occurred. Key: pMEO_2MA (★); Superose 6 prep grade series (D1 – □, D2 – ○, D3 – △).

The LCST at 50% optical transmittance ($T_{50\%}$) for MEO_2MA was reported at 28 °C (Lutz and Hoth, 2006) and sharp transition from fully extended 'hydrophilic coil' ($T_{90\%}$) to fully collapsed 'hydrophobic globule' ($T_{0.4\%}$) occurred between 27 and 31 °C (dashed line traces in Fig. 4.3 a & b). The low level substitution of AAc into MEO_2MA's backbone 'D1' at the expense of 5.7% of its MEO_2MA content (Table 4.2), had the effect of lowering the LCST by 1.2 °C for 'D1' and broadening the transition temperature range in both directions, i.e. 24.5 to 32.3 °C. With mounting MEO_2MA replacement ('D2' and 'D3'), smart thermoresponsive behaviour became increasingly compromised. The LCST of 'D2' and 'D3' reached to 28.5 and 30.2 °C and temperature range over which full 'coil – globule' transition range of 'D2' and 'D3' extended as well. (i.e. from 25 to 35 °C for 'D2' and from 22 to 39 °C for 'D3').

4.4.2 Temperature dependent batch adsorption of LF on thermoCEX-PEG-S6PG

Fig. 4.4 demonstrates the equilibrium isotherms for the adsorption of LF to thermoCEX-PEG-S6PG supports series 'D1', 'D2' and 'D3', respectively at 10 °C, 20 °C, 35 °C and 50 °C. Fig. 4.5a illustrates the effect of temperature on the maximum LF adsorption capacity (q_{max}) for all three thermoCEX-PEG-S6PG supports. In all cases, LF binding capacity is increased linearly with the examined incremental temperature (10 – 50°C), It is surprisingly however, that the LF binding capacity at 10 °C of thermoCEX-PEG-S6PG 'D2' support ($q_{max,\ 10\ °C}$' = 2.0, Table 4.3) is at the same magnitude to that of 'D1', although there were nearly two-fold amount of AAc integrated into 'D2' than 'D1' (AAc% in 'D2' = 10.7%, AAc% in 'D1' = 5.7%, Table 4.2). In stark contrast, 'D2'

possessed almost double binding capacity at 50 °C compared to ‘D1’ (19.8 vs. 10.2 mg/mL, respectively), as the optimal thermoCEX-PEG-S6PG adsorbent in terms of combination of thermoresponsiveness and LF binding capacity (i.e. reasonable $q_{max,\ 50\ °C}$ and low $q_{max,\ 10\ °C}$ values), ‘D2’ was consequently employed for further analysis.

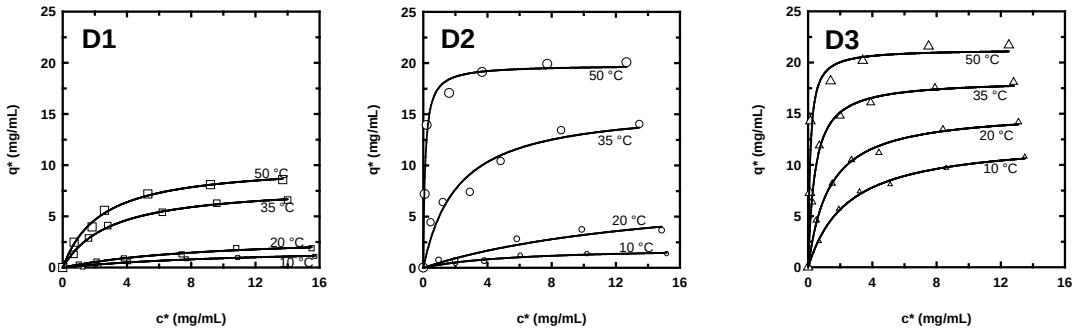

Fig. 4.4 Equilibrium isotherms for the adsorption of LF to thermoCEX-PEG-S6PG supports series D1, D2 and D3, respectively at 10 °C, 20 °C, 35 °C and 50 °C. The solid lines through the data points represent fitted Langmuir curves with parameter values presented in Table 4.3.

For all three thermoCEX-PEG-S6PG adsorbents, the ion exchange capacity rises with increased temperature (Fig. 4.5b), which means the electrostatic interaction between adsorbents and LF is stronger at higher temperature. A possible explanation is that the negative charges of tethered polymer chains become more exposed due to the conformation change of immobilised copolymer from hydrophilic coil to hydrophobic globule with the temperature increases across the LCST.

Table 4.3 Langmuir parameters describing the adsorption of LF at 10, 20, 35 and 50 ºC to the Superose 6 PG based thermoCEX-PEG supports prepared and used in this work. See text for details.

Support ID	Temperature (°C)	q_{max} (mg/mL)	K_d (mg/mL)	Initial slope, q_{max}/K_d (mL/mL)
D1	10	2.0 ± 0.4	12.26 ± 4.75	0.2
	20	3.2 ± 0.4	9.43 ± 2.56	0.3
	35	8.1 ± 0.2	2.95 ± 0.25	2.8
	50	10.2 ± 0.3	2.36 ± 0.25	4.3
D2	10	2.0 ± 0.3	5.66 ± 2.29	0.4
	20	8.3 ± 4.7	15.72 ± 14.47	0.5
	35	15.9 ± 1.6	2.14 ± 0.71	7.4
	50	19.8 ± 0.6	0.12 ± 0.02	165.0
D3	10	12.6 ± 0.4	2.43 ± 0.23	5.2
	20	15.3 ± 0.4	1.29 ± 0.12	11.9
	35	18.3 ± 0.3	0.42 ± 0.03	43.6
	50	21.3 ± 1.1	0.13 ± 0.04	163.8

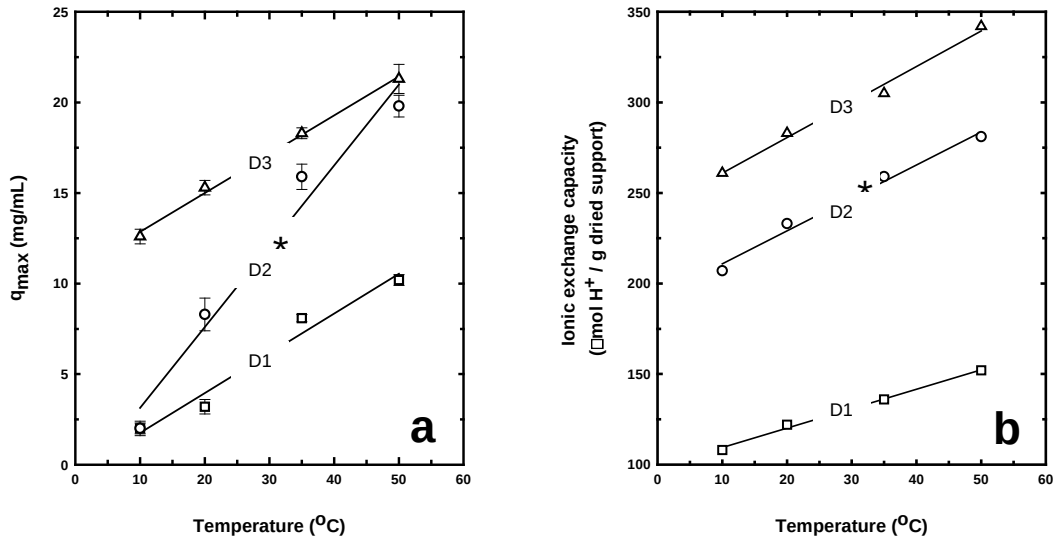

Fig. 4.5 (a) Effect of temperature on the maximum adsorption capacity (q_{max}) of LF on thermoCEX-PEG-S6PG supports and (b) effect of temperature on the ionic capacity of thermoCEX-PEG-S6PG supports. The asterisk next to supports D2 indicates that initially selected for TCZR chromatography. The solid lines represent linear fits to the data.

4.4.3 Chromatography of LF in batchwise TCZR containing thermoCEX-PEG-S6PG support

Based on the advantages of TCZR chromatography over conventional jacketed column, i.e. sharp elution peaks without tailing effects, and continuous operation (see Section 2.4.4), the created optimal thermoCEX-PEG-S6PG support 'D2' was directly applied to TCZR system in order to explore its dynamic performance in this study.

The chromatogram arising from the first test of the TCZR system employing thermoCEX-PEG-S6PG resin 'D2' and LF as the model binding species is illustrated in Fig. 4.6. With the column held at a temperature of 35 °C, LF was supplied until near saturation of matrix 'D2' had been achieved. Following washing with loading buffer, eight successive temperature-mediated elution steps were then conducted by driving the cooling assembly at its lowest possible axial velocity, v_c, of 0.1 mm/s (corresponding to ~5% of u_i). Nearly 36.9% of the previously adsorbed LF was eluted from the column (Table 4.4), and the residually bound LF was subsequently desorbed at 35 °C using equilibration buffer supplemented 1 M NaCl. The first peak's LF concentration was actually slightly higher than that of the feed. This peak alone accounted for 34.1% of total LF eluted via temperature-mediated elution (i.e. all 8 peaks combined; Table 4.4), and protein was still being eluted in all subsequent cycles (even in the 8th); most likely because of matrix D2's slow intra-particle pore diffusion kinetics. By moving the cooling zone along the separation column, proteins are desorbed with the region of reduced temperature because of the reduced binding affinity under these conditions (Table 4.3).

Although the thermoresponsiveness of thermoCEX-PEG-S6PG ‘D2’ is even better than that of thermoCEX-CL6B ‘A2’, thermoCEX-S6PG ‘B2’, and thermoCEX-S12PG ‘C1’ (‘$q_{max,\ 50°C}$ / $q_{max,\ 10°C}$’ ratios of 9.9 for ‘D2’, 3.3 for ‘A2’, 2.3 for ‘B2’, and 2.8 for ‘C1’), the dynamic protein binding performance of ‘D2’ is limited in TCZR due to its relatively lower LF binding capacity at higher temperature (i.e. $q_{max,\ 50°C}$ of only 19.8 mg/mL for ‘D2’, compared to 55.9 mg/mL for ‘A2’, 28.6 mg/mL for ‘B2’, and 44.7 mg/mL for ‘C1’).

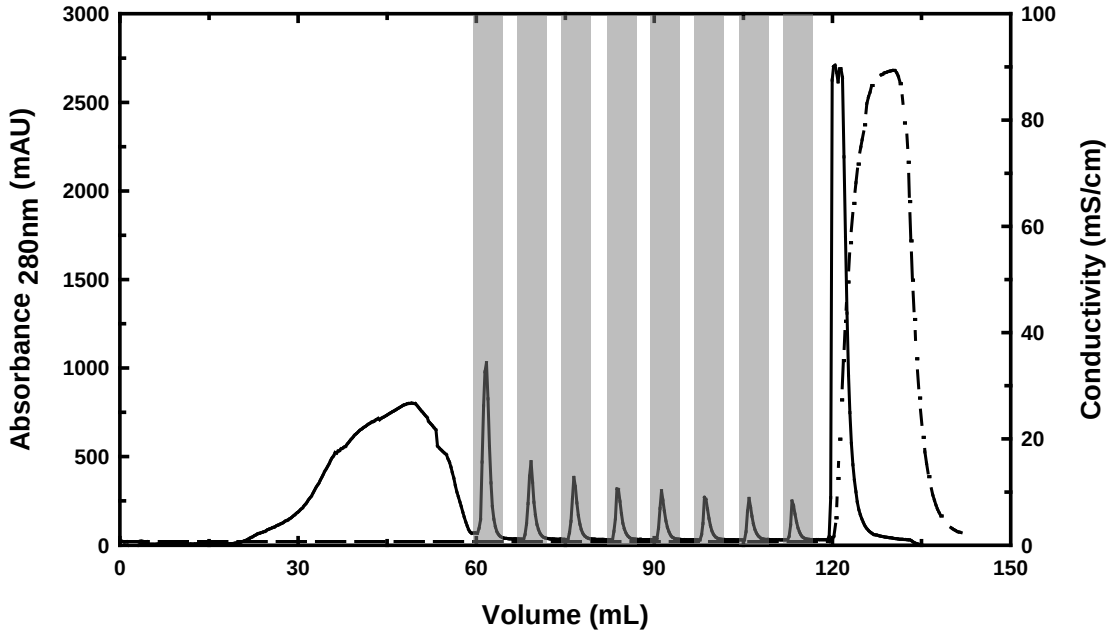

Fig. 4.6 Chromatogram arising from a TCZR test employing eight movements of the cooling zone at a velocity, v_c, of 0.1 mm/s. The unshaded areas indicate column operating temperature of 35 °C, the shaded grey zones indicate movement of the cooling zone. The solid and dashed lines represent the absorbance and conductivity signals, respectively.

Fig. 4.7 displays the second TCZR test of examining the impact of changing the ratio of the velocities of the elution front and the cooling zone on chromatographic performance. For this, using identical LF loading, mobile phase velocity and column temperatures to those employed in the first test

(Fig. 4.6), the cooling zone was moved along the whole column a total of six times at different speeds. For the first and second movements of the cooling zone, v_c was set at values corresponding to 1.9 mm/s and 1.0 mm/s, and the remaining four movements were conducted at v_c = 0.1 mm/s, i.e. the same as that employed in the first test. It is clear that the 'v_c = 0.1 mm/s' elution incidents in the second test closely resemble those in the first (compare Fig. 4.6 and Fig. 4.7). For this reason, only the first three movements are considered in the discussion of the influence of v_c on system performance. Clearly, the amount of protein eluted by a single movement of cooling zone increases strongly with decreasing v_c. For example, only 0.3% of total bound LF was eluted from the column at v_c = 1.9 mm/s, increasing to ~0.5% at v_c = 1 mm/s, and reaching 11% at v_c = 0.1 mm/s (Table 4.4). These dramatic differences are similar to the previous study of thermoCEX-CL6B 'A2' adsorbent, and the possible explanation can be found based on the impact of cooling zone velocity on the minimum temperatures attained within the discrete regions of the column it contacts. At v_c = 1 mm/s the temperature in the cooling zone is ca. 10.1 °C higher than that at v_c = 0.1 mm/s, and thus the eluting power of the cooling zone is considerably reduced.

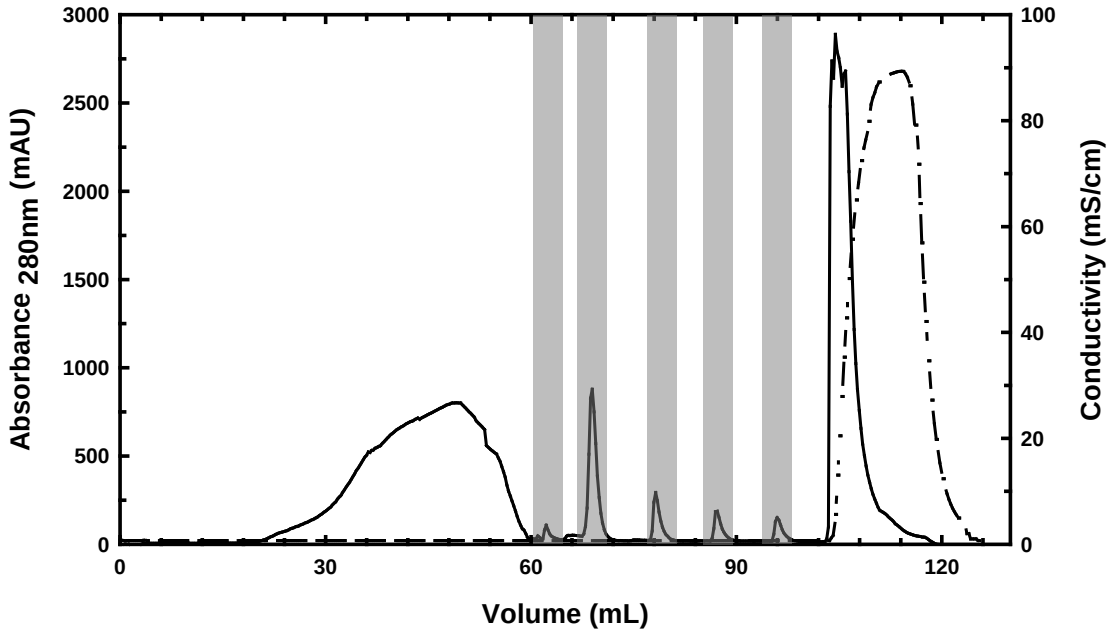

Fig. 4.7 Chromatogram arising from a TCZR test employing six movements of the cooling zone at different velocities, i.e. 1.9 mm/s for the first, 1mm/s for the second and 0.1 mm/s for the subsequent movements. The unshaded areas indicate column operating temperature of 35 °C, the shaded grey zones indicate movement of the cooling zone. The solid and dashed lines represent the absorbance and conductivity signals, respectively.

Table 4.4 LF recoveries from packed beds of thermoCEX-PEG-S6PG adsorbent D2 during multi-cycle TCZR controlled chromatography (see Fig. 4.6 and Fig. 4.7 and text for details). At u = 106 cm/h, u_i was calculated as 303 cm/h (0.70 mm/s).

TCZR test (Figure 4.6)	Temperature mediated elution at v_c = 0.1 mm/s (5% of u_i)									Post elution with	Mass balance
Step:	1	2	3	4	5	6	7	8	1-8 combined	1 M NaCl @ 35 ^{o}C	(%)
LF recovered[a] (%)	12.6	5.5	4.9	3.4	3.1	2.8	2.5	2.1	36.9	52.0	88.9

TCZR test (Figure 4.7)	Temperature mediated elution (varying v_c)							Post elution with	Mass balance
Step:	1	2	3	4	5	6	1-6 combined	1 M NaCl @ 35 ^{o}C	(%)
v_c (mm/s):	1.9	1.0	0.1	0.1	0.1	0.1			
v_c as % of u_i	100	53	5.3	5.3	5.3	5.3			
LF recovered[a] (%)	0.3	0.5	11.0	3.1	2.6	2.1	19.6	64.0	83.6

4.5 Conclusions

A more cost-effective and environmentally friendly thermoresponsive polymer-PEG is introduced to replace NIPAAm for synthesis of a new type of thermoCEX-PEG support based on Superose 6 prep grade (due to it's smaller particle diameters and adequately sized pores), and sequentially this thermoCEX-PEG adsorbent is employed to demonstrate the novel travelling cooling zone reactor (TCZR) arrangement for exploring the dynamic 'adsorption-desorption' behaviour. Although the thermoresponsiveness of thermoCEX-PEG-S6PG has been found even better than those of thermoCEX-CL6B 'A2', thermoCEX-S6PG 'B2', and thermoCEX-S12PG 'C1', the dynamic protein binding performance of 'D2' is limited due to its relatively lower LF binding capacity at higher temperature.

Notwithstanding the low binding capacity of thermoCEX-PEG adsorbents prepared in this study, some further investigations i.e. testing of more monomers compositions for the polymerisation, substitution of AAc with alternative anionic monomers, uncoupling 'thermoresponsiveness' from 'charge' through grafting thermoresponsive chains directly into the surfaces of commercial high capacity ion exchangers may be the optional approaches to improve the 'adsorption-desorption' behaviour of thermoCEX-PEG adsorbents in future works.

5 Integrated system for temperature-controlled fast protein liquid chromatography. IV. Thermoresponsive anion exchange adsorbents in TCZR chromatography

5.1 Abstract

Following the preparation and characterisation of thermoCEX, and the investigation of protein binding with thermoCEX in our previous studies, we fabricated thermoAEX with the base matrices of both Sepharose CL-6B and Superose 6 prep grade in this study. The procedures of synthesis are exactly same to that of thermoCEX, except tBAAm was replaced by BMA as hydrophobic monomer, and anionic monomer AAc was substituted with cationic monomer ATMAC. Through using of different monomers composition in the polymerisation, the thermoAEX matrices with the optimal combination of thermoresponsiveness and ovalbumin binding capacity has been identified. The thermoAEX adsorbents formed from Sepharose CL-6B ('E2') and Superose 6 prep grade ('F2') under identical conditions (ratio of NIPAAm: BMA: ATMAC = 90:5:5) display the optimal combination of thermoresponsiveness ($q_{max,50°C}$ / $q_{max,10°C}$ ratios of 1.4 and 1.6 for adsorbents 'E2' and 'F2', respectively) and OVA binding capacity ($q_{max,50°C}$ ~28 and 25 mg/mL for supports 'E2' and 'F2', respectively) and were consequently selected for TCZR chromatography. However, with temperature increases, the weaker electrostatic interaction between thermoAEX matrices and OVA offsets the contributions from the enhanced hydrophobic interaction, which result in the reduced performance of static and dynamic binding capacity of

support ‘E2’ and ‘F2’ to OVA. Only 19.8% and 28.6% of the ovalbumin bound at 35 °C can be recovered via 8 successive movements of the cooling zone at a velocity of 0.1 mm/s via thermoAEX-CL6B, E2 and thermoAEX-S6PG, F2 respectively.

5.2 Introduction

The ion-exchange chromatography is one of the most common tools to isolate large macromolecules (globular proteins, nucleic acids, viruses) in food and pharmaceutical industries. The high salt concentration of elution buffer, however, hinders its further application in this area (Maharjan et al., 2008). Consequently, synthesis of thermo-responsive chromatographic adsorbents has attracted more attentions in last decades, in order to provide a cost-effective and environmentally friendly bioseparation strategy (Theodossiou and Thomas, 2002; Kobayashi et al., 2003; Pan and Chien, 2003; Ayano et al., 2006a; Maharjan et al., 2008, 2009). However, it is surprising that the majority of the studies on temperature-sensitive chromatography have focused on cation exchange adsorbents. In this context, following the successful manufactures of thermoCEX-CL6B (see Chapter 2) and thermoCEX-S6PG materials (see Chapter 3) in our previous work, we converted both Sepharose CL-6B and Superose 6 prep grade into thermoAEX adsorbents grafted with a methylene bisacrylamide (MBAAm) cross-linked ‘smart’ temperature-sensitive cationic copolymer, i.e. poly(*N*-isopropylacrylamide-*co*-butyl methacrylate-*co*-(3-acrylamidopropyl) trimethylammonium chloride) (abbreviated to pNIPAAm-*co*-BMA-*co*-ATMAC), and exploit their ‘adsorption-desorption’ behaviour in TCZR in this study.

We first describe the preparation, characterisation and comparison of thermoAEX-CL6B and thermoAEX-S6PG adsorbents prepared for this study. Subsequently, we investigate their static and TCZR-dynamic binding behaviours respectively, and further, discuss and identify the main mechanism of preventing their binding capacity with Albumin from chicken egg white (OVA). Finally, we address the possible solutions and future work for the above problems.

5.3 Experimental

5.3.1 Materials

Albumin from chicken egg white (OVA, Cat. no. A5503, lyophilised powder, ≥98% by agarose gel electrophoresis) was purchased from the Sigma-Aldrich Company Ltd (Poole, Dorset, UK). The base matrices Sepharose CL-6B (Cat. no. 170160-01, Lot no. 10040943) and Superose 6 prep grade (Cat. no. 17-0489-01, Lot. no. 10037732) were obtained from GE Healthcare Life Sciences (Little Chalfont, Bucks, UK). The chemicals, *N*-isopropylacrylamide (Cat. no. 415324, 97%; NIPAAm), butyl methacrylate (Cat. no. 235865, 99%; BMA), (3-acrylamidopropyl) trimethylammonium chloride solution (75 wt.% in H_2O, ATMAC, Cat. no. 448281), 2-ethoxy-1-ethoxycabonyl-1,2-dihydroquinoline (Cat. no. 149837, ≥99%; EEDQ), 4,4'-azobis(4-cyanovaleric acid) (Cat. no. 11590, ≥98%; ACV), *N,N*-dimethylformamide (Cat. no. 270547, >99.9%; DMF), *N,N'*-methylenebisacrylamide (Cat. no. 146072, 99%; MBAAm),

epichlorohydrin (Cat. no. E1055, 99%; ECH), tetrahydrofuran (Cat. no. 34865, >99%; THF), diethyl ether (Cat. no. 309966, >99.9%), trizma hydrochloride (Cat. no. T5941, ≥99%; Tris-HCl), trizma base (Cat. no. T6066, ≥99.9%; Tris-base), sodium borohydride (Cat. no. 71321, >99%) and sodium hydroxide (Cat. no. S5881, anhydrous, >98%) were purchased from the Sigma-Aldrich Company Ltd (Poole, Dorset, UK), whereas absolute ethanol (Cat. no. E/0650DF/17, 99.8+%) and ammonia solution (Cat. no. A/3280/PB15, AR grade, 0.88 S.G., 35%) were acquired from Fisher Scientific UK Ltd (Loughborough, Leics, UK), and bottled oxygen-free nitrogen gas was supplied by the British Oxygen Co Ltd (Windlesham, Surrey, UK).

5.3.2 Preparation of thermoAEX adsorbents

Followed our previous researches, both Sepharose CL-6B and Superose 6 prep grade were employed for synthesis of thermoAEX adsorbents in this study. The methods used to convert base matrices into thermoresponsive anion exchange particles (named as thermoAEX-CL6B and thermoAEX-S6PG respectively) involve four successive steps – epoxide activation, amine capping, initiator immobilisation and ‘graft from’ polymerisation. These are detailed below and summarised schematically in Fig. 5.1.

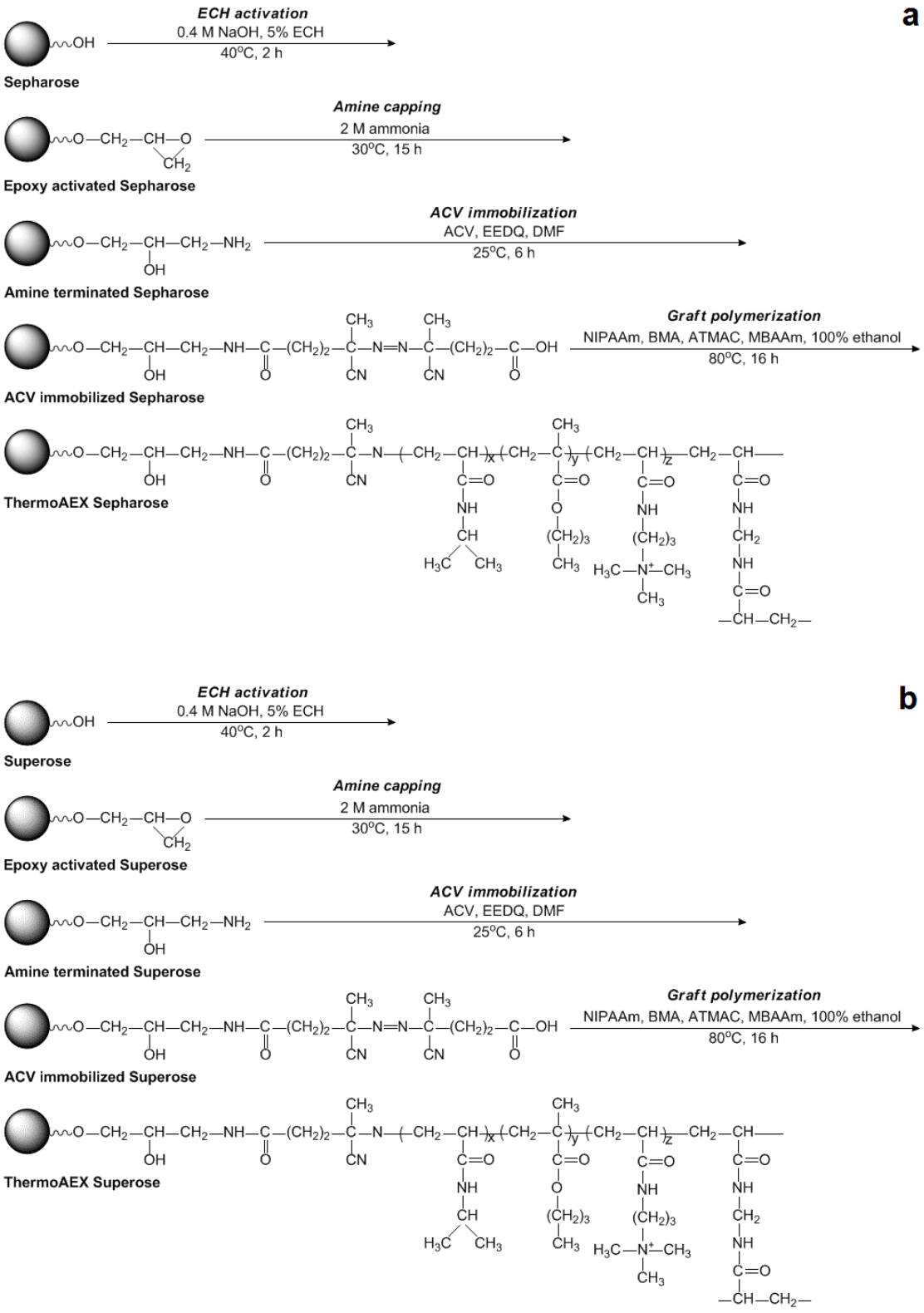

Fig. 5.1 Schematic illustration of steps involved in converting (a) Sepharose CL-6B into thermoAEX-CL6B and (b) Superose 6 prep grade into thermoAEX-S6PG adsorbents (see text for details).

5.3.2.1 **Epoxy activation** (Matsumoto et al., 1979)

Washed suction-drained Sepharose CL-6B (50 g, 71 mL) / Superose 6 prep grade (50 g, 68 mL) were mixed with 85 mL of water in 250 mL Pyrex® conical flasks and 40 mL of 2 M NaOH before placing in a 40 °C shaking water bath (Julabo SW22, Labortechnik GmbH, Seelbach, Germany) reciprocating at 150 rpm for 0.5 h. Ten millilitres of ECH (99%) was then added to a final concentration of ~5% (v/v), and reaction was allowed to proceed at 40 °C with shaking for an additional 2 h. The resulting epoxy-activated supports were washed copiously with water under vacuum.

5.3.2.2 **Amine capping**

After washing, the oxirane groups of epoxy-activated Sepharose CL-6B / epoxy-activated Superose 6 prep grade were reacted and capped with ammonium ions using a procedure adapted from Hermansson et al. (1992). The epoxy-activated Sepharose CL-6B (47.5 g, 65 mL) / epoxy-activated Superose 6 prep grade (47.5 g, 61 mL) were resuspended as a ~57% (v/v) slurry with 50 mL of 2 M ammonium hydroxide. After incubating overnight (~20 h) at ~30 °C with shaking at 150 rpm, the amine-terminated supports were recovered, washed exhaustively at room temperature with water in a sintered glass filter under vacuum, and then stored in 20% (v/v) ethanol at 4 °C until required.

5.3.2.3 Initiator immobilisation

The radical initiator ACV was coupled to amine-terminated Sepharose CL-6B / amine-terminated Superose 6 prep grade using a modified version of Maharjan and co-workers' procedure (2009), one adapted from methods originally applied to aminated silica matrices (Kanazawa et al., 1997; Yakushiji et al., 1999; Sakamoto et al., 2004; Ayano et al., 2006a), employing EEDQ as the condensing agent. Amine-terminated supports were washed sequentially with 5 volumes each of 50%, 75% and 100% (v/v) ethanol. For each wash, the supports were mixed 'end-over-end' (0.25 h, RT, 35 rpm) on a Stuart Scientific SB1 tube rotator (Bibby Scientific Ltd, Stone, Staffs, UK), before recovering by vacuum filtration and resuspending in the next wash solution in the series. Subsequently, the drained amine-terminated Sepharose CL-6B (45 g, 56 mL) / amine-terminated Superose 6 prep grade supports (45 g, 52 mL) were resuspended with 145 mL of DMF containing 75 mM ACV and 150 mM EEDQ. While housed in a zipper-locked inflatable glove box (AtmosBag, Sigma-Aldrich, UK), nitrogen gas was bubbled through the support slurries, before tightly sealing the reaction flasks with suba-Seal® rubber stoppers (Sigma-Aldrich, UK) and transferring to a shaking (150 rpm) water bath for 6 h of reaction at ~25 °C. The ACV coupled matrices were recovered from reaction solvent by vacuum filtration and then washed by end-over-end mixing (0.33 h, RT) and recovered by vacuum filtration, first with 5 volumes of DMF and subsequently with 5 volumes of absolute ethanol.

5.3.2.4 Graft from polymerisation of poly(NIPAAm-*co*-BMA-*co*-ATMAC-*co*-MBAAm)

In this study, NIPAAm was employed as thermoresponsive monomer, BMA was selected as hydrophobic monomer, and ATMAC was used as cationic monomer. Four different compositions of monomers (NIPAAm: BMA: ATMAC = 90: 5: 5/10/15/20) were employed in order to identify the optimal monomers ratio for preparation of thermoAEX-CL6B and thermoAEX-S6PG adsorbents (see all supports ID in Table 5.1). The surfaces of ACV-Sepharose CL-6B / ACV-Superose 6 prep grade were grafted with an immobilised lightly cross-linked (i.e. MBAAm as 1% of the total monomers) copolymer network of poly(NIPAAm-*co*-BMA-*co*-ATMAC-*co*-MBAAm). The method employed in this work was essentially that described by Maharjan et al. (2009), with minor modifications to pre and post washing regimes and reaction conditions. Suction-dried ACV-linked Sepharose CL-6B (25 g, 35 mL) / ACV-linked Superose 6 prep grade adsorbents (25 g, 31 mL) were sequentially washed with 125 mL aliquots of 20%, 50%, 75% and 100% (v/v) ethanol in cycles of resuspension, 'end-over-end' mixing (0.33 h, RT, 20 rpm) and vacuum filtration. Subsequently, the supports were resuspended with 125 mL of ethanol containing the dissolved monomers NIPAAm (900 mM), BMA (50 mM) and ATMAC (50 mM/ 100 mM/ 150 mM/ 200 mM), and the cross-linking monomer MBAAm (10 mM/ 10.50 mM/ 11 mM/ 11.50 mM), before transferring to the environment of a glove box and bubbling nitrogen gas through the reaction slurries. After 0.5 h the reaction flasks were tightly stoppered, and placed in a shaking water bath operated at 150 rpm and 80 °C for 16 h. The reaction mixtures were cooled to room temperature and the poly(NIPAAm-*co*-

BMA-*co*-ATMAC-*co*-MBAAm) grafted supports were recovered by vacuum filtration, before successively cycling through a descending ethanol concentration wash series (100%, 75%, 50%, 20%, v/v) and then with water. Each cycle involved mixing the support with 5 volumes of the appropriate solvent (0.33 h, RT, 20 rpm), followed by vacuum filtration. After the final wash, the polymer grafted supports were resuspended with 20% (v/v) ethanol and stored at 4 °C until required. The washes were retained for subsequent analysis (see Section 5.3.5).

5.3.3 Batch adsorption experiments with OVA

For batch binding tests, pure OVA solutions of defined concentrations (c_0 = 1-15 mg/mL) were prepared in 50 mM Tris-HCl pH 7.5. Aliquots (0.9 mL) of these OVA solutions were added to 0.1 mL volumes of settled thermoAEX-CL6B / thermoAEX-S6PG supports before mixing at various temperatures between 10 and 50 °C, for 1 h with shaking (1000 rpm, Thermomixer Comfort shaker, Eppendorf, Hamburg, Germany). After an additional 0.5 h at the selected incubation temperature without shaking, the supernatants were analysed for residual protein content (see Section 5.3.5). The protein bound to the supports was determined from the difference between the protein concentration in the starting binding solution and the supernatant after binding, and where appropriate the data were fitted to the Langmuir equation (see Eq 2.1 in Section 2.3.3). Data were fitted to the model using the x^2 minimisation procedure of SigmaPlot software version 12.5 (Systat Software Inc, CA, USA).

5.3.4 ThermoAEX supports chromatography of OVA in the batchwise TCZR

The tests conducted with the TCZR were performed using a constant surrounding temperature, Φ_u, of 35 °C, and the lowest possible axial velocity of the cooling zone (v_c) of 0.1 mm/s, which generates a maximum temperature difference of 22.6 °C (i.e. during the cooling zone's progress along the column, parts of the column immediately adjacent to the centre of the cooling assembly were temporarily cooled down to 12.4 °C). The separation column (volume = 2.83 mL) was packed with supports 'E2' and 'F2' (packing factor = 1.2), and u was maintained at 212 cm/h and 106 cm/h respectively. Using the calculated bed voidage (ε) of 0.32 and 0.42, the interstitial velocity (u_i) at this mobile phase velocity was determined as 682 cm/h and 252 cm/h correspondingly. After initial equilibration of the column with 2 CV of 50 mM Tris-HCl buffer, pH 7.5, 4 CV (in 'E2' test) and 3 CV (in 'F2' test) of a 2 mg/mL suspension of OVA (made up in the equilibration buffer) were applied to the column, before washing with a further 5 CV of the same buffer. Thereafter, the cooling zone assembly was moved along the entire column length three successive times at v_c = 0.1 mm/s, before finally eluting residually bound OVA with 5 CV of 50 mM Tris-HCl, pH 7.5, supplemented with 1 M NaCl.

Fractions generated during the above experiments were subsequently analysed off-line for protein content (see Section 5.3.5).

5.3.5 Analysis

5.3.5.1 Epoxide density measurement

The reactive epoxide group content introduced into Sepharose CL-6B / Superose 6 prep grade following activation with epichlorohydrin was determined exactly as described by Sundberg and Porath (1974). The epoxy-activated Sepharose CL-6B (0.5 g, 0.68 mL) / epoxy-activated Superose (0.5 g, 0.64mL) was 'end-over-end' mixed (1.3 h, RT, 20 rpm) with 1.5 mL of 1.3 M sodium thiosulphate solution of pH 7.0, results in the release of OH^- due to ring opening of oxiranes, which is followed by titration with 0.1 M HCl. The support's epoxide density was determined from the amount of HCl required to maintain neutrality.

5.3.5.2 FT-IR and ATR-FTIR analysis

FT-IR analysis was employed in two ways, i.e. qualitatively for direct detection of chemical changes introduced into Sepharose CL-6B / Superose 6 prep grade at various stages during the creation of thermoAEX-CL6B / thermoAEX-S6PG supports, and quantitatively on liquid samples, in order to determine consumption of 'NIPAAm + BMA' monomers, and thereby quantify the amount of 'NIPAAm + BMA' installed on thermoAEX-CL6B / thermoAEX-S6PG supports. For solid samples, aliquots of aqueous particle suspension were pipetted onto watchglasses and dried in an oven (60 °C, 20 h). Small quantities (~3 mg) of dried support samples were then blended with 300 mg of potassium bromide by grinding in agate mortar, until a fine, homogenous powder was produced, before pressing the mixtures into a 13 mm die using a

15 tonne Atlas manual hydraulic press (Model GS15011, Specac Ltd, Orpington, Kent, UK), producing FT-IR suitable tablets. FT-IR spectra of each tablet were recorded using a Nicolet 380 FT-IR (Nicolet 380, Thermo Fischer Scientific, Waltham, MA, USA) in direct beam mode. Sixty-four scans were averaged to yield spectra at a resolution of 2 cm^{-1}. Attenuated total reflectance FT-IR (ATR FT-IR) was employed for estimation of 'NIPAAm + BMA' in liquid samples. Routinely, 150 µl of each solution was applied to the surface of the Smart 53 Orbit diamond accessory of the Nicolet 380 FT-IR, and scanned 64 times at a resolution of 2 cm^{-1} in attenuated total reflection mode. A measurement without any sample in the beam was used as background to keep a relative scale for the adsorption intensity. Background measurements were taken every 0.5 h during sample measurements. NIPAAm, BMA, ATMAC and MBAAm give one characteristic peak in FT-IR, i.e. at ~1670 cm^{-1} corresponding to amide C=O stretching was employed for determination of 'NIPAAm + BMA + ATMAC + MBAAm'. The ATR spectrum of standards, i.e. various dilutions of the initial monomer mixtures NIPAAm: BMA: ATMAC: MBAAm (employed in a ratio of 90: 5: 5/10/15/20: 1/1.05/1.1/1.15), were obtained by subtracting the spectrum of pure water from the aqueous solutions spectra. The version 7.3 OMNIC™ DS (Data Security) software (Thermo Fischer Scientific, Waltham, MA, USA), was used as the interface for data collection and processing (interpretations of interferograms and peak area measurements). The area under the C=O stretching peak of each spectrum was calculated, keeping the same region and baseline at 1765-1600 cm^{-1} during all the readings, and the combined concentration of 'NIPAAm + BMA + ATMAC + MBAAm' in samples was estimated by reference to

standard curves (R^2 > 0.99). The contributions to this signal from the cationic monomer, ATMAC, which accounted for 5.0, 9.4, 13.5 and 17.2% (corresponding to the four different compositions of monomers employed in polymerisation step, see Section 5.3.2.4), and the cross-linking monomer, MBAAm, which accounted for 0.99% of the total monomer concentration, were subtracted to give a value for 'NIPAAm + BMA'.

5.3.5.3 Gravimetric analysis

Gravimetric analysis was routinely performed on solid supports and on dried residues arising from liquid samples, obtained throughout the different stages of thermoAEX-CL6B / thermoAEX-S6PG synthesis, and was used to allow determination of support immobilised ACV and copolymer contents, as well as the amount of free copolymer and unreacted monomers in solution at the end of the polymerisation reaction following their separation from one another (detailed below). For solid support measurements, approximately 1 g quantities of suction-drained support samples were accurately weighed in pre-weighed glass crucibles before drying to constant weight in a 60 °C oven (~20 h), cooling to room temperature in a desiccator jar and weighing accurately on an analytical balance. Post polymer grafting (Section 5.3.2.4), the reaction supernatant and wash solutions were pooled together and evaporated to dryness in a Buchi Rotavapor-RE Rotary Evaporator KRvr-TD-65/45 (Buchi Labortechnik AG, Flawil, Switzerland). The dried residue containing ungrafted free poly(NIPAAm-*co*-BMA-*co*-ATMAC-*co*-MBAAm) and unreacted monomers was resuspended in a small volume of tetrahydrofuran (THF). The free copolymer was then precipitated from solution by the addition of 10 volumes

of diethyl ether. The supernatant fraction containing dissolved monomers was carefully removed, rotary evaporated to dryness, and then redissolved in 100% (v/v) ethanol for ATR FT-IR analysis. The precipitated polymer was subsequently washed with diethyl ether, dried in a 60 °C oven for 20 h and accurately weighed, before finally dissolving in deuterated chloroform ($CDCl_3$) and analysing the relative amounts of NIPAAm and BMA from the ^1H NMR spectrum of the polymer in a Bruker AV400 Nuclear Magnetic Resonance (NMR) Spectrometer (Bruker-BioSpin Corporation, Billerica, MA, USA).

5.3.5.4 LCST measurement

The lower critical solution temperature (LCST) of the copolymer was determined in the standard way (Kanazawa et al., 1997; Sakamoto et al., 2004; Ayano et al., 2006a; Maharjan et al., 2009). The copolymer was resuspended at a concentration of 0.5% (w/v) in 50 mM Tris-HCl buffer, pH 7.5, and its optical transmittance at 500 nm was measured at various temperatures in a Cecil CE7500 UV/visible dual beam spectrophotometer (Cecil Instruments Ltd, Cambridge, UK) equipped with a water thermostatted cuvette holder.

5.3.5.5 Ionic capacity analysis

The Cl^- exchange capacities of the thermoAEX-CL6B / thermoAEX-S6PG were measured by the methods from Theodossiou et al. (Theodossiou and Thomas, 2002) with minor modifications. The thermoAEX adsorbents (0.5 mL) were mixed (1.5 h, 150 rpm) with 50 mL of 2 M NaCl, in a shaking water bath

(Julabo SW22, Labortechnik GmbH, Seelbach, Germany) in order to transform them into the hydrochloride salt or quaternary alkyl ammonium chloride form. The adsorbents were following washed three times with 50 mL of water on the purpose of removing excess acid. For replacing Cl^- ions on the beads by excess OH^- ions, the drained supports were subsequently incubated (16 h, 150 rpm) with 50 mL of 0.1 M NaOH, before settled and 1 mL aliquots of liquid phase were taken for Cl^- ion determination (Theodossiou and Thomas, 2002). For each thermoAEX support, the above procedures were operated at 10, 20, 35 and 50 °C respectively in order to explore the influence of various temperatures on resin's ionic capacity.

The assay for the Cl^- ions content presented in the thermoAEX supports is based on the principle of colorimetric method (A.I. Vogel, 1989) and the reaction is shown below. 100 µl of 0.25 M ammonium iron (III) sulphate in 9 M HNO_3 and 100 µl of a saturated solution of mercury (II) thiocyanate in 96% ethanol were added into the 1 mL aliquots of liquid phase sequentially, before vigorous mixed (10 min, RT, 1000rpm) on a Thermomixer Comfort shaker, (Eppendorf, Hamburg, Germany). The concentration of Cl^- ions was measured through the absorbance measurement at 460 nm of the solution of Iron (III) thiocyanate complex which appears as yellow coloured in a Lambda 20 UV-vis spectrophotometer (PerkinElmer Analytical Instruments, Shelton, CT, USA) (Theodossiou and Thomas, 2002).

$$2Cl^- + Hg(SCN)_2 + 2\ Fe^{3+} \longrightarrow HgCl_2 + 2[(FeSCN)]^{2+}$$

5.3.5.6 Protein contents determination

Protein contents in samples arising from batch binding and chromatography experiments were determined by UV spectrophotometry at 280 nm in quartz cuvettes in a Lambda 20 UV-vis spectrophotometer (PerkinElmer Analytical Instruments, Shelton, CT, USA).

5.4 Results and Discussion

In contrast to the preparation of thermoCEX adsorbents, the methods employed in this study are exactly same except the hydrophobic monomer changed to BMA and ionic monomer changed to ATMAC, respectively. The loading and composition of immobilised poly(NIPAAm-*co*-BMA-*co*-ATMAC-*co*-MBAAm) on the final thermoAEX, and the temperature dependent OVA binding behaviour, were thoroughly investigated, followed by the integrated approach comprising the optimal thermoAEX matrices ('E2' & 'F2') and TCZR batchwise arrangement were detailed investigated.

5.4.1 Manufacture and characterisation of thermoAEX

In order to investigate physico-chemical characterisation of support base material, intermediate supports at every stage of the conversion (Fig. 5.1), pre and post polymerisation reaction supernatants, and the final thermoAEX-CL6B / thermoAEX-S6PG adsorbents themselves, we employed a series of tests (FT-IR, ATR-FTIR, ^{1}NMR, gravimetric measurements, titration based

assays for oxirane content and colorimetric methods for ion exchange capacity). The main results from these are demonstrated in Fig. 5.2, Fig. 5.3 and Table 5.1, and described in the following text.

Fig. 5.2 a & b show FT-IR spectra for dried supports from each stage during fabrication of thermoAEX-CL6B / thermoAEX-S6PG matrices. All spectra are normalised for peak height at 934 cm^{-1}, as this is characteristic for the 3,6-anhydro moiety of Sepharose (Oza et al., 2010). Both the spectra for unmodified Sepharose CL-6B and Superose 6 prep grade show peaks corresponding to the functional groups expected of cross-linked agarose, i.e. alkyl CH_2 bending (at 1474, 1419 and 1378 cm^{-1}), alcohol C-O stretching (1190 and 1159 cm^{-1}) and ether C-O-C stretching (1068 and 1042 cm^{-1}). A pronounced broad peak at 1653 cm^{-1} corresponding to water H-O-H bending is also observed. This peak arises due to the hygroscopic nature of Sepharose, which tends to absorb atmospheric water after being dried.

There were no new peaks introduced in the Sepharose CL-6B & Superose 6 prep grade's FT-IR spectra following activation with epichlorohydrin, but increases in peak heights in the 1474-1378 cm^{-1} region (alkyl, CH2 bend) and areas of peaks at 1068 and 1042 cm^{-1}, were noted. The most striking of these changes, an enhanced peak at 1378 cm^{-1}, is consistent with a rise in alkyl group content arising from additional CH_2 groups of anchored glycidyl functions. Evidence for the introduction of oxirane moieties was tentatively indicated by a less obvious increase in length of the 'shoulder' at 1000-1030

cm^{-1} in the FT-IR spectrum, and was categorically confirmed by independent chemical assay (Table 5.1, 662 µmol/g dried epoxy-activated Sepharose CL-6B; 878 µmol/g dried epoxy-activated Superose 6 prep grade).

No changes in FT-IR spectra were observed following the amination of epoxy activated Sepharose CL-6B / epoxy activated Superose 6 prep grade. Given the relatively low epoxide density, this was not surprised. Further, the loss of oxirane groups in 1200-1000 cm^{-1} range is likely offset by increases in peak signals corresponding to resulting secondary alcohols (C-O stretch, 1080 cm^{-1}) and amines (C-N stretch, 1200-1025 cm^{-1}). The expected amine N-H bending peak at ca. 1600 cm^{-1} is not clearly seen, and is likely obscured by the broad water peak at 1653 cm^{-1}.

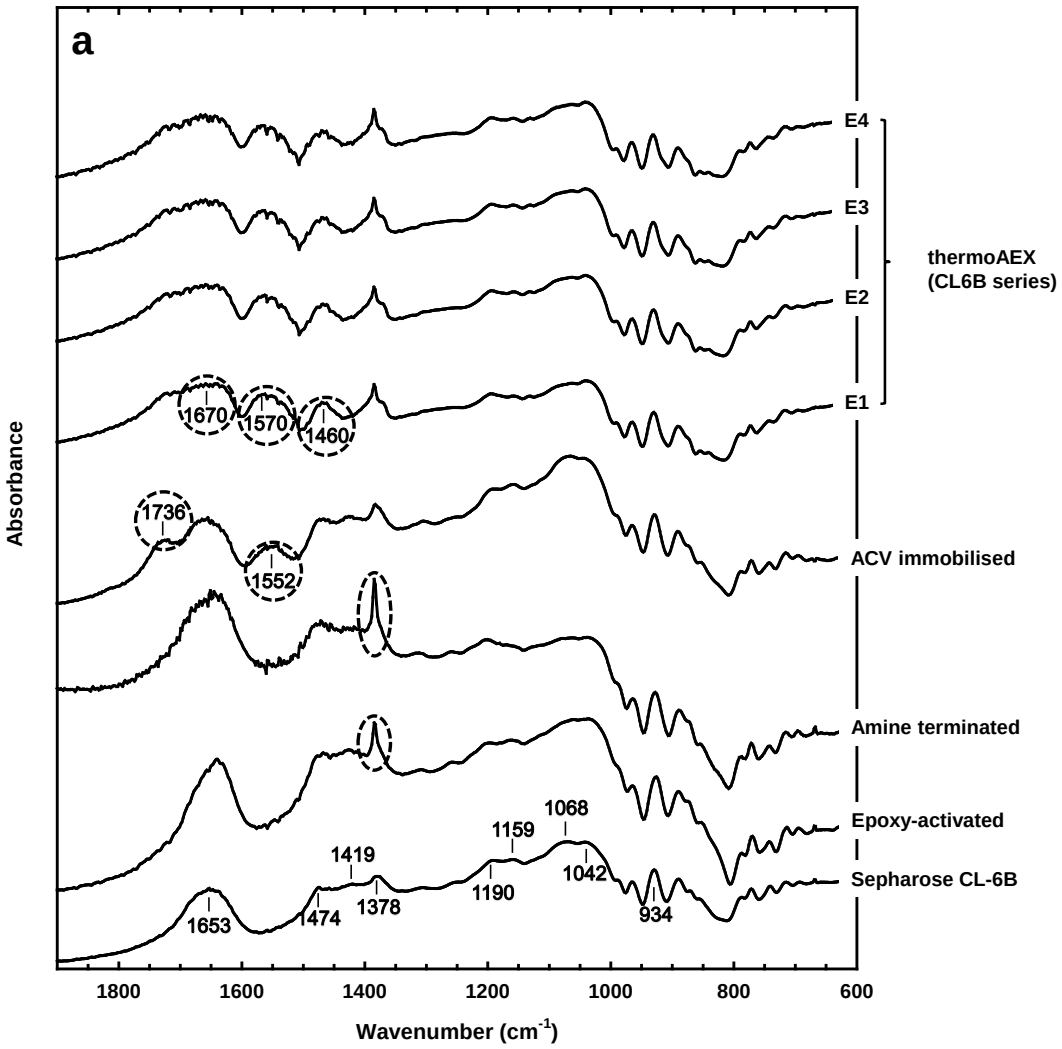
a
E4
E3
E2
E1
thermoAEX
(CL6B series)
1670
1570
1460
1736
1552
ACV immobilised
Amine terminated
1068
1159
1419
1042
1190
Epoxy-activated
Sepharose CL-6B
1653
1474
1378
934
Absorbance
1800
1600
1400
1200
1000
800
600
Wavenumber (cm-1)

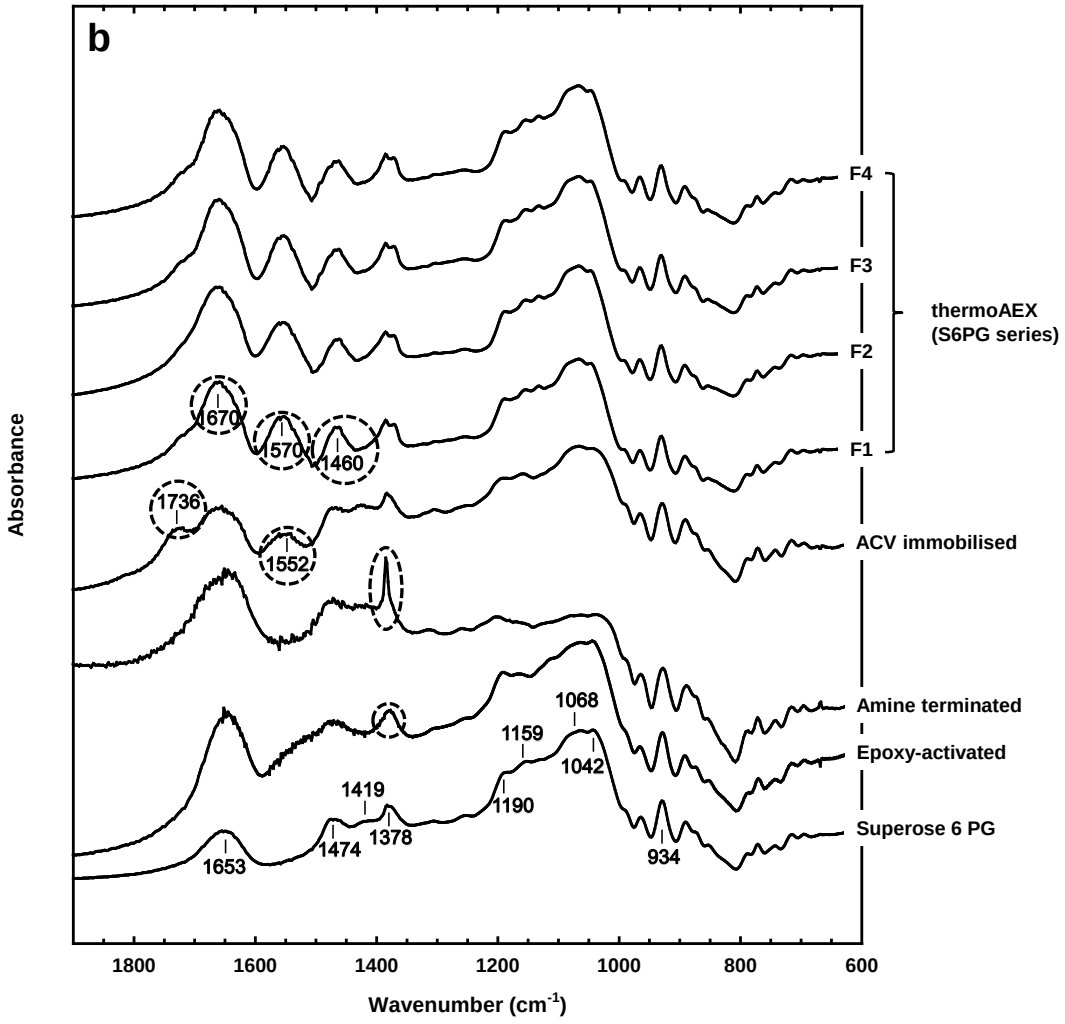

Fig. 5.2 FT-IR spectra recorded at various stages during the conversion of (a) Sepharose CL-6B into thermoAEX-CL6B, and (b) Superose 6 prep grade into thermoAEX-S6PG adsorbents series

Successful addition of the ACV initiator was confirmed following reaction with ACV, by two striking changes in the both FT-IR spectra, i.e. new peaks at 1736 cm^{-1} (carboxylic acid C=O stretch) and 1552 cm^{-1} (azo N=N stretch and/or amide N-H bend). Some broadening between 1653 cm^{-1} (water H-O-H bending) and 1736 cm^{-1} (carboxylic acid C=O stretch) consistent with the expectation of increased absorbance at ~1670 cm^{-1} corresponding to amide C=O stretching, was also observed. Gravimetric analysis indicated ACV had, following the amine capping step, been coupled to nearly 60% and 65% of the

initially installed reactive epoxide sites in Sepharose CL-6B and Superose 6 prep grade (Table 5.1, 380 µmol/g dried ACV-Sepharose CL-6B; 568 µmol/g dried ACV-Superose 6 prep grade), respectively.

The thermoAEX-CL6B supports ID (i.e. ‘E1’, ‘E2’, ‘E3’ and ‘E4’) and thermoAEX-S6PG supports ID (i.e. ‘F1’, ‘F2’, ‘F3’ and ‘F4’) refer to the resins prepared with different initial monomers compositions (detailed information see Table 5.1). The spectra of the thermoAEX-CL6B and thermoAEX-S6PG activated matrices show considerable growth of the peak at 1570 cm^{-1} (amide N-H bend), indicating presence of additional amide groups from the grafted copolymer chains (arising from NIPAAm, ATMAC and MBAAm). Peak at 1670 cm^{-1} (amide C=O stretch) also appear to have grown, indicating that the amide-containing units from NIPAAM, ATMAC and MBAAm have been successfully grafted in significant amounts.

Table 5.1 Characterisation of the Sepharose CL-6B based and Superose 6 prep grade based thermoAEX supports prepared and used in this work.

Parameter	ThermoAEX-CL6B			
Support ID (symbol)	E1	E2	E3	E4
Base matrix	Sepharose CL-6B (lot 10061497)			
Particle size distribution	45 – 165 µm (98%)			
Globular protein fractionation range, M_r	$1 \times 10^4 – 4 \times 10^6$ Da			
Step 1 Immobilised oxirane content (µmol/g dried support) [a]	662			
Step 3. Immobilised ACV content (µmol/g dried support) [b]	380			
Step 4. Free monomers entering reaction:				
'NIPAAm: BMA: ATMAC' (mM)	900: 50: 50	900: 50: 100	900: 50: 150	900: 50: 200
'NIPAAm: BMA: ATMAC' ratio	90:5:5	90:5:10	90:5:15	90:5:20
Immobilised copolymer composition of thermoCEX support:				
'pNIPAAm + BMA' content (µmol/ g dried support) [b,c]	3917	3852	3806	3710
pNIPAAm: BMA ratio[d]	89:11	87:13	83:17	79:21
NIPAAm content (µmol/ g dried support)	3486	3351	3159	2931
BMA content (µmol/ g dried support)	431	501	647	779
Ion exchange capacity (µmol Cl^-/ g dried support)[e]	197	337	480	628
'pNIPAAm + BMA + ATMAC' content (µmol/ g dried support)	4114	4189	4286	4338
'NIPAAm: BMA: ATMAC' ratio	84.7:10.5:4.8	80.0:12.0:8.0	73.7:15.1:11.2	67.5:18.0:14.5
% monomer consumed by support:				
NIPAAm + BMA + ATMAC	13.3	12.9	12.6	12.2
NIPAAm	12.5	12.0	11.3	10.5
BMA	27.9	32.5	42.0	50.5
ATMAC	12.8	10.9	10.4	10.2

Parameter	ThermoAEX-S6PG			
Support ID (symbol)	F1	F2	F3	F4
Base matrix	Superose 6 PG (lot 10037732)			
Particle size distribution	20 – 40 µm (83%)			
Globular protein fractionation range, M_r	5×10^3 – 5×10^6 Da			
Step 1 Immobilised oxirane content (µmol/g dried support) [a]	878			
Step 3. Immobilised ACV content (µmol/g dried support) [b]	568			
Step 4. Free monomers entering reaction:				
'NIPAAm: BMA: ATMAC' (mM)	900: 50: 50	900: 50: 100	900: 50: 150	900: 50: 200
'NIPAAm: BMA: ATMAC' ratio	90:5:5	90:5:10	90:5:15	90:5:20
Immobilised copolymer composition of thermoCEX support:				
'pNIPAAm + BMA' content (µmol/ g dried support) [b,c]	4182	4176	4127	4078
pNIPAAm: BMA ratio[d]	90:10	87:13	84:16	81:19
NIPAAm content (µmol/ g dried support)	3764	3633	3467	3303
BMA content (µmol/ g dried support)	418	543	660	775
Ion exchange capacity (µmol Cl^-/ g dried support)[e]	210	338	465	580
'pNIPAAm + BMA + ATMAC' content (µmol/ g dried support)	4392	4514	4592	4658
'NIPAAm: BMA: ATMAC' ratio	85.7:9.5:4.8	80.5:12.0:7.5	75.5:14.4:10.1	70.9:16.6:12.5
% monomer consumed by support:				
NIPAAm + BMA + ATMAC	14.2	13.9	13.5	13.1
NIPAAm	13.5	13.0	12.4	11.9
BMA	27.1	35.2	42.8	50.2
ATMAC	13.6	11.0	10.1	9.4

Key: Determined by: [a]oxirane ring opening reaction followed by titration [Sundberg and Porath, 1974]; [b]gravimetric measurement; [c]ATR-FTIR spectrometry of supernatant samples before and after polymerisation reactions, [d]Proton NMR of the ungrafted free copolymer in $CDCl_3$; [e]anion-exchange.

Utilising the optimal ECH activation conditions described by Matsumoto and co-workers (Matsumoto et al., 1979), i.e. 5% ECH, 0.4 M NaOH, 2 h at 40 °C (previously described in Sections 2.4.1 & 3.4.1), the oxirane density of 662 µmol/g dried matrix was determined using Sepharose CL-6B, and 878 µmol/g dried matrix was determined using Superose 6 prep grade (Table 5.1), respectively. The increased immobilised ACV initiator densities, and the following high yields of the polymer grafting reaction, were consequently obtained arising from high and consistent levels of oxirane activation accompanied with the benefits of minimal cross-linking (Table 5.1).

Grafting of polymer chains on the matrices was accompanied by the generation of significant amounts of free polymer in the supernatant (detailed explanation see Section 2.4.1), gravimetrically determined as i.e. 25.2% (in support ‘E2’ synthesis), and 27.2% (in support ‘F2’ synthesis) of the total monomers supplied. Both of them are roughly 2-fold higher to their corresponding conversion ratios of grafted polymer (12.9% (for support ‘E2’), and 13.9% (for support ‘F2’)) to the total monomers provided respectively, which are in line with the expecting ratio of free to grafted polymer (2: 1) in theoretical calculation.

The temperature dependent phase transition behaviour of ungrafted free copolymer solutions emanating from various grafting reactions with ACV-immobilised Sepharose CL-6B and Superose prep grade are compared in Fig. 5.3. Fig. 5.3a and Fig. 5.3b display the raw transmittance vs. temperature

profiles, and Fig. 5.3c examines the wider impact of NIPAAm replacement on the LCST and full transition temperature ranges of the copolymers.

The characteristic steep decrease in optical transmittance across a relatively narrow temperature range has been found in all eight thermoAEX matrices prepared in this study arising from the conformation of poly(NIPAAm-*co*-BMA-*co*-ATMAC-*co*-MBAAm) changing from hydrophilic coil to hydrophobic globule. However, with NIPAAm content of copolymer reduces in thermoAEX-CL6B (from 'E1'-84.7% to 'E4'-67.5%), and in thermoAEX-S6PG (from 'F1'-85.7% to 'F4'-70.9%), the temperature range over which the full phase transition occurs become wider and the LCST become higher, which completely in line with the rules reported in previous studies (Kobayashi et al., 2002, 2003; Sakamoto et al., 2004; Ayano et al., 2006b). Despite the differences in NIPAAm content and monomer composition (Table 5.1), the LCST shift of thermoAEX matrices is at a relatively narrow range, i.e. 30.5 °C for support 'E1' cf. 36.7 °C for support 'E4' (Fig. 5.3a), and 30 °C for support 'F1' cf. 36 °C for support 'F4' (Fig. 5.3b). In accord with literature reports (Heskins and Guillet, 1968; Kubota et al., 1990; Schild, 1992), the LCST at 50% optical transmittance ($T_{50\%}$) for the 'smart' homopolymer pNIPAAm was 32.3 °C and sharp transition from fully extended 'hydrophilic coil' ($T_{90\%}$) to fully collapsed 'hydrophobic globule' ($T_{0.4\%}$) occurred between 31 and 35 °C (dashed line traces in Fig. 5.3a-c). Copolymerising NIPAAm with more hydrophobic monomers leads to a reduction in the LCST (Hoffman et al., 2000; Yoshimatsu et al., 2012), whereas incorporation of more hydrophilic species increases it (Hoffman et al., 2000). Here, simultaneous low level substitution

of ATMAC and BMA into pNIPAAm's backbone ('E1' & 'F1') at the expense of 15.3 & 14.3% of its NIPAAm content (Table 5.1), had the effect of lowering the LCST (by 1.8 °C for 'E1' and 2.3 °C for 'F1') and broadening the transition temperature range in both directions (i.e. 27.8 to 36.2 °C for 'E1' and 26.2 to 36.3 °C for 'F1'). With mounting NIPAAm replacement, smart thermoresponsive behaviour became increasingly compromised. For example, the LCST for the '67.5:18.0:14.5' copolymer (Fig. 3.5c, 'E4') reached 36.7 °C and temperature range over which full 'coil – globule' transition range extended >25 °C, i.e. from 19.6 to 45 °C.

Under the identical monomers composition of NIPAAm: tBAAm (for thermoCEX) or BMA (for thermoAEX): AAc (for thermoCEX) or ATMAC (for thermoAEX), the NIPAAm was introduced heavier in Superose 6 prep grade based final resins than in Sepharose CL-6B based final supports in both thermoCEX and thermoAEX series (i.e. 86.6% NIPAAm in 'B2' > 79.1% NIPAAm in 'A2', (Table 3.1 & Table 3.2); 80.5% NIPAAm in 'F2' > 80% NIPAAm in 'E2' (Table 5.1)), which is not surprisingly corresponding to the findings in LCST measurements (i.e. LCST of 'B2' < LCST of 'A2'; LCST of 'F2' < LCST of 'E2'). The principle is integrating more hydrophobic monomers (i.e. NIPAAm) leads to a reduction in LCST (Hoffman et al., 2000; Yoshimatsu et al., 2012).

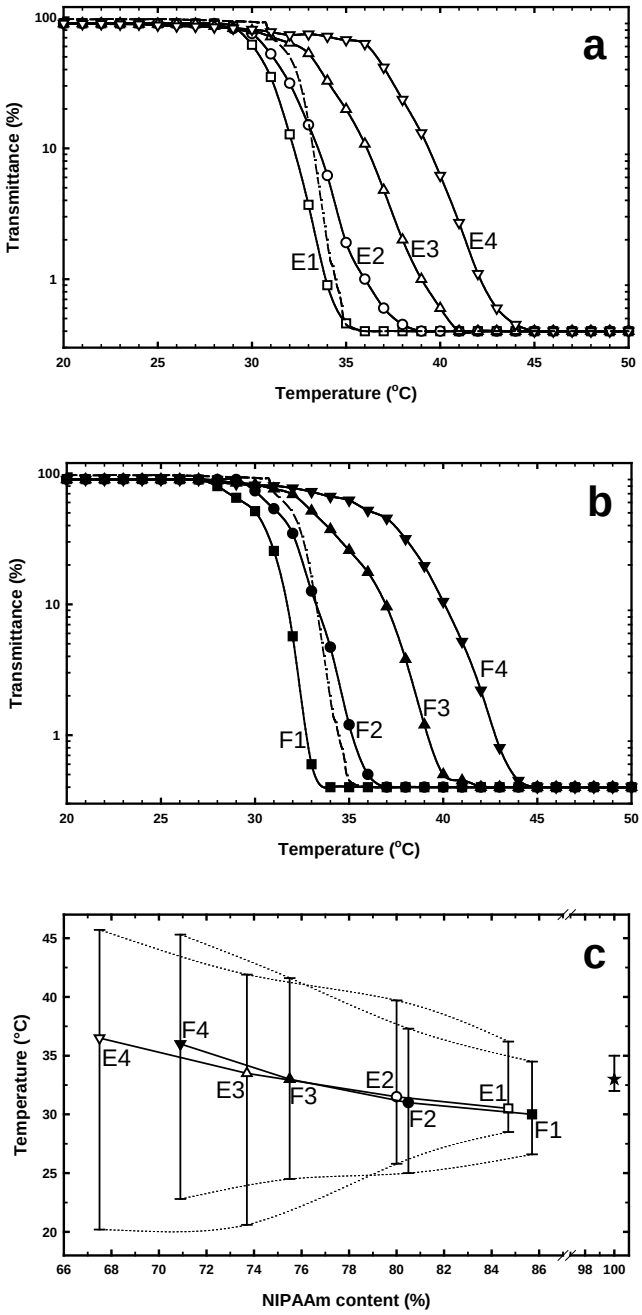

Fig. 5.3 Optical transmittance (500 nm) vs. temperature profiles for 0.5% (w/v) solutions of ungrafted free poly(NIPAAm-*co*-BMA-*co*-ATMAC-*co*-MBAAm) arising during fabrication of (a) Sepharose CL-6B and (b) Superose 6 prep grade, and (c) the influence of NIPAAm content on temperature transition behaviour of the copolymers. The symbols in 'c' indicate the determined LCST values at 50% transmittance ($T_{50\%}$), capped bars define the temperature range over which phase transition occurred, and the lower dotted and upper dashed lines respectively delineate the temperatures at which full collapse ($T_{0.4\%}$) and extension ($T_{90\%}$) of the copolymer chains occurred. Key: pNIPAAm (★); Sepharose CL6B series (E1 – □, E2 – ○, E3 – △, E4 – ▽); Superose series (F1 – ■, F2 – ●, F3 – ▲, F4 – ▼).

5.4.2 Temperature dependent batch adsorption of OVA on thermoAEX adsorbents

Fig. 5.4 shows adsorption isotherms obtained for the binding of OVA to these at different temperatures, Fig. 5.5 a & b compare the effect of temperature on the adsorption of OVA to all eight thermoAEX-CL6B / thermoAEX-S6PG adsorbents series prepared in this work in a 50 mM Tris-HCl buffer, pH 7.5, at temperature of 10, 20, 35 and 50 °C, respectively, and Table 5.2 summarises the Langmuir binding parameters fitted to the data sets of thermoAEX adsorbents ‘E2’ and ‘F2’. In all cases, OVA binding capacity is increased linearly with the examined incremental temperature (10 – 50°C), it is clear however, that the effect is more pronounced for adsorbent ‘E2’ in thermoAEX-CL6B supports series, and adsorbent ‘F2’ in thermoAEX-S6PG matrices series. For adsorbents ‘E2’ and ‘F2’, the binding capacity rises approximately 1.4-fold from 19.8 mg/mL at 10 °C to 28.1 mg/mL at 50 °C, and 1.6-fold from 16.1 mg/mL at 10 °C to 25.1 mg/mL at 50 °C, respectively (Table 5.2). As the results, ‘E2’ and ‘F2’ were consequently selected for further study.

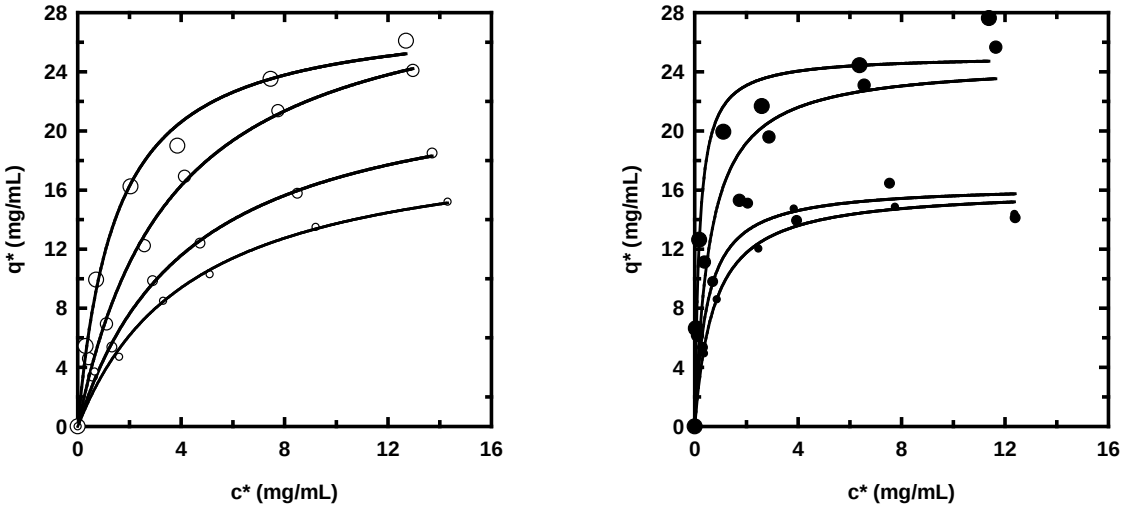

Fig. 5.4 Equilibrium isotherms for the adsorption of OVA to thermoAEX supports E2 and F2 initially selected for TCZR chromatography at 10, 20, 35 and 50 °C. The solid lines through the data points represent fitted Langmuir curves with parameter values presented in Table 5.2.

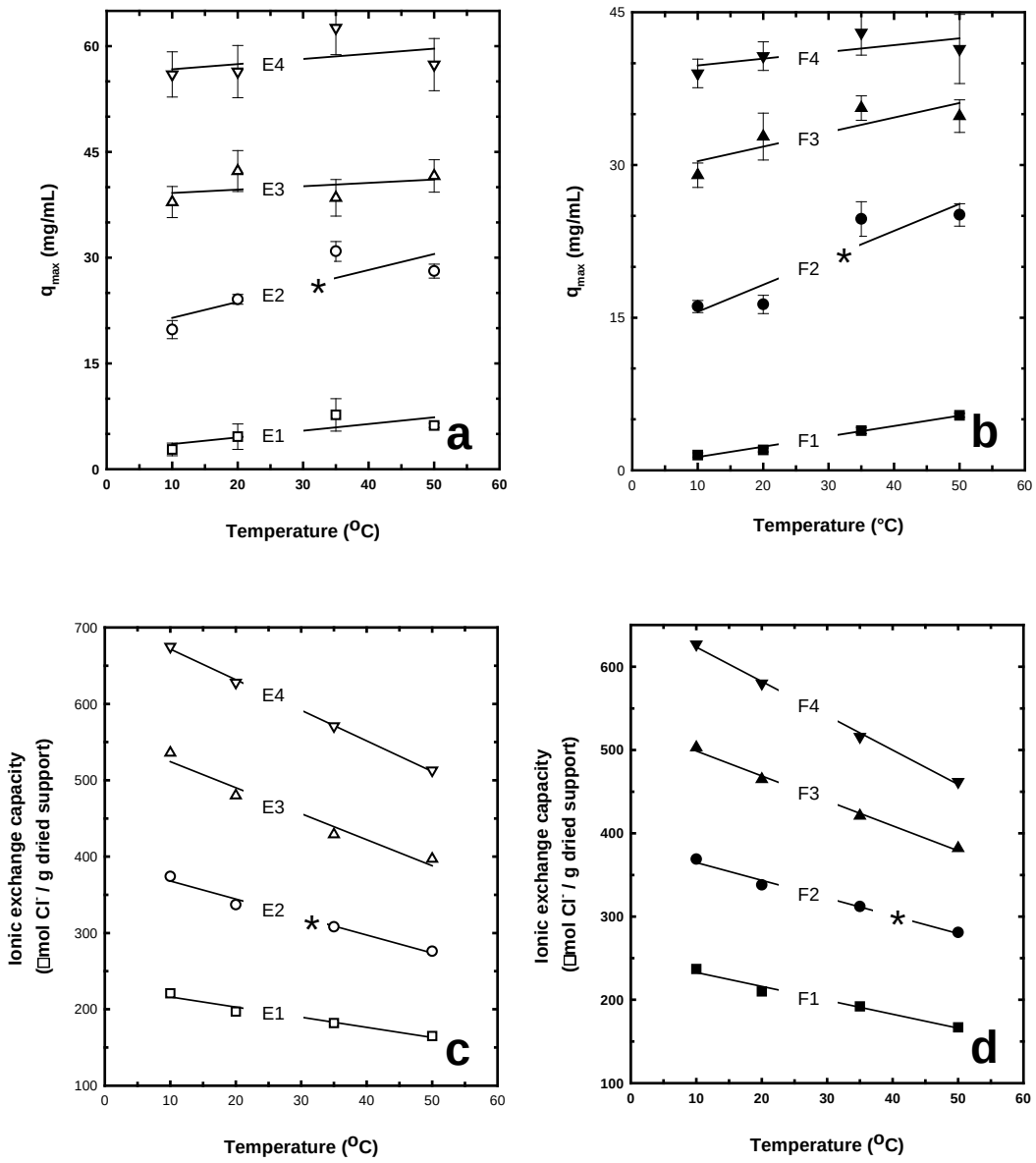

Fig. 5.5 Effect of temperature on the maximum adsorption capacity (q_{max}) of OVA on (a) thermoAEX-CL6B supports (open circles) and (b) thermoAEX-S6PG (filled black circles); and effect of temperature on the ionic capacity of (c) thermoAEX-CL6B supports (open circles) and (d) thermoAEX-S6PG (filled black circles). The asterisks next to supports E2, and F2 indicate those initially selected for TCZR chromatography. The solid lines represent linear fits to the data.

The ionic exchange capacity of every thermoCEX adsorbents prepared in our previous studies is increased with temperature shifting from low to high degree (Fig. 3.6 and Fig. 4.5). However, the completely opposite relationship was found in the cases of both thermoAEX-CL6B and thermoAEX-S6PG (Fig.

5.5 c&d). With the temperature rises across LCST (from 10 to 50 °C), the charge density of each thermoAEX adsorbent reduces at various extents, which indicates the electrostatic interaction between thermoAEX adsorbents and OVA is stronger at low temperature. In contrast to the results observed in thermoCEX adsorbents, the anion-exchange groups of immobilised polymer chains on thermoAEX matrices act a completely inverse behaviour, similar results have also been found in other researches (Ayano et al., 2006a; Nishio et al., 2011). We cannot explain the completely inverse behaviour occurred in thermoAEX adsorbents at present time, however, one possible reason may be that non-uniform distribution of the positive charged monomers within the copolymer network could lead to it happened, for example, the anion-exchange groups are hiding on the bottom of the ligand and therefore immersing in the hydrophobic polymer chain, result in the reduced electrostatic interaction between OVA and thermoAEX adsorbents.

Table 5.2 Langmuir parameters describing the adsorption of OVA at 10, 20, 35, and 50 °C to the (a) Sepharose CL-6B based thermoAEX supports and (b) Superose 6 prep grade based thermoAEX supports prepared and used in this work. See text for details

Support (ionic capacity)	Temperature (°C)	q_{max} (mg/mL)	K_d (mg/mL)	Initial slope, q_{max}/K_d (mL/mL)
thermoAEX-CL6B E2 (32.2 µmolCl^-/mL support)	10	19.8 ± 1.3	4.44 ± 0.72	4.5
	20	24.1 ± 0.7	4.31 ± 0.31	5.6
	35	30.9 ± 1.4	3.58 ± 0.44	9.6
	50	28.1 ± 1.0	1.46 ± 0.18	19.3
thermoAEX-S6PG F2 (30.9 µmolCl^-/mL support)	10	16.1 ± 0.6	0.74 ± 0.12	21.8
	20	16.3 ± 0.9	0.47 ± 0.14	34.7
	35	24.7 ± 1.7	0.57 ± 0.20	43.3
	50	25.1 ± 1.1	0.18 ± 0.05	139.4

It is interesting and therefore deserves comment that the high ratios of '$q_{max,\ 50°C}$ / $q_{max,\ 10°C}$' have been found in the optimal thermoCEX-CL6B support 'A2' (3.3-fold) and thermoCEX-S6PG support 'B2' (2.3-fold), respectively, however, the relatively lower ratios of '$q_{max,\ 50°C}$ / $q_{max,\ 10°C}$' have been observed in the optimal thermoAEX-CL6B support 'E2' (1.4-fold) and thermoAEX-S6PG support 'F2' (1.6-fold). From Fig. 3.5 and Fig. 5.3, the characteristic sharp decrease in optical transmittance across a relatively narrow temperature range is observed in all NIPAAm copolymers, which confirms that at the lower temperature all copolymers are fully extended and hydrophilic, however, with the temperature raises across the LCST, the grafted copolymers start to collapse, becoming hydrophobic and globule. Nonetheless, the completely opposite behavior of ion exchange capacity on temperature tuning has been found between thermoCEX and thermoAEX matrices (Fig. 3.6 and Fig. 5.5). With incremental increase in temperature from 10 to 50 °C, the ion exchange capacity rises for all thermoCEX adsorbents, whist conversely, drops for all thermoAEX matrices. The hydrophobic and electrostatic interactions play main roles to determine the binding capacity between ionic exchangers and proteins (Ayano et al., 2006a; Maharjan et al., 2009), consequently, the weaker electrostatic interaction at higher temperature for thermoAEX adsorbents is possibly the key factor to hinder the improvement of protein binding capacity, although the hydrophobic interaction is stronger at higher temperature for both thermoAEX and thermoCEX matrices.

In our previous studies, thermoCEX matrices 'A3' and 'B3', which are fabricated with the identical monomers composition to thermoAEX adsorbents

‘E2’ and ‘F2’ (thermoresponsive monomer: hydrophobic monomer: ionic monomer = 18: 1: 2), the q_{max} are 39.6 and 32.5 mg/mL respectively at 10 °C, but rises to 59.5 and 38.4 mg/mL respectively at 50 °C. The big magnitude difference of capacity between thermoCEX and thermoAEX can also be attributed to their converse behavior of ion exchange capacity on temperature shifting.

5.4.3 Chromatography of OVA in TCZR containing thermoAEX supports

Due to the advantages of TCZR chromatography over conventional jacketed column, i.e. sharp elution peaks without tailing effects, and continuous operation (see Section 2.4.4), the fabricated optimal support ‘E2’ in thermoAEX-CL6B and adsorbent ‘F2’ in thermoAEX-S6PG were directly applied to TCZR system in order to explore its dynamic performance in this study.

The chromatograms arising from the tests of the TCZR system employing thermoAEX-CL6B adsorbent ‘E2’ and thermoAEX-S6PG support ‘F2’ with OVA as the model binding species are demonstrated in Fig. 5.6 a & b, respectively. With the column held at a temperature of 35 °C, OVA were provided until near saturation of matrix had been achieved. Following washing with loading buffer, the amount of protein was estimated to be only 23.9 mg (equivalent to 6.5 mg/mL) bound to the support ‘E2’, and 14.4 mg (equivalent to 3.9 mg/mL) to the support ‘F2’. Three successive temperature-mediated elution steps were then conducted by driving the cooling assembly at its

lowest possible axial velocity, v_c, of 0.1 mm/s. Only 19.8% (4.7 mg) in 'E2' test and 28.6% (4.1 mg) in 'F2' test of the previously adsorbed OVA were eluted from the column (Table 5.3) respectively, and the residually bound OVA was subsequently desorbed at 35 °C using equilibration buffer supplemented 1 M NaCl. It is not surprising that the dynamic 'adsorption-desorption' performance of thermoAEX adsorbents (i.e. 'E2' and 'F2') is considerably worse than that of thermo-CEX matrices (i.e. 'A2' and 'B2') due to the loss of ionic strength with increased temperature, although hydrophobic interaction rises simultaneously (see Section 5.4.2). Despite much reduced amount of protein binding to thermoAEX matrices, the three successive peaks arising from the continuous movement of narrow travelling cooling zone display similar behaviour to which happened in thermoCEX adsorbents. The first peak accounted for 51.5% (in 'E2' test) and 52.8% (in 'F2' test) of total OVA eluted through temperature-mediated elution (i.e. all 3 peaks combined; Table 5.3), respectively.

OVA unfolding could be another reason for the worse dynamic 'adsorption-desorption' behaviours of thermoAEX adsorbents in TCZR. A loss of recovery for OVA has been found on silica-based matrix in HPLC test due to irreversible protein unfolding even the ambient temperature is at 37 °C (Patananan et al., 2008), although the denaturing temperature of OVA has been reported at 84 °C via Sigma-Aldrich. It is possible arising from the catalysis of protein via the surfaces of resin occurred at a lower temperature than it would be in bulk solution (Somasundaran, 2006).

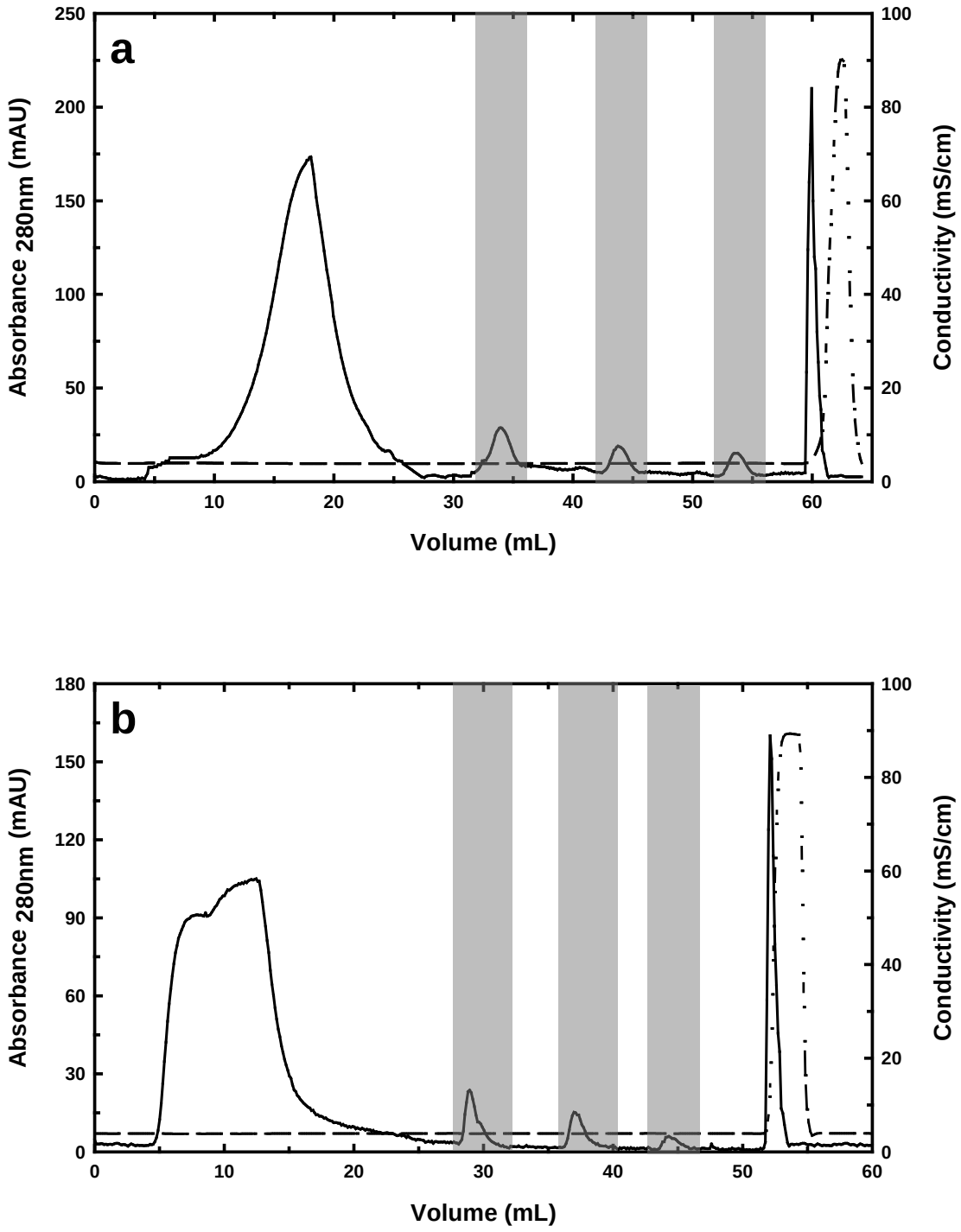

Fig. 5.6 Chromatograms arising from TCZR tests with (a) thermoAEX-CL6B support E2, and (b) thermoAEX-S6PG support F2, employing three movements of the cooling zone at a velocity, v_c, of 0.1 mm/s. The unshaded areas indicate column operating temperature of 35 °C, the shaded grey zones indicate movement of the cooling zone. The solid and dashed lines represent the absorbance and conductivity signals, respectively.

Table 5.3 OVA recoveries from packed beds of thermoAEX-CL6B support E2 and thermoAEX-S6PG support F2, during multi-cycle TCZR controlled chromatography (see Fig. 5.6 and text for details).

TCZR test (Figure 5.7)	Temperature mediated elution at v_c = 0.1 mm/s				Post elution with	Mass Balance
Step:	1	2	3	1-3 combined	1 M NaCl @ 35 ^{o}C	(%)
OVA recovered[a] (%) of E2	10.2	6.0	3.6	19.8	64.9	84.7
OVA recovered[a] (%) of F2	15.1	10.0	3.5	28.6	55.3	83.9

5.5 Conclusions

In this study, a novel travelling cooling zone reactor (TCZR) packed with thermoAEX adsorbents which grafted with pNIPAAm based copolymer was applied to examine the 'adsorption-desorption' performance of OVA. Based on our previous protocol of preparing for thermoCEX supports (see Chapters 2 & 3), the underivatised Sepharose CL-6B and Superose 6 prep grade were transformed into thermoresponsive anion exchange (thermoAEX) adsorbents, respectively. Instead of employing tBAAm and AAc in thermoCEX synthesis, BMA was used as hydrophobic monomer and AAC was employed as cationic monomer in this study.

Through FT-IR, ^{1}H NMR, gravimetric and chemical assays, it has been confirmed that the poly(NIPAAm-*co*-BMA-*co*-ATMAC-*co*-MBAAm) was successfully grafted on the thermoAEX matrices. However, with elevated temperature, the weaker electrostatic interaction between thermoAEX matrices and OVA possibly caused by charge non-uniform distribution within the copolymer network offsets the contributions from the enhanced hydrophobic interaction, which results in the reduced performance of static and dynamic binding capacity of support 'E2' and 'F2' to OVA. OVA unfolding at a lower temperature on the surface of chromatographic supports than it would be in bulk solution is another factor to impact the 'adsorption-desorption' performance of thermoAEX adsorbents with OVA.

Despite the ‘adsorption-desorption’ performance of thermoAEX matrices prepared in this study is not as good as the thermoCEX adsorbents produced in our previous research, the future works should focus on (i) finding alternative thermo-stable targets with more hydrophilic property which could benefit from both strong hydrophilic and electrostatic interaction at lower temperature; and consequently (ii) exploiting an integrated approach to temperature-controlled chromatography, comprising thermoAEX adsorbents and a novel travelling heating zone reactor (THZR) arrangement, where the elution occurs on heating, and (iii) replacing NIPAAm with PEG to prepare more environment-friendly thermoAEX supports.

6 Conclusions and future work

Since liquid chromatography plays an increasingly important role in bioseparation field, more and more attentions have been drawn to the solutions of its drawbacks. It is not only focused on reducing the processing costs, but also on creating a more convenient, more environmentally friendly approach of chromatography process.

Following Chapter 1 which explains the DSP process, especially emphasis on the introduction of liquid chromatography including its drawbacks, an integrated approach to temperature-controlled chromatography, comprising pNIPAAm modified thermoCEX-CL6B adsorbents and TCZR arrangement, is described in Chapter 2. The resulting thermoCEX-CL6B adsorbents displayed superior LF 'adsorption-desorption' behaviour with TCZR. As the cooling zone travelled along the column, previously adsorbed LF on the supports at 35 °C, was desorbed in the form of sharp, concentrated peaks. Intra-particle diffusion of desorbed protein out of the pores of the adsorbent and the ratio between the velocities of the cooling zone and mobile phase were identified as the main parameters affecting the TCZR's performance. Consequently, the fabrication and detailed characterisation of porous beaded thermoCEX adsorbents varying in particle size, pore dimensions and grafted poly(*N*-isopropylacrylamide-*co*-*N*-tert-butylacrylamide-*co*-acrylic acid) composition has been done in Chapter 3. It has been confirmed that a small particle diameter combined with sufficiently large pores is necessary in the TCZR

application (hence Superose 6 prep grade's superiority over Sepharose CL-6B and Superose 12 prep grade). It leads to reduced times for the diffusion process, culminating practically in fewer numbers of movements of the TCZ to achieve a desired target desorption yield. Simultaneously, a continuous steady state accumulation on and regular cyclic elution of LF, from a fixed bed of the created thermoCEX adsorbents in the form of sharp uniformly sized peaks has also been investigated in Chapter 3. The time required to reach quasi steady state operation and the degree of concentration attained on TCZ mediated elution appear inversely related to the concentration of LF being continuously supplied to the bed. The addition of non-binding species, BSA, to the LF feed had unexpectedly deleterious effects on LF accumulation and recovery; the latter being tentatively attributed to fouling of the thermoCEX matrix by lipids carried into the feed by serum albumin.

In Chapter 4, with introducing cheaper and more environmentally friendly PEG, a new type of thermoCEX-PEG adsorbent was created based on Superose 6 prep grade, and sequentially applied to demonstrate TCZR arrangement for investigating the dynamic protein 'adsorption-desorption' behaviour. It has been found that the dynamic protein 'adsorption-desorption' performance of thermoCEX-PEG adsorbents is limited due to its relatively low LF binding capacity, although its thermoresponsiveness is superior to thermoCEX.

Chapter 5 is the only chapter in this thesis to investigate the thermoAEX adsorbents and the TCZR arrangement. With increased temperature, the

weaker electrostatic interaction between thermoAEX adsorbents and OVA possibly caused by charge non-uniform distribution within the copolymer network offsets the contributions from the enhanced hydrophobic interaction, which leads to the reduced performance of static and dynamic binding capacity. OVA unfolding at a lower temperature on the surface of chromatographic supports than it would be in bulk solution is another reason to impact the ‘adsorption-desorption’ performance of thermoAEX adsorbents with OVA.

The thermoresponsive behaviour of all thermoresponsive ion exchange adsorbents fabricated in this study are listed in Table 6.1.

Table 6.1 Thermoresponsive adsorbents prepared in this study, see individual chapters for more details, especially for protein adsorption-desorption behaviour.

ID	Base matrix	Adsorbent type	LCST (°C)	Ionic capacity at 20 °C	$q_{max,50°C}$ / $q_{max,10°C}$
A1	S CL-6B	thermoCEX	30.9	330 µmol H^+/g oven dried support	2.2
A2	S CL-6B	thermoCEX	31.8	469 µmol H^+/g oven dried support	3.3
A3	S CL-6B	thermoCEX	34.1	582 µmol H^+/g oven dried support	1.5
A4	S CL-6B	thermoCEX	36.6	811 µmol H^+/g oven dried support	1.1
B1	S6 PG	thermoCEX	29.7	268 µmol H^+/g oven dried support	3.3
B2	S6 PG	thermoCEX	30.8	293 µmol H^+/g oven dried support	2.2
B3	S6 PG	thermoCEX	33.5	382 µmol H^+/g oven dried support	1.2
B4	S6 PG	thermoCEX	36.1	416 µmol H^+/g oven dried support	1.1
C1	S12 PG	thermoCEX	31.4	391 µmol H^+/g oven dried support	2.8
D1	S6 PG	thermoCEX	26.8	122 µmol H^+/g oven dried support	5.1
D2	S6 PG	thermoCEX	28.5	233 µmol H^+/g oven dried support	9.9
D3	S6 PG	thermoCEX	30.2	283 µmol H^+/g oven dried support	1.7
E1	S CL-6B	thermoAEX	30.5	197 µmol Cl^-/g oven dried support	2.2
E2	S CL-6B	thermoAEX	32.1	337 µmol Cl^-/g oven dried support	1.4
E3	S CL-6B	thermoAEX	33.4	480 µmol Cl^-/g oven dried support	1.1
E4	S CL-6B	thermoAEX	36.7	628 µmol Cl^-/g oven dried support	1.0
F1	S6 PG	thermoAEX	30.0	210 µmol Cl^-/g oven dried support	3.6
F2	S6 PG	thermoAEX	32.3	338 µmol Cl^-/g oven dried support	1.6
F3	S6 PG	thermoAEX	33.4	465 µmol Cl^-/g oven dried support	1.2
F4	S6 PG	thermoAEX	36.0	580 µmol Cl^-/g oven dried support	1.1

Future work should focus on (i) creating functionalised monolithic chromatography media which is not subject to diffusion-controlled mass transfer, (ii) improving protein binding capacity and desorption efficiency, instead of combining thermoresponsive and charged monomers within the same polymeric chains or network, uncoupling ‘thermoresponsiveness’ from ‘charge’ may be the solution, and could conceivably be achieved by grafting thermoresponsive chains directly into the surfaces of commercial high capacity ion exchangers in order to deliver temperature-sensitive ion exchange adsorbents possessing charge densities and protein binding capacities similar to those commercial ion exchangers, whist simultaneously retaining desirable thermoresponsive properties. (iii) lowering the operating temperature range, i.e. via increasing the content of hydrophobic monomers. (iv) finding alternative thermo-stable targets with more hydrophilic property which could benefit from both strong hydrophilic and electrostatic interaction at lower temperature in the case of thermoAEX adsorbents application, (v) exploiting an integrated approach to temperature-controlled chromatography, comprising thermoAEX adsorbents and a novel travelling heating zone reactor (THZR) arrangement, where the elution occurs on heating, and consequently (vi) focusing on the scale-up of TCZR operation, instead of simply increasing the column diameter of TCZR due to heat transfer issue, a design of multiple small columns (with the same size as we used in current study) embedded or encased in a common cooling block could be a possibility for scale-up of TCZR.

7 Appendix

7.1 LF calibration curve for analysis in Chapter 2, 3 and 4

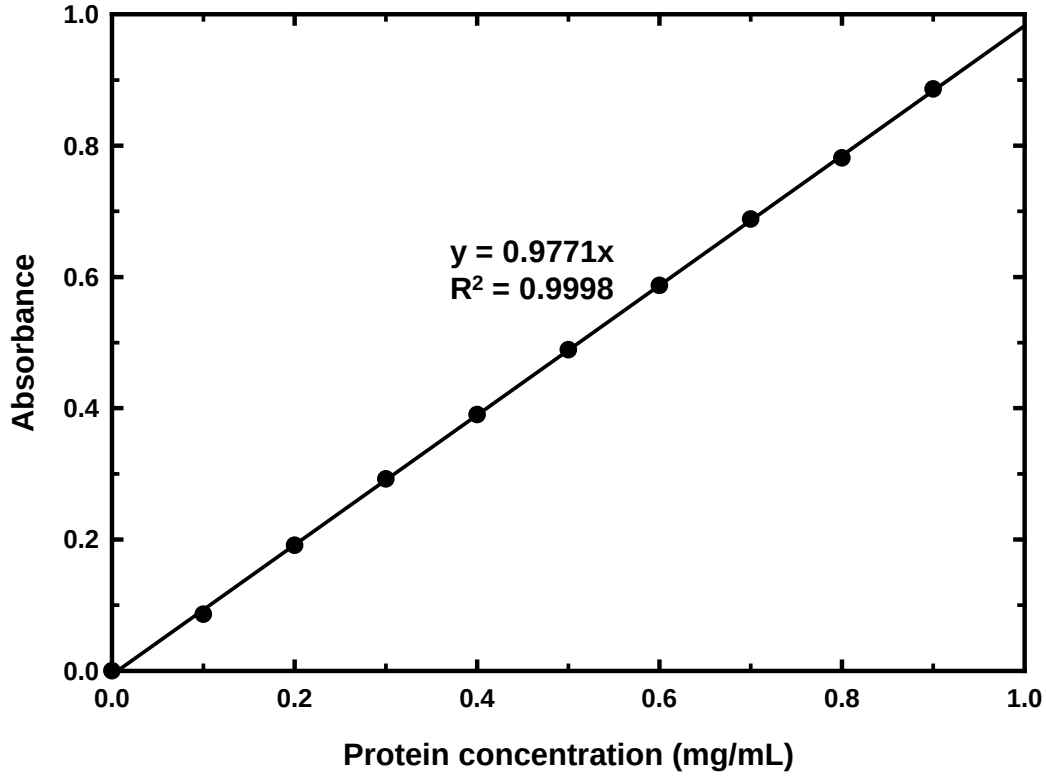

Fig. 7.1 Calibration curve used for calculation of LF concentration via absorbance measurements (280 nm). Equation for line of best fit and corresponding R^2 values are shown in the figure.

7.2 NMR spectra of thermoCEX-CL6B adsorbents ‘A1’-‘A4’ in Chapter 3

^{1}H NMR spectra of ungrafted free copolymer in $CDCl_3$ from the preparation of thermoCEX-CL6B adsorbents ‘A1’-‘A4’ (Fig. 7.2) indicated the successful inclusion of NIPAAm and tBAAm units into the polymer chains. A peak seen at 2.16 ppm corresponds to protons on the carbon α to the carbon of the amide carbonyl group in the NIPAAm and tBAAm monomers, or possibly the carboxylic acid group on AAc. The methyl protons marked ‘A’ and ‘B’ give the characteristic chemical shifts seen at 1.15 and 1.34 ppm, respectively (Spectral Database for Organic Compounds, National Institute of Advanced Industrial Science and Technology, Japan). Comparison of peak heights associated with these ‘A’ and ‘B’ protons (Fig. 7.2) indicated that monomers had been grafted with a NIPAAm to tBAAm ratio of 90: 10 (for support ‘A1’), 88: 12 (for support ‘A2’), 85: 15 (for support ‘A3’), and 81: 19 (for support ‘A4’) in the ungrafted copolymer. Assuming that the compositions of the free and matrix grafted copolymers are identical, then the ratio of NIPAAm: tBAAm: AAc of the subunits grafted onto the matrices are 83.5: 9.3: 7.2 (for support ‘A1’), 79.1: 10.8: 10.1 (for support ‘A2’), 74.5: 13.2: 12.3 (for support ‘A3’), and 67.3: 15.8: 16.9 (for support ‘A4’) (Table 3.1).

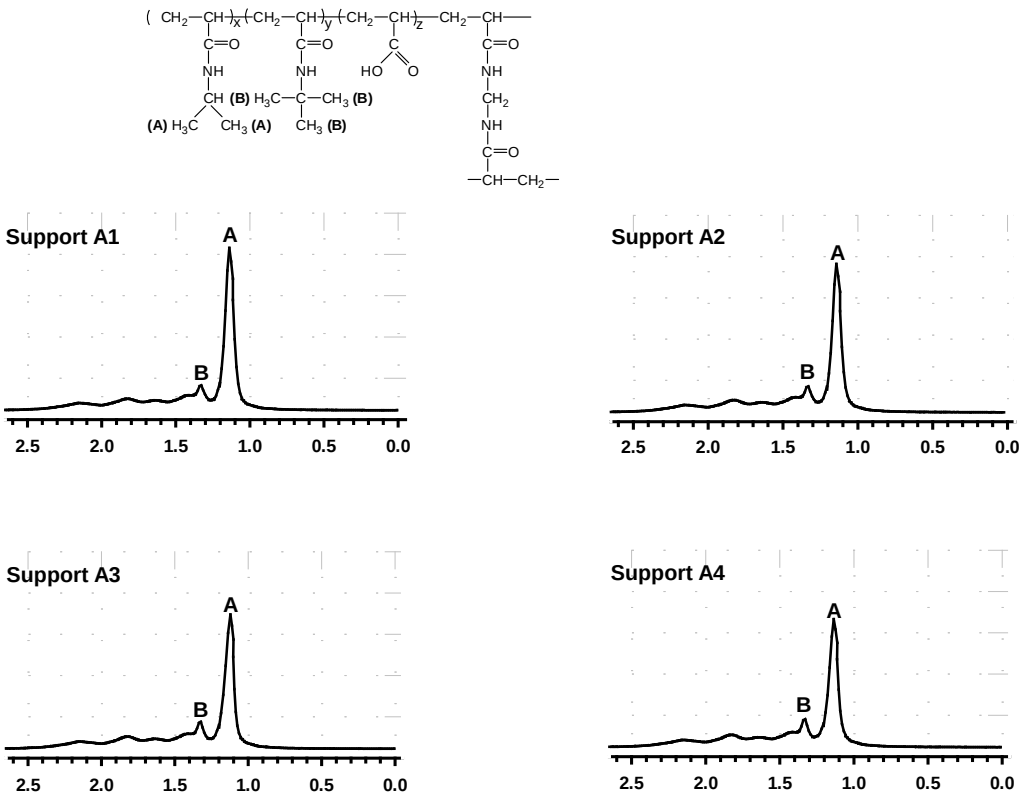

Fig. 7.2 ^{1}H NMR spectra of free ungrafted copolymer in $CDCl_3$ from the preparation of thermoCEX-CL6B adsorbents A1-A4. Peaks corresponding to hydrogen atoms of isopropylacrylamide and *t*-butylacrylamide side chains in the partial structure shown in the upper are indicated by A and B, respectively.

7.3 NMR spectra of thermoCEX-S6PG adsorbents ‘B1’-‘B4’ and thermoCEX-S12PG adsorbent ‘C1’ in Chapter 3

^{1}H NMR spectra of ungrafted free copolymer in $CDCl_3$ from the preparation of thermoCEX-S6PG adsorbents ‘B1’-‘B4’, and thermoCEX-S12PG adsorbent ‘C1’ (Fig. 7.3) indicated the successful inclusion of NIPAAm and tBAAm units into the polymer chains. Comparison of peak heights associated with these ‘A’ and ‘B’ protons (Fig. 7.3) indicated that monomers had been grafted with a NIPAAm to tBAAm ratio of 92: 8 (for support ‘B1’), 91: 9 (for support ‘B2’), 87: 13 (for support ‘B3’), 84: 16 (for support ‘B4’) and 89: 11 (for support ‘C1’) in the ungrafted copolymer. Assuming that the compositions of the free and matrix grafted copolymers are identical, then the ratio of NIPAAm: tBAAm: AAc of the subunits grafted onto the matrices are 87.9: 7.6: 4.5 (for support ‘B1’), 86.6: 8.5: 4.9 (for support ‘B2’), 81.5: 12.2: 6.3 (for support ‘B3’), 78.2: 14.9: 6.9 (for support ‘B4’) and 83.1: 10.3: 6.6 (for support ‘C1’) (Table 3.2).

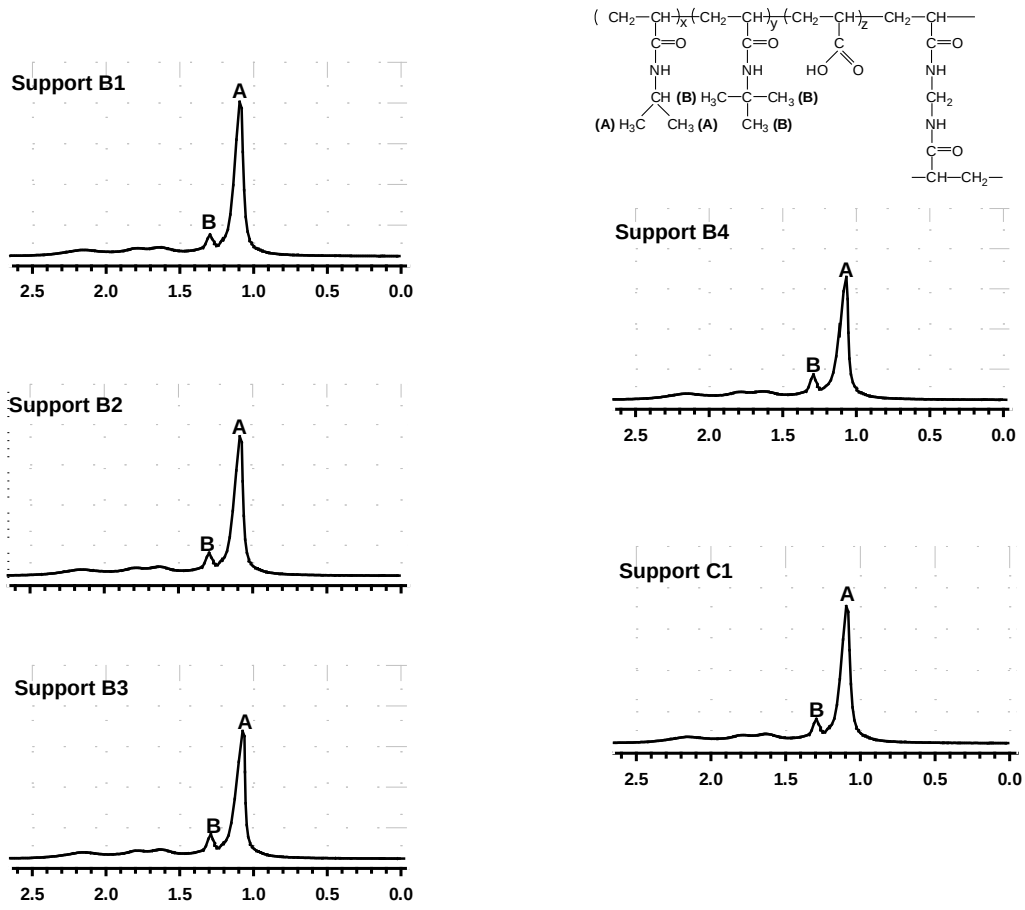

Fig. 7.3 ^{1}H NMR spectra of free ungrafted copolymer in $CDCl_3$ from the preparation of thermoCEX-S6PG adsorbents B1-B4, and thermoCEX-S12PG adsorbent C1. Peaks corresponding to hydrogen atoms of isopropylacrylamide and *t*-butylacrylamide side chains in the partial structure shown in the upper are indicated by A and B, respectively.

7.4 OVA calibration curve for analysis in Chapter 5

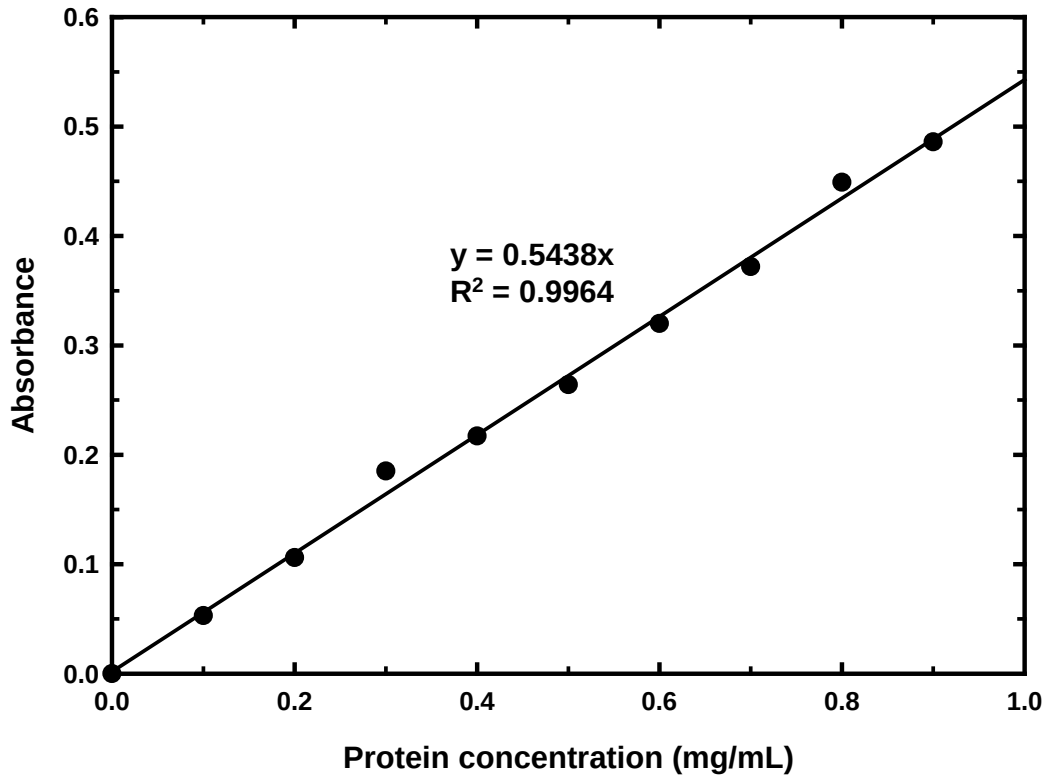

Fig. 7.4 Calibration curve used for calculation of OVA concentration via absorbance measurements (280 nm). Equation for line of best fit and corresponding R^2 values are shown in the figure.

7.5 NMR spectra of thermoAEX adsorbents in Chapter 5

The successful introduction of NIPAAm and BMA units into the polymer chains of thermoAEX adsorbents were evidenced via ^{1}H NMR spectra of ungrafted free copolymer in $CDCl_3$ (Fig. 7.5). The methyl protons marked 'A' and 'B' give the characteristic chemical shifts seen at 1.15 and 0.95 ppm, respectively (Spectral Database for Organic Compounds, National Institute of Advanced Industrial Science and Technology, Japan). Comparison of peak heights associated with these 'A' and 'B' protons (Fig. 7.5) indicated that monomers had been grafted with a NIPAAm to BMA ratio of 89: 11 (for support 'E1'), 87: 13 (for support 'E2'), 83: 17 (for support 'E3'), and 79: 21 (for support 'E4') in the ungrafted copolymers from the preparation of thermoAEX-CL6B adsorbents series; and 90: 10 (for support 'F1'), 87: 13 (for support 'F2'), 84: 16 (for support 'F3'), and 81: 19 (for support 'F4') in the ungrafted copolymers from the preparation of thermoAEX-S6PG adsorbents series. Assuming that the compositions of the free and matrix grafted copolymers are identical, then the ratio of NIPAAm: BMA: ATMAC of the subunits grafted onto the thermoAEX-CL6B matrices are 84.7: 10.5: 4.8 (for support 'E1'), 80.0: 12.0: 8.0 (for support 'E2'), 73.7: 15.1: 11.2 (for support 'E3'), and 67.5: 18.0: 14.5 (for support 'E4') (Table 5.1); also the ratio of NIPAAm: BMA: ATMAC of the subunits grafted onto the thermoAEX-S6PG matrices are 85.7: 9.5: 4.8 (for support 'F1'), 80.5: 12.0: 7.5 (for support 'F2'), 75.5: 14.4: 10.1 (for support 'F3'), and 70.9: 16.6: 12.5 (for support 'F4') (Table 5.1).

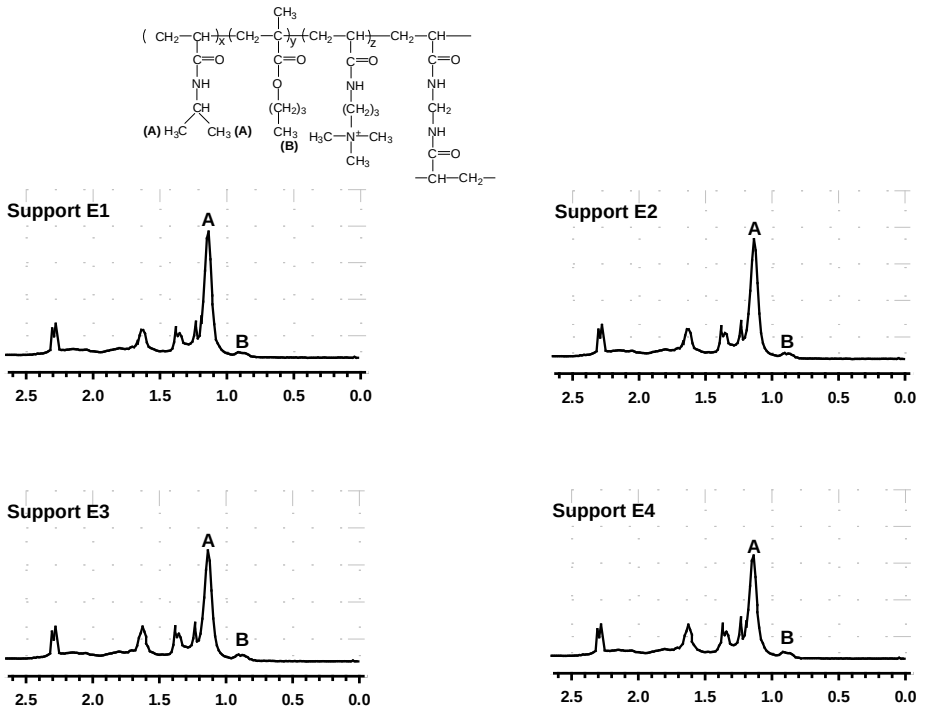

a

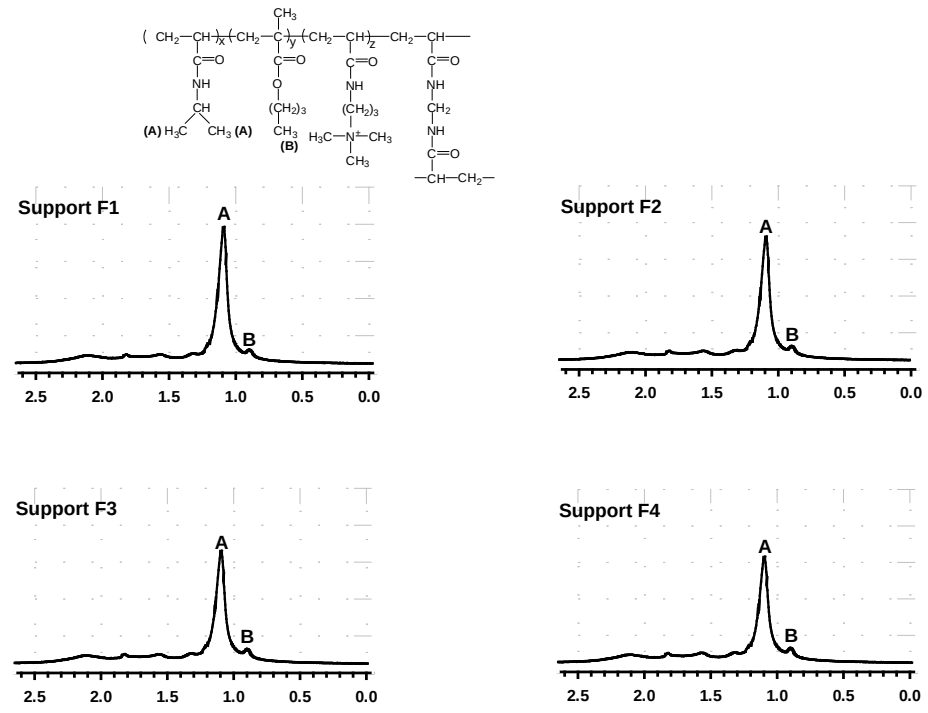

b

Fig. 7.5 ^{1}H NMR spectra of free ungrafted copolymer in $CDCl_3$ from the preparation of thermoAEX-CL6B adsorbents E1-E4. Peaks corresponding to hydrogen atoms of isopropylacrylamide and butyl methacrylate side chains in the partial structure shown in the upper are indicated by A and B, respectively.

7.6 Design of TCZR scale-up

Instead of simply increasing the column diameter of TCZR due to heat transfer issue, a design of multiple small columns (maximum inner diameter could be reached to 2 cm) nested in a common cooling block could be a possibility for scale-up of TCZR.

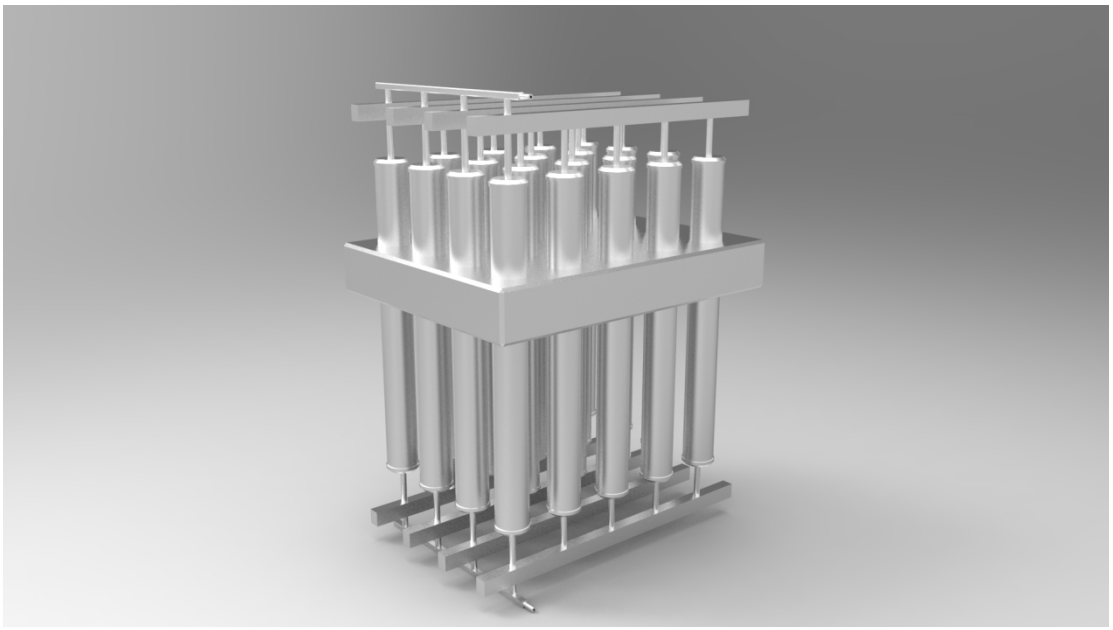

Fig. 7.6 Scale-up of TCZR: a possible configuration (Source: Jonas Wohlgemuth at KIT).

7.7 Permission to Publish of Fig 1.1, 1.2, 1.3, 1.4 and 1.5 from GE Healthcare

GE Healthcare

Permission to Publish

26/11/2015

GE Healthcare Bio-Sciences AB (the "Licensor") hereby grants Ping Cao (the "Licensee"), the non-exclusive, non-transferable, perpetual, worldwide right to reproduce the following material (the "Licensor's Material"):

Fig 1.1 Process of Gel Filtration (taken from Gel Filtration - Principles and Methods, 18-1022-18)
Fig 5 Steps in a HIC Separation (taken from Hydrophobic Interaction and Reversed Phase Chromatography - Principles and Methods, 11-0012-69)
Fig 2 Typical Affinity Purification (taken from Affinity Chromatography - Principles and Mehtods, 18-1022-29)
Fig 2 Theoretical protein titration curves, showing how net surface charge varies with pH (taken from Ion Exchange Chromatography & Chromatofocusing - Principles and Methods, 11-0004-21)
Fig 3 Principles of an anion exchange separation (taken from Ion Exchange Chromatography & Chromatofocusing - Principles and Methods, 11-0004-21)

for the following use:
To illustrate the principles of various chromatography methods in the introduction of my thesis

The Licensee shall not alter the Licensor's Material in any way without the prior permission of the Licensor and shall always include the proper trademark and copyright notice and the following credit line in all versions of the Work:
© XXXX General Electric Company – Reproduced by permission of the owner

This Permission Form has been executed in two originals, of which the Licensor and the Licensee have taken one each.

7.8 List of Publications

Poster presentation:

Thermo-responsive ion exchangers: Preparation, characterisation and protein adsorption-desorption behaviour – '10th Annual bioProcess UK Conference', 3-4 December, 2013, BMA House, London.

Paper:

Müller, T.K.H., Cao, P., Ewert, S., Wohlgemuth, J., Liu, H., Willett, T.C., et al. (2013). Integrated system for temperature-controlled fast protein liquid chromatography comprising improved copolymer modified beaded agarose adsorbents and a travelling cooling zone reactor arrangement. J. Chromatogr. A *1285*: 97–109.

Cao, P., Müller, T.K.H., Ketterer, B., Ewert, S., Theodosiou, E., Thomas, O.R.T., et al. (2015). Integrated system for temperature-controlled fast protein liquid chromatography. II. Optimized adsorbents and 'single column continuous operation'. J. Chromatogr. A *1403*: 118–131.

8 References

A.I. Vogel (1989). Vogel's Textbook of quantitative chemical analysis (Avon: Bath Press).

Adrados, B.P., Galaev, I.Y., Nilsson, K., and Mattiasson, B. (2001). Size exclusion behavior of hydroxypropylcellulose beads with temperature-dependent porosity. J. Chromatogr. A *930*: 73–78.

Affinity chromatography - Principles and Methods (2007). Affinity chromatography - Principles and Methods. GE Healthc. 1–159.

Andersson, J., and Mattiasson, B. (2006). Simulated moving bed technology with a simplified approach for protein purification: Separation of lactoperoxidase and lactoferrin from whey protein concentrate. J. Chromatogr. A *1107*: 88–95.

Andersson, M., Hietala, S., Tenhu, H., and Maunu, S.L. (2006). Polystyrene latex particles coated with crosslinked poly(N-isopropylacrylamide). Colloid Polym. Sci. *284*: 1255–1263.

Andersson, M., Ramberg, M., and Johansson, B.L. (1998). The influence of the degree of cross-linking, type of ligand and support on the chemical stability of chromatography media intended for protein purification. Process Biochem. *33*: 47–55.

Andersson, T., Carlsson, M., Hagel, L., and P-A. Pernemalm (1985). Agarose-based media for high-resolution gel filtration of biopolymers. J. Chromatogr. *326*: 33–44.

Asenjo, J.A., and Andrews, B.A. (2009). Protein purification using chromatography: selection of type, modelling and optimization of operating conditions. J. Mol. Recognit. *22*: 65–76.

Axelsson, H.A.C. (1985). Comprehensive Biotechnology.

Ayano, E., Nambu, K., Sakamoto, C., Kanazawa, H., Kikuchi, A., and Okano, T. (2006a). Aqueous chromatography system using pH- and temperature-responsive stationary phase with ion-exchange groups. J. Chromatogr. A *1119*: 58–65.

Ayano, E., Okada, Y., Sakamoto, C., Kanazawa, H., Kikuchi, A., and Okano, T. (2006b). Study of temperature-responsibility on the surfaces of a thermo-responsive polymer modified stationary phase. J. Chromatogr. A *1119*: 51–57.

Ballew, H.W. (1978). Basics of filtration and separation (Nuclepore Corporation).

Bell, D.J., Hoare, M., and Dunnill, P. (1983). Advances in biochemical engineering/biotechnology.

Belter, P.A., Cussler, E.L., and Hu, W.S. (1988). Bioseparations (Downstream Processing for Biotechnology).

Brinck, J., Jönsson, A.S., Jönsson, B., and Lindau, J. (2000). Influence of pH on the adsorptive fouling of ultrafiltration membranes by fatty acid. J. Memb. Sci. *164*: 187–194.

Cao, P., Müller, T.K.H., Ketterer, B., Ewert, S., Theodosiou, E., Thomas, O.R.T., et al. (2015). Integrated system for temperature-controlled fast protein liquid chromatography. II. Optimized adsorbents and ‘single column continuous operation’. J. Chromatogr. A *1403*: 118–131.

Chen, R.F. (1967). Removal of fatty acids from serum albumin by charcoal treatment. J. Biol. Chem. *242*: 173–181.

Duncan, R. (2003). The dawning era of polymer therapeutics. Nat Rev Drug Discov *2*: 347–360.

Dunnill, P. (1987). Biochemical-engineering and biotechnology. Chem. Eng. Res. Des. *65*: 211–217.

Eastmond, G.C., Tipper, C.F.H., and C.H.Bamford (1976). Comprehensive chemical kinetics. (New York: American Elsevier),.

Eveleigh, J.W. (1978). Techniques and instrumentation for preparative immuno-sorbent separations. J. Chromatogr. *159*: 129–145.

Galaev, I.Y., and Mattiasson, B. (1999). Biotechnology and medicine. Trends Biotechnol *17*: 335–340.

Gel filtration - Principles and Methods (2010). Gel filtration - Principles and Methods. GE Healthc. 1–123.

Gewehr, M., Nakamura, K., Ise, N., and Kitano, H. (1992). Gel permeation chromatography using porous glass beads modified with temperature-responsive polymers. Chem. *193*: 249–256.

Giovannini, R., and Freitag, R. (2002). Continuous isolation of plasmid DNA by annular chromatography. Biotechnol. Bioeng. *77*: 445–454.

Godawat, R., Brower, K., Jain, S., Konstantinov, K., Riske, F., and Warikoo, V. (2012). Periodic counter-current chromatography – design and operational considerations for integrated and continuous purification of proteins. Biotechnol. J. *7*: 1496–1508.

Goheen, S.C., and Gibbins, B.M. (2000). Protein losses in ion-exchange and hydrophobic interaction high-performance liquid chromatography. J. Chromatogr. A *890*: 73–80.

Guiochon, G. (2002). Preparative liquid chromatography. J. Chromatogr. A *965*: 129–161.

Haidacher, D., Vailaya, A., and Horváth, C. (1996). Temperature effects in hydrophobic interaction chromatography. Proc. Natl. Acad. Sci. U. S. A. *93*: 2290–2295.

Han, S., Hagiwara, M., and Ishizone, T. (2003). Synthesis of thermally sensitive water-soluble polymethacrylates by living anionic polymerizations of oligo(ethylene glycol) methyl ether methacrylates. Macromolecules *36*: 8312–8319.

Heskins, M., and Guillet, J.E. (1968). Solution properties of poly(N-isopropylacrylamide). J. Macromol. Sci. Part A - Chem. *2*: 1441–1455.

Hjerten, S. (1973). Some general aspects of hydrophobic interaction chromatography. J. Chromatogr. A *87*: 325–331.

Hoare, M., and Dunnill, P. (1989). Biochemical engineering challenges of purifying useful proteins. Philos. Trans. R. Soc. London B Biol. Sci. *324*: 497–507.

Hoffman, A.S., and Stayton, P.S. (2004). Bioconjugates of smart polymers and proteins: synthesis and applications. Macromol. Symp. *207*: 139–151.

Hoffman, A.S., Stayton, P.S., Bulmus, V., Chen, G., Chen, J., Cheung, C., et al. (2000). Really smart bioconjugates of smart polymers and receptor proteins. J. Biomed. Mater. Res. *52*: 577–586.

Hoshino, K., Taniguchi, M., Kitao, T., Morohashi, S., and Sasakura, T. (1998). Preparation of a new thermo-responsive adsorbent with maltose as a ligand and its application to affinity precipitation. Biotechnol. Bioeng. *60*: 568–579.

Hosoya, K., Kimata, K., Araki, T., Tanaka, N., and Frechet, J.M.J. (1995). Temperature-controlled high-performance liquid chromatography using a uniformly sized temperature-responsive polymer-based packing material. Anal. Chem. *67*: 1907–1911.

Hosoya, K., Sawada, E., Kimata, K., Araki, T., Tanaka, N., and Frechet, J.M.J. (1994). In situ surface-selective modification of uniform size macroporous polymer particles with temperature-responsive poly-N-isopropylacrylamide. Macromolecules *27*: 3973–3976.

Hydrophobic Interaction and Reversed Phase Chromatography Handbook (2006). Hydrophobic Interaction and Reversed Phase Chromatography handbook. GE Healthc. 1–168.

Ion Exchange Chromatography & Chromatofocusing - Principles and Methods (2004). Ion Exchange Chromatography & Chromatofocusing - Principles and Methods. GE Healthc. 1–188.

J.A. Queiroz, C.T. Tomaz, J.M.S.C. (2001). Hydrophobic interaction chromatography of proteins. J. Biotechonology *87*: 143–159.

Jagschies, G. (2008). Where is biopharmaceutical manufacturing heading. BioPharm Inter. *21*: 72.

Jain, M., Vora, R. a., and Satpathy, U.S. (2003). Kinetics of emulsion copolymerization of methylmethacrylate and ethylacrylate: effect of type and concentration of initiator in unseeded polymerization system. Eur. Polym. J. *39*: 2069–2076.

Janson, J.C., and Rydén, L. (1998). Protein purification: principles, high-resolution methods, and applications (Wiley).

Jin, J., Chhatre, S., Titchener-Hooker, N.J., and Bracewell, D.G. (2010). Evaluation of the impact of lipid fouling during the chromatographic purification of virus-like particles from Saccharomyces cerevisiae. J. Chem. Technol. Biotechnol. *85*: 209–215.

Kanazawa, H., Kashiwase, Y., Yamamoto, K., Matsushima, Y., Kikuchi, A., Sakurai, Y., et al. (1997). Temperature-responsive liquid chromatography effects of hydrophobic groups in N-isopropylacrylamide copolymer-modified silica. Anal. Chem. *69*: 823–830.

Kanazawa, H., Nishikawa, M., Mizutani, A., Sakamoto, C., Morita-Murase, Y., Nagata, Y., et al. (2008). Aqueous chromatographic system for separation of biomolecules using thermoresponsive polymer modified stationary phase. J. Chromatogr. A *1191*: 157–161.

Kanazawa, H., Yamamoto, K., Matsushima, Y., Takai, N., Kikuchi, A., Sakurai, Y., et al. (1996). Temperature-responsive chromatography using poly(N-isopropylacrylamide)-modified silica. Anal. Chem. *68*: 100–105.

Kennedy, J.F., and Cabral, J.S. (1993). Recovery processes for biological materials (Wiley).

Kobayashi, J., Kikuchi, A., Sakai, K., and Okano, T. (2002). Aqueous chromatography utilizing hydrophobicity-modified anionic temperature-responsive hydrogel for stationary phases. J. Chromatogr. A *958*: 109–119.

Kobayashi, J., Kikuchi, A., Sakai, K., and Okano, T. (2003). Cross-linked thermoresponsive anionic polymer-grafted surfaces to separate bioactive basic peptides. Anal. Chem *75*: 3244–3249.

Kubota, K., Fujishige, S., and Ando, I. (1990). Single-chain transition of poly(N-isopropylacrylamide) in water. J. Phys. Chem. *94*: 5154–5158.

L, P., and J.Sundberg (1972). High capacity chemisorbents for protein immobilization. New Biol. *238*: 261–262.

Laemmli (1970). Cleavage of structural proteins during the assembly of the head of bacteriophage T4. Nature *227*: 680–685.

Langford, J.F., Schure, M.R., Yao, Y., Maloney, S.F., and Lenhoff, a. M. (2006). Effects of pore structure and molecular size on diffusion in chromatographic adsorbents. J. Chromatogr. A *1126*: 95–106.

Lay, M.C., Fee, C.J., and Swan, J.E. (2006). Continuous radial flow chromatography of proteins. Food Bioprod. Process. *84*: 78–83.

Leser, E.W., and Asenjo, J.A. (1994). Protein recovery, separation and purification. Selection of optimal techniques using an expert system. Mem. Inst. Oswaldo Cruz *89*: 99–109.

Li, N., Qi, L., Shen, Y., Li, Y., and Chen, Y. (2013). Thermoresponsive oligo(ethylene glycol)-based polymer brushes on polymer monoliths for all-aqueous chromatography. ACS Appl. Mater. Interfaces *5*: 12441–12448.

Lindgren, G.E.S. (1986). Method of cross-linking a porous polysaccharide gel (US Patent 4,973,683).

Lowe, C.R., and Dean, P.D.G. (1974). Affinity chromatography (New York: John Wiley & Sons).

Lutz, J.-F., Akdemir, O., and Hoth, A. (2006). Point by point comparison of two thermosensitive polymers exhibiting a similar LCST: is the age of poly(NIPAM) over? J. Am. Chem. Soc. *128*: 13046–13047.

Lutz, J.-F., and Hoth, A. (2006). Preparation of ideal PEG analogues with a tunable thermosensitivity by controlled radical copolymerization of 2-(2-methoxyethoxy)ethyl methacrylate and oligo(ethylene glycol) methacrylate. Macromolecules *39*: 893–896.

Magnusson, J.P., Khan, A., Pasparakis, G., Saeed, A.O., Wang, W., and Alexander, C. (2008). Ion-sensitive 'isothermal' responsive polymers prepared in water. J. Am. Chem. Soc. *130*: 10852–10853.

Maharjan, P., Hearn, M.T.W., Jackson, W.R., Silva, K. De, and Woonton, B.W. (2009). Development of a temperature-responsive agarose-based ion-exchange chromatographic resin. J. Chromatogr. A *1216*: 8722–8729.

Maharjan, P., Woonton, B.W., Bennett, L.E., Smithers, G.W., DeSilva, K., and Hearn, M.T.W. (2008). Novel chromatographic separation — The potential of smart polymers. Innov. Food Sci. Emerg. Technol. *9*: 232–242.

Matsuda, N., Shimizu, T., Yamato, M., and Okano, T. (2007). Tissue engineering based on cell sheet technology. Adv. Mater. *19*: 3089–3099.

Matsumoto, I., Mizuno, Y., and Seno, N. (1979). Activation of Sepharose with epichlorohydrin and subsequent immobilization of ligand for affinity adsorbent. J. Biochem. *85*: 1091–1098.

Mendez, S., Curro, J.G., McCoy, J.D., and Lopez, G.P. (2005). Computational modeling of the temperature-induced structural changes of tethered poly(N-isopropylacrylamide) with self-consistent field theory. Macromolecules *38*: 174–181.

Muca, R., Piatkowski, W., and Antos, D. (2009a). Altering efficiency of hydrophobic interaction chromatography by combined salt and temperature effects. J. Chromatogr. A *1216*: 8712–8721.

Muca, R., Piatkowski, W., and Antos, D. (2009b). Effects of thermal heterogeneity in hydrophobic interaction chromatography. J. Chromatogr. A *1216*: 6716–6727.

Müller, T.K.H., Cao, P., Ewert, S., Wohlgemuth, J., Liu, H., Willett, T.C., et al. (2013). Integrated system for temperature-controlled fast protein liquid chromatography comprising improved copolymer modified beaded agarose adsorbents and a travelling cooling zone reactor arrangement. J. Chromatogr. A *1285*: 97–109.

Munro, P.A., Dunnill, P., and Lilly, M.D. (1977). Nonporous magnetic materials as enzyme supports: Studies with immobilized chymotrypsin. Biotechnol. Bioeng. *19*: 101–124.

Nagase, K., Kobayashi, J., Kikuchi, A., Akiyama, Y., Kanazawa, H., Annaka, M., et al. (2010). Preparation of thermoresponsive anionic copolymer brush surfaces for separating basic biomolecules. Biomacromolecules *11*: 215–223.

Nagase, K., Kobayashi, J., Kikuchi, A., Akiyama, Y., Kanazawa, H., and Okano, T. (2013). Thermally modulated cationic copolymer brush on monolithic silica rods for high-speed separation of acidic biomolecules. ACS Appl. Mater. Interfaces *5*: 1442–1452.

Nagase, K., Yuk, S.F., Kobayashi, J., Kikuchi, A., Akiyama, Y., Kanazawa, H., et al. (2011). Thermo-responsive protein adsorbing materials for purifying pharmaceutical protein on exposed charging surface. J. Mater. Chem. *21*: 2590–2593.

Nishio, T., Ayano, E., Suzuki, Y., Kanazawa, H., and Okano, T. (2011). Separation of phosphorylated peptides utilizing dual pH- and temperature-responsive chromatography. J. Chromatogr. A *1218*: 2079–2084.

Odian, G. (2004). Principles of polymerization (NY, USA: Wiley-Interscience).

Oza, M.D., Meena, R., Prasad, K., Paul, P., and Siddhanta, a. K. (2010). Functional modification of agarose: A facile synthesis of a fluorescent agarose–guanine derivative. Carbohydr. Polym. *81*: 878–884.

Palani, S., Gueorguieva, L., Rinas, U., Seidel-Morgenstern, A., and Jayaraman, G. (2011). Recombinant protein purification using gradient-assisted simulated moving bed hydrophobic interaction chromatography. Part I: Selection of chromatographic system and estimation of adsorption isotherms. J. Chromatogr. A *1218*: 6396–6401.

Pan, L.-C., and Chien, C.-C. (2003). A novel application of thermo-responsive polymer to affinity precipitation of polysaccharide. J. Biochem. Biophys. Methods *55*: 87–94.

Park, B.J., Lee, C.H., Mun, S., and Koo, Y.M. (2006). Novel application of simulated moving bed chromatography to protein refolding. Process Biochem. *41*: 1072–1082.

Patananan, N., Angeles, L., Sciences, B., Angeles, L., Genetics, M., Undergraduate, U., et al. (2008). The surface-mediated unfolding kinetics of globular proteins is dependent on molecular weight and tempearture. U.S. Dep. Energy J. Undergrad. Res. 97–104.

Pernemalm, P.A., Carlsson, M., and G. Lindgren (1987). 32 (European Patent EP 0132244).

Peters, E.C., Svec, F., and Fréchet, J.M.J. (1997). Thermally responsive rigid polymer monoliths. Adv. Mater. *9*: 630–633.

Plunkett, K.N., Zhu, X., Moore, J.S., and Leckband, D.E. (2006). PNIPAM chain collapse depends on the molecular weight and grafting density. Langmuir *22*: 4259–4266.

Porath, J., and Fornstedt, N. (1970). Group fraction of plasma proteins on dipolar ion exchangers. J. Chromatogr. *51*: 479–489.

Porath, J., Janson, J.-C., and Laas, T. (1971). Agar derivatives for chromatography, electrophoresis and gel-bound enzymes. J. Chromatogr. *60*: 167–177.

Przybycien, T.M., Pujar, N.S., and Steele, L.M. (2004). Alternative bioseparation operations: life beyond packed-bed chromatography. Curr. Opin. Biotechnol. *15*: 469–478.

Sakamoto, C., Okada, Y., Kanazawa, H., Ayano, E., Nishimura, T., Ando, M., et al. (2004). Temperature- and pH-responsive aminopropyl-silica ion-exchange columns grafted with copolymers of N-isopropylacrylamide. J. Chromatogr. A *1030*: 247–253.

Schild, H.G. (1992). Poly(N-isopropylacrylamide): experiment , theory and application. Polym. Sci *17*: 163–249.

Schneider, C.A., Rasband, W.S., and Eliceiri, K.W. (2012). NIH Image to ImageJ: 25 years of image analysis. Nat Meth *9*: 671–675.

Scopes, R.K. (1982). Protein purification: principles and practice (WILEY-VCH Verlag GmbH).

Shi, Y., Xiang, R., Horváth, C., and Wilkins, J. a. (2004). The role of liquid chromatography in proteomics. J. Chromatogr. A *1053*: 27–36.

Shuler, M.L., and Kargi, F. (1992). Bioprocess engineering: basic concepts.

Somasundaran, P. (2006). Encyclopedia of surface and colloid science (Taylor & Francis).

Spector, a a, John, K., and Fletcher, J.E. (1969). Binding of long-chain fatty acids to bovine serum albumin. J. Lipid Res. *10*: 56–67.

Sundberg, L., and Porath, J. (1974). Preparation matography i. attachment polymers. J. Chromatogr. *90*: 87–98.

Tallarek, U., Vergeldt, F.J., and As, H. Van (1999). Stagnant mobile phase mass transfer in chromatographic media: Intraparticle diffusion and exchange kinetics. J. Phys. Chem. B *103*: 7654–7664.

Taylor, L.D., and Cerankowski, L.D. (1975). Preparation of films exhibiting a balanced temperature dependence to permeation by aqueous solutions-a study of lower consolute behavior. J. Polym. Sci. Polym. Chem. Ed. *13*: 2551–2570.

Teal, H.E., Hu, Z., and Root, D.D. (2000). Native purification of biomolecules with temperature-mediated hydrophobic modulation liquid chromatography. Anal. Biochem. *283*: 159–165.

Terefe, N.S., Glagovskaia, O., Silva, K. De, and Stockmann, R. (2014). Application of stimuli responsive polymers for sustainable ion exchange chromatography. Food Bioprod. Process. *92*: 208–225.

Theodossiou, I., Collins, I.J., Ward, J.M., Thomas, O.R. t., and Dunnill, P. (1997). The processing of a plasmid-based gene from E. coli.: Filtration as a primary recovery step. Bioprocess Eng. *16*: 175–183.

Theodossiou, I., and Thomas, O.R.T. (2002). DNA-induced inter-particle cross-linking during expanded bed adsorption chromatography Impact on future support design. J. Chromatogr. A *971*: 73–86.

Thomas, O.R.. (2008). Bioserarations. Course notes University of Birmingham.

Thömmes, J., and Etzel, M. (2007). Alternatives to chromatographic separations. Biotechnol. Prog. *23*: 42–45.

Tiainen, P., Gustavsson, P.E., Månsson, M.O., and Larsson, P.O. (2007). Plasmid purification using non-porous anion - exchange silica fibres. J. Chromatogr. A *1149*: 158–168.

Venkatramani, C.J., and Zelechonok, Y. (2003). An automated orthogonal two-dimensional liquid chromatography. Anal. Chem. *75*: 3484–3494.

Wang, D.I., Cooney, C.L., Demain, A.L., Dunnill, P., Humphrey, A.E., and Lillly, M.D. (1979). Fermentation and enzyme technology (Chichester and New York: John Wiley & Sons, Ltd).

Weerts, P.A., Loos, J.L.M. van der, and German, A.L. (1989). Emulsion polymerization of butadiene, 1. The effects of initiator and emulsifier concentration. Die Makromol. Chemie *190*: 777–788.

Yagi, H., Yamamoto, K., and Aoyagi, T. (2008). New liquid chromatography method combining thermo-responsive material and inductive heating via alternating magnetic field. J. Chromatogr. B. Analyt. Technol. Biomed. Life Sci. *876*: 97–102.

Yakushiji, T., Sakai, K., Kikuchi, A., Aoyagi, T., Sakurai, Y., and Okano, T. (1999). Effects of cross-linked structure on temperature-responsive hydrophobic interaction of poly(N-isopropylacrylamide) hydrogel-modified surfaces with steroids. Anal. Chem. *71*: 1125–1130.

Yim, H., Kent, M.S., Huber, D.L., Satija, S., Majewski, J., and Smith, G.S. (2003). Conformation of end-tethered PNIPAM chains in water and in acetone by neutron reflectivity. Macromolecules *36*: 5244–5251.

Yoshimatsu, K., Lesel, B.K., Yonamine, Y., Beierle, J.M., Hoshino, Y., and Shea, K.J. (2012). Temperature-responsive ‘catch and release’ of proteins by using multifunctional polymer-based nanoparticles. Angew. Chemie Int. Ed. *51*: 2405–2408.

Yoshizako, K., Akiyama, Y., Yamanaka, H., Shinohara, Y., Hasegawa, Y., Carredano, E., et al. (2002). Regulation of protein binding toward a ligand on chromatographic matrixes by masking and forced-releasing effects using thermoresponsive polymer. Anal. Chem. *74*: 4160–4166.

Zhang, J., and Pelton, R. (1999). The dynamic behavior of poly(N-isopropylacrylamide) at the air/water interface. Colloids Surfaces A Physicochem. Eng. Asp. *156*: 111–122.